University of Bergen

Master Thesis in Applied and Computational Mathematics

Acoustic and Boundary Layer Comparisons Between Navier-Stokes and Svärd's Modified Navier-Stokes Equations

Author:
Karl Munthe

December 22, 2021

Abstract

In this thesis we examine the validity and predictive value of the Navier-Stokes-Svärd equations, first introduced in [22]. We compare the acoustic attenuation between the Navier-Stokes and Navier-Stokes-Svärd equations. The comparison is done by numerically solving both equations with initial conditions small enough such that non-linearities are negligible (i.e., linear theory is still valid). The numerical solution is then compared against analytically solution to the linearized Navier-Stokes and Navier-Stokes-Svärd equations as well as experimental results found in the literature. Additionally, we examine the boundary layer obtained from the Navier-Stokes-Svärd equations and compare it with the Blasius boundary layer.

The acoustic simulations show that if both systems are in the linear regime, the difference between the models is much smaller than what can be measured with equipment being used in experimental acoustics today. The boundary layer simulations also show a good agreement between the Blasius boundary layer and the boundary layer obtained from the Navier-Stokes-Svärd equations.

Acknowledgements

First and foremost I want to express my gratitude to Professor Magnus Svärd who has guided me through this masters thesis. Thank you for your guidance and interesting discussions.

Furthermore, I would like to thank my friends Calvin, Devan, Evan, and Gracy for introducing me to science. Had it not been for you, I would probably never had studied science at all. My life has become much richer after receiving a formal education in physics and math and I am extremely grateful for the inspiration and motivation you guys gave me to pursue a masters in mathematics. Additionally, I want to thank Professor Nancy Emery from the University of Colorado, Boulder, who was the first professor I had who really showed me how interesting and awesome nature really is.

Last but not least, I want to thank my family and partner, Birgitte, for supporting me in all my endeavours. Without your continued support I would never have come this far.

Contents

List of Figures

List of Tables

Introduction

Fluid mechanics is the study of the behavior of gases and liquids and is used in all domains of modern society. It is important for the understanding of everything from bodily fluids to spaceships. One of the earliest and most popular set of fluid equations model adiabatic and inviscid flow and are known as the Euler equations:

$$\begin{aligned} \frac{\partial \rho}{\partial t} + \nabla \cdot (\rho \mathbf{u}) &= 0 \\ \frac{\partial (\rho \mathbf{u})}{\partial t} + \nabla \cdot (\rho \mathbf{u} \otimes \mathbf{u}) + \nabla p &= 0 \\ \frac{\partial E}{\partial t} + \nabla \cdot (E\mathbf{u} + p\mathbf{u}) &= 0, \end{aligned}$$

where ρ is the density, $\mathbf{u}$ is the velocity, p is the pressure, and E is the total energy. Since most fluid phenomena occur in the presence of viscosity and/or heat transfer there have been attempts at modelling these effects as well. The most well-known and widely used model is the Navier-Stokes (NS) equations. In the absence of body forces, the NS equations are:

$$\begin{aligned} \frac{\partial \rho}{\partial t} + \nabla \cdot (\rho \mathbf{u}) &= 0 \\ \frac{\partial (\rho \mathbf{u})}{\partial t} + \nabla \cdot (\rho \mathbf{u} \otimes \mathbf{u}) + \nabla p &= \nabla \cdot \sigma \\ \frac{\partial E}{\partial t} + \nabla \cdot (E\mathbf{u} + p\mathbf{u}) &= \nabla \cdot (\sigma \cdot \mathbf{u}) + \nabla \cdot (\kappa \nabla T) \end{aligned}$$

where κ is the thermal diffusivity and σ is the viscous stress tensor. For a Newtonian fluid, the viscous stress tensor, σ, is

$$\sigma = \zeta \nabla \cdot \mathbf{u} \mathbb{I} + \mu \left(\nabla \mathbf{u} + (\nabla \mathbf{u})^\top - \frac{2}{3} (\nabla \cdot \mathbf{u}) \mathbb{I} \right).$$

Despite the success of the Navier-Stokes equations, there is still no well-posedness proof (no proof of existence, uniqueness, or stability). In fact, the well-posedness of the incompressible Navier-Stokes equations has been questioned in [26]. Other

attempts have therefore been made to model viscosity and heat transfer for fluid flow. This thesis will focus on is the Navier-Stokes-Svärd equations (NSS) first proposed in [22], which among other things, introduced mass diffusion. For other mass diffusive models, see the citations in [22]. The NSS equations are:

$$\begin{aligned} \frac{\partial \rho}{\partial t} + \nabla \cdot (\rho \mathbf{u}) &= \nabla \cdot (\nu \nabla \rho) \\ \frac{\partial (\rho \mathbf{u})}{\partial t} + \nabla \cdot (\rho \mathbf{u} \otimes \mathbf{u}) + \nabla p &= \nabla \cdot (\nu \nabla (\rho \mathbf{u})) \\ \frac{\partial E}{\partial t} + \nabla \cdot (E\mathbf{u} + p\mathbf{u}) &= \nabla \cdot (\nu \nabla E). \end{aligned}$$

The difference between the NSS and NS equations is solely in the diffusive terms. The NSS equations are conservative and the non-linear phenomena are a result of the convective terms which are the exact same as the NS equations (and Euler equations) indicating that all the non-linear phenomena generated by the NS equations must also be generated by the NSS equations. The equations differ in how they diffuse ρ, $\mathbf{u}$, and E, and all the equations in the NSS system are parabolic, while the NS system has one hyperbolic and two parabolic equations.

This thesis will examine the validity and predictive value of the NSS equations. Specifically we will compare how the NSS and NS equations predict acoustic attenuation. This is done by comparing the numerical solution to the analytical solution of the linearized equations and to experimental results found in the literature. Additionally, we compare the Blasius boundary layer with the NSS equations on a domain approximating the assumptions used to derive the Blasius boundary layer.

The acoustic simulations of both the NS and NSS equations show an experimentally indistinguishable difference in their predictions of acoustic attenuation for acoustic waves in the linear regime. The boundary layer simulations of the NSS equations show a good agreement with the Blasius boundary layer.

All the code written for this thesis has been written from scratch by the author and can be found here: https://github.com/KarlMunthe/MasterThesis.

Thesis Outline

Chapter 1: derive core equations that will be used in the succeeding chapters. The equations used in derivations for the NSS equations that are not needed in

derivations for the NS equations will derived. (Equations needed for the NS equations can be found in [13], [12], or [1]).

Chapter 2: explain the concept of entropy for a system of conservation laws from a mathematical point of view and derive the mathematical equivalent of the second law of thermodynamics. Furthermore, we will derive the physically relevant entropy vector and equations for both the NS and NSS systems and prove that they satisfy the second law of thermodynamics.

Chapter 3: derive the coefficient of absorption for both the NS and NSS systems with help from the entropy equations derived in chapter 2.

Chapter 4: present the spectral methods and derive the n'th order difference matrix for an equispaced grid.

Chapter 5: introduce the basic ideas behind time discretization techniques and derive the fourth order Runge-Kutta method.

Chapter 6: show that the scheme used to solve the NS and NSS systems converges with a spectral convergence rate by help of the method of the method of manufactured solution.

Chapter 7: discuss various sources of errors and then present the results of the sound wave simulations.

Chapter 8: show that the incompressible NS and NSS equations are the same. Then we will derive the boundary layer equations and then derive the Blasius ordinary differential equation.

Chapter 9: present the results from the numerical solution to the non-dimensionalized boundary layer problem and compare the boundary layer obtained from the NSS system with the boundary layer solved by the Blasius equations.

Chapter 0

Useful Equations, Operators, and Identities

This chapter presents useful equations, operators, and identities that will be used throughout this thesis. For a derivation and/or explanation of the various equations consult [14] and [13].

0.1 Equations

Throughout this thesis we will use the following notation to describe various entities. Unless stated otherwise, $\mathbf{u}$ is velocity vector, $\mathbf{m}$ is momentum vector, ρ is density, E is total energy, e is internal energy, T is temperature, p is pressure, c_p is heat capacity at constant pressure, c_V is heat capacity at constant volume, γ is heat capacity ratio, R is *specific* gas constant, μ is the dynamic viscosity, ν is the kinematic viscosity, β is the linear thermal expansion coefficient, and S is the *specific* entropy. The following is a list of standard fluid mechanics equations

that will be used frequently throughout this thesis.

$$\mathbf{m} = \rho\mathbf{u} \tag{1}$$

$$E = \rho\left(\frac{|\mathbf{m}|^2}{2} + e\right) \tag{2}$$

$$e = c_V T \tag{3}$$

$$p = \rho R T \tag{4}$$

$$\gamma = \frac{c_p}{c_V} \tag{5}$$

$$R = c_p - c_V \tag{6}$$

$$\nu = \frac{\mu}{\rho} \tag{7}$$

$$Tds = nc_V dT + pdV \tag{8}$$

$$S = c_V \ln\left(\frac{p}{\rho^\gamma}\right) \tag{9}$$

$$\frac{\partial T}{\partial x} = \frac{c\beta T}{c_p}\frac{\partial u}{\partial x} \tag{10}$$

$$\frac{T\beta^2 c^2}{c_p} = \frac{c_p}{c_v} - 1 \tag{11}$$

0.2 Operators

Definition 0.2.1 (Material derivative)**.** *The material derivative of some scalar function f is the sum of the time derivative of f and the dot product between gradient of f and the velocity field.*

$$\frac{D}{Dt}f = \frac{\partial}{\partial t}f + \mathbf{u}\cdot\nabla f. \tag{12}$$

Definition 0.2.2 (Tensor product)**.** *The tensor product between two vectors, $\mathbf{a}\otimes\mathbf{b}$, is a matrix where each entry in $\mathbf{a}$ is multiplied by the transpose of $\mathbf{b}$.*

$$\mathbf{a}\otimes\mathbf{b} = \begin{bmatrix} a_1\mathbf{b}^\top \\ \vdots \\ a_N\mathbf{b}^\top \end{bmatrix} = \begin{bmatrix} a_1b_1 & a_1b_2 & a_1b_3 & \cdots & a_1b_N \\ a_2b_1 & a_2b_2 & a_2b_3 & \cdots & a_2b_N \\ \vdots & \ddots & \ddots & \ddots & \vdots \\ a_Nb_1 & a_Nb_2 & a_Nb_3 & \cdots & a_Nb_N \end{bmatrix}$$

Definition 0.2.3 (Hadamard product)**.** *The Hadamard operator product, $\circ$, acts on matrices of the same size. The Hadamard product between two matrices, A and B, results in a new matrix C which is the same size as A and B but each entry in*

C is the product of the same entry in both A and B. Given two vectors, $\mathbf{a}$ and $\mathbf{b}$, their Hadamard product is

$$\mathbf{a} \circ \mathbf{b} = \begin{bmatrix} a_1 b_1 \\ \vdots \\ a_N b_N \end{bmatrix}$$

and between two matrices, A and B, is

$$A \circ B = \begin{bmatrix} A_{11}B_{11} & A_{12}B_{12} & A_{13}B_{13} & \cdots & A_{1N}B_{1N} \\ A_{21}B_{21} & A_{22}B_{22} & A_{23}B_{23} & \cdots & A_{2N}B_{2N} \\ \vdots & \ddots & \ddots & \ddots & \vdots \\ A_{N1}B_{N1} & A_{N2}B_{N2} & A_{N3}B_{N3} & \cdots & A_{NN}B_{NN} \end{bmatrix}$$

Definition 0.2.4 (Frobenius inner product/double dot product)**.** *The Frobenius inner product between two matrices, $A : B$, returns the sum of the product of each entry in A multiplied by the entry with the same index in B.*

$$\begin{aligned} A : B = \sum_i \sum_j A_{ij}B_{ij} =& A_{11}B_{11} + A_{12}B_{12} + \cdots + A_{1N}B_{1N} + \\ & A_{21}B_{21} + A_{22}B_{22} + \cdots + A_{2N}B_{2N} + \\ & \vdots \\ & A_{N1}B_{N1} + A_{N2}B_{N2} + \cdots + A_{NN}B_{NN}. \end{aligned}$$

Note that the Frobenius inner product between two matrices A and B is the sum of all the entries in the Hadamard product between A and B.
In this thesis we will be working with systems of PDE's that can be cast in conservative form. Therefore it is convenient to write the system of equations in *container form*

PDE's are often coupled where parts of the system are scalars, vectors or tensors. Often the same operation is done on a vector as a tensor. To simplify notation we introduce the *container*, which is best explained by an example

Definition 0.2.5 (Container)**.** *The Euler equations can be expressed as*

$$\frac{\partial}{\partial t}\mathbf{U} + \sum_n \frac{\partial}{\partial x_n} F = 0$$

where $\mathbf{U} = (\rho, \mathbf{m}, E)^\top$ and

$$\sum_n \frac{\partial}{\partial x_n} F = \begin{bmatrix} \nabla \cdot (\mathbf{m}) \\ \nabla \cdot (\mathbf{m} \otimes \frac{\mathbf{m}}{\rho}) + \nabla p \\ \nabla \cdot (E\frac{\mathbf{m}}{\rho} + p\frac{\mathbf{m}}{\rho}) \end{bmatrix}$$

Since every term has a "$\nabla\cdot$", the mathematics becomes simpler if we express this as

$$\nabla \odot F$$

where

$$F = \begin{Bmatrix} \mathbf{m} \\ (\mathbf{m} \otimes \frac{\mathbf{m}}{\rho}) + p\mathbb{I} \\ E\frac{\mathbf{m}}{\rho} + p\frac{\mathbf{m}}{\rho} \end{Bmatrix}. \tag{13}$$

$\nabla\odot$ will be defined in the next definition. We will refer to (13) as a container which is denoted with curly brackets. The container contains three first entries, $\mathbf{m}$, $(\mathbf{m}\otimes\mathbf{m}/\rho)+p\mathbb{I}$, $E\mathbf{m}/\rho + p\mathbf{m}/\rho$.

Definition 0.2.6 (O divergence)**.** *Given a system of PDE's*

$$\frac{\partial \mathbf{u}}{\partial t} = \begin{bmatrix} \nabla\cdot\mathbf{f}_1(\mathbf{u}) \\ \nabla\cdot\mathbf{f}_2(\mathbf{u}) \\ \vdots \\ \nabla\cdot\mathbf{f}_N(\mathbf{u}) \end{bmatrix}$$

we can express this as

$$\frac{\partial \mathbf{u}}{\partial t} = \nabla \odot F.$$

where $F = (\mathbf{f}_1, \mathbf{f}_2, \cdots, \mathbf{f}_N)^\top$. The rule is that the operator acting on F gets moved inside such that it acts on all the first *indices of F. We emphasize first because if F is a vector containing vectors and/or tensors then the operator acts on the vectors and/or tensors in F and* not *the entries of the vectors and/or tensors in F.*

Definition 0.2.7 (O dot product)**.** *Given a vector $\mathbf{g}$ and a container $F = (\mathbf{f}_1, \mathbf{f}_2, \cdots, \mathbf{f}_N)^\top$ the O dot prodcut, $\odot$, between the two is as follows*

$$\mathbf{g} \odot F = \sum_n \mathbf{g}\mathbf{f}_n = \mathbf{g}\cdot\mathbf{f}_1 + \mathbf{g}\cdot\mathbf{f}_2 + \cdots + \mathbf{g}\cdot\mathbf{f}_N.$$

$\mathbf{f}_n$ might not necessarily be a vector, and in the case that it is a scalar, f_n, we multiply f_n by a vector with unit entries such that $\mathbf{g}\cdot\mathbf{f}_n$ returns a scalar. Or, we can dot $\mathbf{g}$ with a vector with the same length as $\mathbf{g}$ with unit entries such that we end up with the same scalar. See appendix A for an example.

In this thesis we will abuse notation for containers in the two following ways. Given a vector g and a container $F = (\mathbf{f}_1, \mathbf{f}_2, \cdots, \mathbf{f}_N)^\top$ the "normal" dot product

is

$$\mathbf{g} \cdot F = \begin{bmatrix} \mathbf{g} \cdot \mathbf{f}_1 \\ \mathbf{g} \cdot \mathbf{f}_2 \\ \vdots \\ \mathbf{g} \cdot \mathbf{f}_N \end{bmatrix}. \tag{14}$$

One can think of the $\mathbf{g}\cdot$ being sent into the container and dotted with its entries. In the case that $\mathbf{f}_n$ is not a vector the same rules apply as stated in definition 9.5.

Given two containers, $G = (\mathbf{g}_1, \mathbf{g}_2, \cdots, \mathbf{g}_N)^\top$, and $F = (\mathbf{f}_1, \mathbf{f}_2, \cdots, \mathbf{f}_N)^\top$ the double dot product between F and G is

$$G : F = \sum_n \mathbf{g}_n \mathbf{f}_n = \mathbf{g}_1 \cdot \mathbf{f}_1 + \mathbf{g}_2 \cdot \mathbf{f}_2 + \cdots + \mathbf{g}_N \cdot \mathbf{f}_N \tag{15}$$

which technically is not the same as the Frobenius inner product, but is similar enough so we use the same notation. In the case that $\mathbf{f}_n$ is not a vector the same rules apply as stated in definition 9.5.

0.3 Identities

Definition 0.3.1 (Various Product Rules)**.** *Given a scalar a and a vector $\mathbf{b}$ the product rule is:*

$$\nabla \cdot (a\mathbf{b}) = \mathbf{b} \cdot \nabla a + a \nabla \cdot \mathbf{b}. \tag{16}$$

Given a vector $\mathbf{a}$ and a vector $\mathbf{b}$ the product rule is:

$$\nabla \cdot (\mathbf{a} \otimes \mathbf{b}) = (\nabla \cdot \mathbf{a})\mathbf{b} + \mathbf{a} \cdot \nabla \mathbf{b}. \tag{17}$$

Given a second order tensor A and a vector $\mathbf{b}$ the product rule is:

$$\nabla \cdot (A \cdot \mathbf{b}) = \mathbf{b} \cdot \nabla \cdot A + A : \nabla \mathbf{b}. \tag{18}$$

Chapter 1

Elementary Physics

In this chapter we will outline the most important physical principles and relations that are necessary for the analysis of acoustic attenuation and boundary layer simulations of the Navier-Stokes-Svärd equations. All derivations in this chapter are used for the Navier-Stokes equations as well, except for (1.13). For more information about these derivations consult [13] and [28].

1.1 Simple Harmonic Motion

It is well known that the energy of small and linear waves is expressed in terms of the potential and kinetic energy as follows

$$E = \frac{1}{2}mu^2 + \frac{1}{2}kx^2 \tag{1.1}$$

where m is mass, u is velocity, k is some proportionality constant, and x is displacement. Assuming the waves are so small that energy dissipation is negligible we can assume the energy to be constant. Moreover, we assume that x, and therefore u, is a simple sinusoidal function. Setting $x = A\sin(kx - \omega t)$ we get

$$E = \frac{1}{2}m(-A\omega\cos(kx - \omega t))^2 + \frac{1}{2}k(A\sin(kx - \omega t))^2$$

since u is the time derivative of the displacement. Now we simply integrate over one temporal wavelength and get

$$\begin{aligned} E &= \int_0^\lambda \frac{1}{2}m(-A\omega\cos(kx - \omega t))^2 dx + \int_0^\lambda \frac{1}{2}k(A\sin(kx - \omega t))^2 dx \\ &= \frac{1}{4}mA^2\omega^2 + \frac{1}{4}kA^2. \end{aligned}$$

Since m and ω are all constants we can safely assume that the energy is proportional to the amplitude squared, namely

$$E \propto A^2.$$

Moreover, ω can be derived by Newton's second law and one finds that $\omega^2 = k/m$. The magnitude of the kinetic energy, KE, must be equal to the magnitude of the potential energy, PE. Therefore, the total energy can be expressed as twice the kinetic or potential energy.

$$E = 2KE = 2PE$$

According to Landau and Lifshitz [13], the decay of mechanical energy is

$$E = C \exp\left(\frac{d}{dt}\ln(KE)t\right) = C \exp\left(\frac{\frac{d}{dt}KE}{KE}t\right) = C \exp\left(\Gamma t\right). \tag{1.2}$$

1.2 Entropy

We will now derive the entropy function. Since the derivation mostly contains substitutions of thermodynamic relations we will show the substitutions needed in order to get to the next line to the right of the equation. Here, n is the number of moles m is mass. We begin with the fundamental thermodynamic relation:

$$\begin{aligned}
Tds &= nc_V dT + pdV, \qquad V = \frac{m}{\rho} \\
ds &= nc_V \frac{dT}{T} - \frac{mp}{T\rho^2}d\rho, \qquad pV = nRT \Leftrightarrow \frac{mp}{\rho T} = nR \\
&= nc_V \frac{dT}{T} - nR\frac{d\rho}{\rho}, \qquad \int_{t_0}^{t} dt \\
s &= nc_V \ln(T) - nR\ln(\rho) + C, \qquad R = c_p - c_v \Leftrightarrow R = c_V(\gamma - 1) \\
&= nc_V \ln(T) - nc_V \ln(\rho^{\gamma-1}) + C, \qquad T = \frac{p}{\rho R} \\
&= nc_V \ln\left(\frac{p}{\rho^\gamma}\frac{1}{R}\right) + C \\
S &= c_V \ln\left(\frac{p}{\rho^\gamma}\right)
\end{aligned} \tag{1.3}$$

where $S = s/n$ and is referred to as the *specific entropy*. We have used the definite integral because entropy is a relative quantity, meaning that there is no absolute zero measure of entropy in the continuum realm. From (1.3) we can deduce that in isentropic phenomena (no change in entropy), $p = p_0\rho^\gamma$.

1.3 The Newtonian Viscous Stress Tensor

The viscous stress tensor for a Newtonian fluid is

$$\sigma = \lambda(\nabla \cdot \mathbf{u})I + \mu(\nabla\mathbf{u} + (\nabla\mathbf{u})^T). \tag{1.4}$$

(A rigorous derivation of (1.5) can be found in [1] and a less detailed but more intuitive approach can be found in [12]). The first term arises because for any parcel of fluid there will always be a perpendicular force acting on the surface of the parcel. The second term is the deformation tensor and describes how the parcel deforms when subjected to stresses. The first term determines the change of volume and the second term determines the change of shape. The viscous stress tensor, σ, for the Newtonian fluid can be expressed as the sum of the trace of the viscous stress tensor and everything that isn't the trace of the viscous stress tensor. The trace of the first term on the right side is simply three times the value λ and the trace on the second term is simply the divergence of the velocity field, which is straight forward to show in indicial notation:

$$\begin{aligned}
\mu(\nabla\mathbf{u} + (\nabla\mathbf{u})^\top) &= \mu\left(\frac{\partial u_i}{\partial x_j} + \frac{\partial u_j}{\partial x_i}\right) \\
\operatorname{tr}(\mu(\nabla\mathbf{u} + (\nabla\mathbf{u})^\top)) &= \mu\sum_{i=j=1}^{3}\left(\frac{\partial u_i}{\partial x_j} + \frac{\partial u_j}{\partial x_i}\right) \\
&= 2\mu\left(\frac{\partial u_1}{\partial x_1} + \frac{\partial u_2}{\partial x_2} + \frac{\partial u_3}{\partial x_3}\right) \\
&= 2\mu\nabla\cdot\mathbf{u}
\end{aligned}$$

so the trace of σ is simply

$$\operatorname{tr}(\sigma) = (3\lambda + 2\mu)(\nabla\cdot\mathbf{u}).$$

Now the viscous stress tensor for a Newtonian fluid can be expressed simply as the sum of the trace with everything else.

$$\begin{aligned}
\sigma &= \operatorname{tr}(\sigma) + (\sigma - \operatorname{tr}(\sigma)) \\
&= \left(\lambda + \frac{2}{3}\mu\right)\nabla\cdot\mathbf{u}\mathbb{I} + \mu\left(\nabla\mathbf{u} + (\nabla\mathbf{u})^\top - \frac{2}{3}(\nabla\cdot\mathbf{u})\mathbb{I}\right) \\
&= \zeta\nabla\cdot\mathbf{u}\mathbb{I} + \mu\left(\nabla\mathbf{u} + (\nabla\mathbf{u})^\top - \frac{2}{3}(\nabla\cdot\mathbf{u})\mathbb{I}\right)
\end{aligned} \tag{1.5}$$

$\zeta = (\lambda + \frac{2}{3}\mu)$ and is referred to as the second viscosity, bulk viscosity, or volume viscosity and is significant when the volume changes significantly. Often this can

be set to equal zero, which is called Stokes assumption. The last term in the parenthesis can be checked to be valid by recognizing that the term in the parenthesis must vanish if you sum over all indices when $i = j$ (the diagonal). In doing so the viscous stress tensor vanishes when a fluid is at rest.

1.4 Small, Irrotational, and Isentropic Sound Waves

In the limit of smaller and longer waves the viscosity becomes negligible and the physics described by the Navier-Stokes equations approximate the Euler equations. Moreover, these waves behave like isentropic waves (constant entropy). The Euler equations with constant entropy are

$$\frac{\partial \rho}{\partial t} + \nabla \cdot (\rho \mathbf{u}) = 0 \tag{1.6}$$

$$\frac{\partial (\rho \mathbf{u})}{\partial t} + \nabla \cdot (\rho \mathbf{u} \otimes \mathbf{u}) + \nabla p = 0 \tag{1.7}$$

$$p = p_0 \rho^\gamma.$$

(1.7) can be recast by using the product rules, (16) and (17), and inserting the $\mathbf{u} \cdot \partial_t \rho$ from (1.7) resulting in:

$$\rho \frac{\partial}{\partial t} \mathbf{u} + \rho \mathbf{u} \nabla \cdot \mathbf{u} + \nabla p = 0.$$

Now we decompose the density and pressure, ρ, p, into the background pressure and density, ρ_0, p_0, and the density and pressure fluctuation, ρ', p', and assume that the fluctuations and their derivatives are small. These assumptions allow us to linearize (1.6) and (1.7) as follows:

$$\frac{\partial \rho'}{\partial t} + \rho_0 \nabla \cdot \mathbf{u} = 0$$

$$\frac{\partial \mathbf{u}}{\partial t} + \frac{1}{\rho_0} \nabla p' = 0$$

$$p = p_0 \rho^\gamma$$

expressing velocity in terms of the velocity potential, $\nabla \phi = \mathbf{u}$, and assuming we can change order of derivation, (1.6) becomes:

$$\frac{\partial \rho'}{\partial t} + \rho_0 \nabla^2 \phi = 0 \tag{1.8}$$

and (1.7) becomes:

$$\begin{aligned} \nabla\frac{\partial\phi}{\partial t} + \frac{1}{\rho_0}\nabla p' &= 0 \\ \frac{\partial\phi}{\partial t} + \frac{1}{\rho_0}p' &= C. \end{aligned} \tag{1.9}$$

We can set $C = 0$ and use the the thermodynamic relation

$$p' = \left(\frac{\partial p}{\partial \rho_0}\right)_s \rho',$$

such that (1.9) becomes

$$\frac{\partial\rho'}{\partial t} = -\frac{\rho_0}{\left(\frac{\partial p}{\partial\rho_0}\right)_s}\frac{\partial^2\phi}{\partial t^2}. \tag{1.10}$$

Inserting (1.10) into the (1.8) we end up with:

$$-\frac{\partial^2\phi}{\partial t^2} + c^2\nabla\cdot\nabla\phi = 0 \tag{1.11}$$

where $c^2 = \partial p/\partial\rho$ is the speed of sound squared. (1.11) is the wave equation and has the solution $\phi = f(\mathbf{x} - ct)$. We will now calculate u and p'.

$$\begin{aligned} \mathbf{u} &= \nabla\phi = \dot{f}(\mathbf{x} - ct) \\ p' &= -\rho_0\frac{\partial\phi}{\partial t} = \rho_0 c\dot{f}(\mathbf{x} - ct) \\ u &= \frac{p'}{\rho_0 c} \\ u &= \frac{c\rho'}{\rho_0} \end{aligned} \tag{1.12}$$

where we've used the fact that $p' = c^2\rho'$ to get to the last equation. Rearranging (1.12) we obtain

$$\frac{\partial\rho}{\partial x} = \frac{\rho_0}{c}\frac{\partial u}{\partial x} \tag{1.13}$$

which will be of relevance when computing the NSS absorption coefficient.

Chapter 2

Mathematical Entropy

Mathematical entropy theory is a theory developed to find scalar functions from conservation laws that satisfy various entropy properties from physics. In addition to deriving the classic entropy equations from physics, the mathematical procedure allows one to find other entropy solutions which is helpful when, for example, proving uniqueness. One of the important reasons for finding entropy solutions is the ability to generate an entropy *inequality* satisfying the second law of thermodynamics. This condition is necessary (but not sufficient) for proving well-posedness of a PDE or a system of PDE's. In this chapter we will give an outline of the basic theory behind mathematical entropy and then find the entropy equation for the Euler, Navier-Stokes, and Navier-Stokes-Svärd equations. For an introduction to mathematical entropy theory, we recommend [5]. For a more in depth writing about entropy and their use in developing numerical schemes, we recommend [25]. The content of this chapter is based on the paper [25].

2.1 Mathematical Entropy Function

Given a system of conservation laws of $\boldsymbol{\Upsilon} : \mathbb{R}^d \to \mathbb{R}^d$ and $\mathbf{f} : \boldsymbol{\Upsilon} \to \mathbb{R}^d$ where $d \in \mathbb{N}$:

$$\frac{\partial}{\partial t}\boldsymbol{\Upsilon} + \sum_{n=1}^{N} \frac{\partial}{\partial x_n}\mathbf{f}(\boldsymbol{\Upsilon}) = 0, \tag{2.1}$$

we can apply the chain rule and obtain

$$\frac{\partial}{\partial t}\boldsymbol{\Upsilon} + \nabla_{\boldsymbol{\Upsilon}}\mathbf{f} \cdot \sum_{n=1}^{N} \frac{\partial}{\partial x_n}\boldsymbol{\Upsilon} = 0. \tag{2.2}$$

We can define its corresponding entropy equation to be a scalar function with the vector $\boldsymbol{\Upsilon}$ as its input as done in [5]

$$\frac{\partial}{\partial t}\phi(\boldsymbol{\Upsilon}) + \sum_{n=1}^{N} \frac{\partial}{\partial x_n}\psi(\boldsymbol{\Upsilon}) = 0.$$

By applying the chain rule, we see that parts of (2.2) appear in the entropy equation

$$\nabla_{\boldsymbol{\Upsilon}}\phi \cdot \frac{\partial}{\partial t}\boldsymbol{\Upsilon} + \nabla_{\boldsymbol{\Upsilon}}\psi \cdot \sum_{n=1}^{N} \frac{\partial}{\partial x_n}\boldsymbol{\Upsilon} = 0, \tag{2.3}$$

where $\nabla_{\boldsymbol{\Upsilon}}$ refers to the gradient with respect to the entries in $\boldsymbol{\Upsilon}$ (dependent variables) in contrast to ∇ which is the gradient with respect to the independent variables, $\mathbf{x}$. If the two following criteria are fulfilled we can be sure that a solution to (2.3) exists if a solution to (2.2) exists.

1. $\nabla_{\boldsymbol{\Upsilon}}\psi = \nabla_{\boldsymbol{\Upsilon}}\phi \cdot \nabla_{\boldsymbol{\Upsilon}}\mathbf{f}(\boldsymbol{\Upsilon})$.

2. $\phi(\boldsymbol{\Upsilon})$ is a convex entropy function of $\boldsymbol{\Upsilon}$ such that

$$\nabla\nabla_{\boldsymbol{\Upsilon}}\phi : \nabla\mathbf{g} > 0$$

where $\mathbf{g}$ is a vector modelling the diffusion. (For a thorough introduction to mathematical entropy functions see the article [25] and the citations therein). The first criteria allows us to show that $\boldsymbol{\Upsilon}$ will satisfy (2.3) by substituting (2.2) into (2.3).

$$\begin{aligned}
\nabla_{\boldsymbol{\Upsilon}}\phi \cdot \frac{\partial}{\partial t}\boldsymbol{\Upsilon} + \nabla_{\boldsymbol{\Upsilon}}\psi \cdot \sum_{n=1}^{N} \frac{\partial}{\partial x_n}\boldsymbol{\Upsilon} &= 0 \\
\nabla_{\boldsymbol{\Upsilon}}\phi \cdot \frac{\partial}{\partial t}\boldsymbol{\Upsilon} + \nabla_{\boldsymbol{\Upsilon}}\phi \cdot \nabla_{\boldsymbol{\Upsilon}}\mathbf{f} \cdot \sum_{n=1}^{N} \frac{\partial}{\partial x_n}\boldsymbol{\Upsilon} &= 0 \\
\nabla_{\boldsymbol{\Upsilon}}\phi \cdot \left(-\nabla_{\boldsymbol{\Upsilon}}\mathbf{f} \cdot \sum_{n=1}^{N} \frac{\partial}{\partial x_n}\Upsilon \right) + \nabla_{\boldsymbol{\Upsilon}}\phi \cdot \nabla_{\boldsymbol{\Upsilon}}\mathbf{f} \cdot \sum_{n=1}^{N} \frac{\partial}{\partial x_n}\boldsymbol{\Upsilon} &= 0.
\end{aligned}$$

This shows that there is no diffusion of entropy. The gain (or loss) of entropy in one part of the fluid is due to loss (or gain) of entropy in another part of the fluid, just as with the other conserved quantities (density, momentum and energy). Additionally, this shows us that the mathematical entropy function $\phi(\boldsymbol{\Upsilon})$ can be found by simply contracting the system of conservation laws with

$\nabla_{\boldsymbol{\Upsilon}}\phi$ as long as the first criteria is fulfilled.

(2.2) as it stands now will not guarantee a unique solution (in the strong sense) as shocks etc. may appear (as is typical with nonlinear hyperbolic PDE's). To circumvent this, we now assume that the conservation laws include friction which is modelled by dissipative, double spatial derivative (Laplacian) of $\mathbf{g}(\boldsymbol{\Upsilon})$,

$$\frac{\partial}{\partial t}\boldsymbol{\Upsilon} + \sum_{n=1}^{N}\frac{\partial}{\partial x_n}\mathbf{f}(\boldsymbol{\Upsilon}) = \epsilon\nabla\cdot(\nabla\mathbf{g}(\boldsymbol{\Upsilon})). \tag{2.4}$$

The physically relevant solution to (2.2) is obtained by taking the limit as $\epsilon \to 0$ in (2.4). Since the second law of thermodynamics must hold we assume that the entropy can never increase. We will now show via integration by parts that the entropy will always be decreasing *if* the second criteria is fulfilled. We begin by contracting (2.4) with $\nabla_{\boldsymbol{\Upsilon}}\phi$

$$\begin{aligned}\nabla_{\boldsymbol{\Upsilon}}\phi\cdot\frac{\partial}{\partial t}\boldsymbol{\Upsilon} + \nabla_{\boldsymbol{\Upsilon}}\phi\cdot\sum_{n=1}^{N}\frac{\partial}{\partial x_n}\mathbf{f}(\boldsymbol{\Upsilon}) &= \nabla_{\boldsymbol{\Upsilon}}\phi\cdot\epsilon\nabla\cdot(\nabla\mathbf{g}(\boldsymbol{\Upsilon}))\\ &= \epsilon\nabla\cdot(\nabla_{\boldsymbol{\Upsilon}}\phi\cdot\nabla\mathbf{g}(\boldsymbol{\Upsilon})) - \epsilon\nabla\nabla_{\boldsymbol{\Upsilon}}\phi : \nabla\mathbf{g}(\boldsymbol{\Upsilon})\\ &\leq \epsilon\nabla\cdot(\nabla_{\boldsymbol{\Upsilon}}\phi\cdot\nabla\mathbf{g}(\boldsymbol{\Upsilon}))\end{aligned} \tag{2.5}$$

where the second criteria ensures that all the terms in $\epsilon\nabla\nabla_{\boldsymbol{\Upsilon}}\phi : \nabla\mathbf{g}(\boldsymbol{\Upsilon}) \geq 0$, enabling us to obtain the inequality which is referred to as the *entropy inequality* and is equivalent to the second law of thermodynamics. By taking the limit as $\epsilon \to 0$ of (2.5) we get:

$$\nabla_{\boldsymbol{\Upsilon}}\phi\cdot\frac{\partial}{\partial t}\boldsymbol{\Upsilon} + \nabla_{\boldsymbol{\Upsilon}}\phi\cdot\sum_{n=1}^{N}\frac{\partial}{\partial x_n}\mathbf{f}(\boldsymbol{\Upsilon}) \leq 0.$$

For our case, (2.1) is the Euler system of equations and (2.4) is the NS and NSS system of equations. In the next sections we will derive the entropy equation for the Euler, NS, and NSS system of equations.

2.2 Mathematical Entropy Function for Euler Equations

Given the Euler equations,

$$\frac{\partial}{\partial t}\rho + \nabla \cdot (\rho \mathbf{u}) = 0 \tag{2.6}$$

$$\frac{\partial}{\partial t}(\rho \mathbf{u}) + \nabla \cdot (\rho \mathbf{u} \otimes \mathbf{u}) - \nabla p = 0 \tag{2.7}$$

$$\frac{\partial}{\partial t}E + \nabla \cdot ((E+p)\mathbf{u}) = 0, \tag{2.8}$$

we can find an entropy function. Since the Euler equations model adiabatic (no transfer of heat or matter) flow we can deduce the behavior of entropy for inviscid, adiabatic flows from the fundamental thermodynamic relation. The fundamental thermodynamic relation is

$$\rho dS = \frac{\rho}{T} de - \frac{p}{\rho T} d\rho \tag{2.9}$$

and recasting this will gives us a mathematical entropy function that coincides with the physical entropy function. To recast (2.9) we begin by using the Euler energy conservation equation (2.8). By using the relations for energy (2) and internal energy (3) as well as the product rule, (16), we can recast the 2.8) as

$$\begin{aligned} \frac{\partial}{\partial t}E + \nabla \cdot (E\mathbf{u} + p\mathbf{u}) &= 0 \\ \frac{\partial}{\partial t}\left(\rho e + \rho \frac{|\mathbf{u}|^2}{2}\right) + \nabla \cdot \left(\rho e \mathbf{u} + \rho \frac{|\mathbf{u}|^2}{2}\mathbf{u}\right) + \nabla \cdot (p\mathbf{u}) &= 0 \\ \frac{\partial \rho}{\partial t}e + \rho \frac{\partial e}{\partial t} + \frac{\partial \rho}{\partial t}\frac{|\mathbf{u}|^2}{2} + \rho \frac{\partial}{\partial t}\left(\frac{|\mathbf{u}|^2}{2}\right) + e\nabla \cdot (\rho \mathbf{u}) + \rho \mathbf{u} \cdot \nabla e & \\ + \rho \mathbf{u} \cdot \nabla \left(\frac{|\mathbf{u}|^2}{2}\right) + \frac{|\mathbf{u}|^2}{2}\nabla \cdot (\rho \mathbf{u}) + \nabla \cdot (p\mathbf{u}) &= 0. \end{aligned} \tag{2.10}$$

If we now insert the conservation of mass equation (2.6) into (2.10) we see that $\partial_t(\rho)e = -e\nabla \cdot (\rho \mathbf{u})$ and $\partial_t(\rho)|\mathbf{u}|^2/2 = -|\mathbf{u}|^2/2\nabla \cdot (\rho \mathbf{u})$. (2.10) is thus simplified to:

$$\rho \frac{\partial e}{\partial t} + \rho \mathbf{u} \nabla e + \rho \frac{\partial}{\partial t}\left(\frac{|\mathbf{u}|^2}{2}\right) + \rho \mathbf{u} \cdot \nabla \frac{|\mathbf{u}|^2}{2} + \nabla \cdot (p\mathbf{u}) = 0. \tag{2.11}$$

The three right most terms are similar to the terms in the conservation of momentum equations (2.7). If we dot (2.7) by $\mathbf{u}$ and once again use the mass

conservation equation (2.6) we get:

$$\begin{aligned}
\mathbf{u}\cdot\frac{\partial}{\partial t}(\rho\mathbf{u})+\mathbf{u}\cdot\nabla\cdot(\rho\mathbf{u}\otimes\mathbf{u})+(\nabla p)\cdot\mathbf{u}&=0\\
\rho\mathbf{u}\cdot\frac{\partial\mathbf{u}}{\partial t}+\cancel{|\mathbf{u}|^2\frac{\partial\rho}{\partial t}}+\cancel{|\mathbf{u}|^2\nabla\cdot(\rho\mathbf{u})}+\rho\mathbf{u}\cdot\nabla\left(\frac{|\mathbf{u}|^2}{2}\right)+(\nabla p)\cdot\mathbf{u}&=0\\
\rho\frac{\partial}{\partial t}\left(\frac{|\mathbf{u}|^2}{2}\right)+\rho\mathbf{u}\cdot\nabla\left(\frac{|\mathbf{u}|^2}{2}\right)+(\nabla p)\cdot\mathbf{u}&=0 \qquad (2.12)
\end{aligned}$$

This is referred to as the *mechanical energy* and inserting (2.12) into (2.11) we are left with

$$\rho\frac{\partial e}{\partial t}+\rho\mathbf{u}\cdot\nabla e=-p\nabla\cdot\mathbf{u} \qquad (2.13)$$

which is referred to as the *internal energy*. Note that the left hand side of (2.13) is the *material derivative*, (12), of the internal energy, e. Since the material derivative is a linear operator it can be used as the differential in the fundamental thermodynamic relation (2.9) as follows

$$\begin{aligned}
\rho dS&=\frac{\rho}{T}de-\frac{p}{\rho T}d\rho\\
\rho\left(\frac{\partial S}{\partial t}+\mathbf{u}\cdot\nabla S\right)&=\frac{\rho}{T}\left(\frac{\partial e}{\partial t}+\mathbf{u}\cdot\nabla e\right)-\frac{p}{\rho T}\left(\frac{\partial\rho}{\partial t}+\mathbf{u}\cdot\nabla\rho\right). \qquad (2.14)
\end{aligned}$$

Now using (2.13) in the first term on the right hand side of (2.14) and

$$\frac{1}{\rho}\frac{\partial\rho}{\partial t}=-\frac{1}{\rho}\nabla\cdot(\rho\mathbf{u})=-\frac{\mathbf{u}}{\rho}\cdot\nabla(\rho)-\nabla\cdot\mathbf{u}$$

(obtained simply by multiplying the conservation of mass equation (2.6) by $1/\rho$) on the last term on the right hand side of (2.14) we obtain the entropy equation

$$\begin{aligned}
\rho\left(\frac{\partial S}{\partial t}+\mathbf{u}\cdot\nabla S\right)&=-\frac{p}{T}\nabla\cdot\mathbf{u}-\frac{p}{T}\left(-\frac{\mathbf{u}}{\rho}\cdot\nabla\rho-\nabla\cdot\mathbf{u}+\frac{\mathbf{u}}{\rho}\cdot\nabla\rho\right)\\
\rho\frac{\partial S}{\partial t}+\rho\mathbf{u}\cdot\nabla S&=0. \qquad (2.15)
\end{aligned}$$

Since (2.15) is simply the material derivative for the entropy, S, multiplied by the density, ρ, it is constant along streamlines. Intuitively, this is because a material volume is made up by connecting the particles to each other such that they encompass a parcel of fluid, so whatever way the boundary particles move they must, by definition, follow the streamlines. (2.15) also holds for a function with S as its variable as noted by Harten in [9]

$$\rho\frac{\partial h(S)}{\partial t}+\rho\mathbf{u}\cdot\nabla h(S)=\rho\frac{\partial h}{\partial S}\frac{DS}{Dt}. \qquad (2.16)$$

where D/Dt is there material derivative (12). Now, by multiplying the conservation of mass equation (2.6) with $-h(S)$ and subtract from it (2.16) we obtain

$$\begin{aligned} -h(S)\frac{\partial \rho}{\partial t} - h(S)\nabla \cdot (\rho \mathbf{u}) - \rho \frac{\partial h(S)}{\partial t} + \rho \mathbf{u} \cdot \nabla h(S) = 0 \\ \frac{\partial}{\partial t}(-\rho h(S)) + \nabla \cdot (-\rho \mathbf{u} h(S)) = 0. \end{aligned} \tag{2.17}$$

The mathematical entropy for the Euler equations is thus

$$\phi(\boldsymbol{\Upsilon}) = -\rho h(S) \tag{2.18}$$

and

$$\sum_{n=1}^{N} \frac{\partial}{\partial x_n} \psi(\boldsymbol{\Upsilon}) = \nabla \cdot (-\rho \mathbf{u} h(S)). \tag{2.19}$$

To find $\nabla_{\boldsymbol{\Upsilon}} \phi$ we simply differentiate with respect to the entries in the vector $\boldsymbol{\Upsilon}$ (which is the vector $[\rho, \mathbf{m}^\top, E]^\top$) and use (1.3) as our entropy S. Since the entries in $\boldsymbol{\Upsilon}$ are the entities ρ, $\mathbf{m}$, and E, we express S in terms of those entities.

$$\begin{aligned} S &= c_V \ln\left(\frac{p}{\rho^\gamma}\right), \qquad p = (\gamma - 1)\left(E - \frac{|\mathbf{m}|^2}{2\rho}\right) \\ &= c_V \ln\left(\frac{(\gamma - 1)\left(E - \frac{|\mathbf{m}|^2}{2\rho}\right)}{\rho^\gamma}\right). \end{aligned}$$

The following calculations will become easier if we express the entropy as

$$S = c_V \left[\ln(\gamma - 1) + \ln\left(E - \frac{|\mathbf{m}|^2}{2\rho}\right) - \gamma \ln(\rho)\right].$$

We now find the various values of the gradient of (2.18), $\nabla_{\boldsymbol{\Upsilon}}\phi$.

$$\begin{aligned}
\frac{\partial\phi}{\partial\rho} &= -h(S) - \rho\frac{\partial h}{\partial S}\frac{\partial S}{\partial\rho} \\
&= -h(S) - \rho\frac{\partial h}{\partial S}c_V\left(\frac{1}{E-\frac{m^2}{2\rho}}\frac{|\mathbf{m}|^2}{2\rho^2} - \frac{\gamma}{\rho}\right) \\
\frac{\partial\phi}{\partial\mathbf{m}} &= -\rho\frac{\partial h}{\partial S}\frac{\partial S}{\partial\mathbf{m}} \\
&= -\rho\frac{\partial h}{\partial S}c_V\left(\frac{1}{E-\frac{|\mathbf{m}|^2}{2\rho}}\left(-\frac{\mathbf{m}}{\rho}\right)\right) \\
\frac{\partial\phi}{\partial E} &= -\rho\frac{\partial h}{\partial S}\frac{\partial S}{\partial E} \\
&= -\rho\frac{\partial h}{\partial S}c_V\left(\frac{1}{E-\frac{|\mathbf{m}|^2}{2\rho}}\right)
\end{aligned}$$

Now using the fact that

$$\frac{1}{E-\frac{|\mathbf{m}|^2}{2\rho}} = \frac{\gamma-1}{p}$$

we can express our entropy vector, $\nabla_{\boldsymbol{\Upsilon}}\phi$, as

$$\nabla_{\boldsymbol{\Upsilon}}\phi = -c_V\frac{\gamma-1}{p}\frac{\partial h}{\partial S}\begin{bmatrix}\frac{|\mathbf{m}|^2}{2\rho}+\frac{p}{\gamma-1}\left(\frac{h}{c_V\frac{\partial h}{\partial S}}-\gamma\right)\\ -m\\ \rho\end{bmatrix}.$$

Using the following equation for internal energy,

$$\frac{p}{\gamma-1} = \rho c_V T \Leftrightarrow -c_V\frac{\gamma-1}{p} = -\frac{1}{\rho T}$$

we can recast the entropy vector as

$$\begin{aligned}
\nabla_{\boldsymbol{\Upsilon}}\phi &= -\frac{1}{\rho T}\frac{\partial h}{\partial S}\begin{bmatrix}\frac{|\mathbf{m}|^2}{2\rho}+\rho c_V T\left(\frac{h}{c_V\frac{\partial h}{\partial S}}-\gamma\right)\\ -m\\ \rho\end{bmatrix} \\
&= -\frac{1}{T}\frac{\partial h}{\partial S}\begin{bmatrix}\frac{|\mathbf{u}|^2}{2}+c_V T\left(\frac{h}{c_V\frac{\partial h}{\partial S}}-\gamma\right)\\ -\mathbf{u}\\ 1\end{bmatrix}.
\end{aligned}$$

For the Navier-Stokes system the only entropy is $h(S) = S$, [11], and in that case the entropy vector simplifies to

$$\nabla_{\boldsymbol{\Upsilon}}\phi = -\frac{1}{T}\begin{bmatrix} \frac{|\mathbf{u}|^2}{2} + c_V T\left(\frac{S}{c_V} - \gamma\right) \\ -\mathbf{u} \\ 1 \end{bmatrix}. \tag{2.20}$$

In [9] Harten proves that the entropy function must satisfy the inequality

$$\frac{\ddot{h}(S)}{\dot{h}(S)} < \frac{1}{\gamma}$$

to guarantee that (1.3), $\phi(\boldsymbol{\Upsilon})$, is convex, and in the case for physical entropy where $h(S) = S$ this inequality is automatically satisfied. To double check our work we can contract the Euler equations with (2.20) and see if we obtain (2.17), which is the subject of the next section.

2.3 Euler Entropy Equation

The Euler equations take the form

$$\frac{\partial}{\partial t}\boldsymbol{\Upsilon} + \nabla \odot \mathbf{f}(\boldsymbol{\Upsilon}) = 0.$$

where we have used definition 0.2.6. Contracting with the entropy vector, (2.20), we obtain

$$\nabla_{\boldsymbol{\Upsilon}}\phi \cdot \frac{\partial}{\partial t}\boldsymbol{\Upsilon} + \nabla_{\boldsymbol{\Upsilon}}\phi \cdot \nabla \odot \mathbf{f}(\boldsymbol{\Upsilon}) = 0 \tag{2.21}$$

Calculating this is relatively straight forward and the two dimensional case is done in [9] and we use the approach used in [24]. Here we present the three dimensional case. We begin by calculating the two terms on the left hand side of (2.21). We need $\nabla_{\boldsymbol{\Upsilon}}\phi$, $\partial_t \mathbf{u}$, and $\nabla \odot \mathbf{f}(\boldsymbol{\Upsilon})$ and we will calculate them in that order. We've already calculated $\nabla_{\boldsymbol{\Upsilon}}\phi$ above (equation (2.20)). $\partial_t[\rho, \rho\mathbf{u}, E]^\top$ is

$$\frac{\partial}{\partial t}\begin{bmatrix} \rho \\ \rho\mathbf{u} \\ \rho c_V T + \rho\frac{|\mathbf{u}|^2}{2} \end{bmatrix} = \begin{bmatrix} \partial_t\rho \\ \partial_t\rho\mathbf{u} + \rho\partial_t\mathbf{u} \\ \partial_t\rho c_V T + \rho c_V \partial_t T + \partial_t\rho\frac{|\mathbf{u}|^2}{2} + \rho\partial_t\frac{|\mathbf{u}|^2}{2} \end{bmatrix}$$

and $\nabla \odot \mathbf{f}(\boldsymbol{\Upsilon})$ is

$$\nabla\odot\mathbf{f}(\boldsymbol{\Upsilon}) = \begin{Bmatrix} \nabla\cdot(\rho\mathbf{u}) \\ \nabla\cdot(\rho\mathbf{u}\otimes\mathbf{u}) + \nabla p \\ \nabla\cdot\left(\rho\frac{|\mathbf{u}|^2}{2}\mathbf{u}\right) + \nabla\rho\cdot c_V T\mathbf{u} + \rho c_V\nabla T\cdot\mathbf{u} + \rho c_V T\nabla\cdot\mathbf{u} + \nabla p\cdot\mathbf{u} + p\nabla\cdot\mathbf{u} \end{Bmatrix}.$$

To calculate the entropy equation we need help from the entropy function, $S = c_V \ln(p/\rho^\gamma)$ and two vector calculus identities. Differentiating S we get

$$\begin{aligned}
\dot{S} &= \dot{\ln}\left(\frac{p}{\rho^\gamma}\right) \\
&= \frac{\dot{p}}{p} - \gamma\frac{\dot{\rho}}{\rho}, \qquad p = \rho RT \Rightarrow \dot{p} = \dot{\rho}RT + \rho R\dot{T} \\
&= \frac{\dot{T}}{T} - (\gamma-1)\frac{\dot{\rho}}{\rho} \\
\gamma\dot{\rho} &= \frac{\dot{T}}{T}\rho + \dot{\rho} - \rho\dot{S}
\end{aligned}$$

where the dot above the function represents differentiation with respect to independent variables (in this case meaning either x or t). Two helpful vector calculus identities are

$$\mathbf{u}\cdot\nabla\cdot(\rho\mathbf{u}\otimes\mathbf{u}) = \nabla\cdot(\rho|\mathbf{u}|^2\mathbf{u}) - \rho\mathbf{u}\otimes\mathbf{u} : \nabla\mathbf{u} \tag{2.22}$$

and

$$\frac{|\mathbf{u}|^2}{2}\nabla\cdot(\rho\mathbf{u}) = \nabla\cdot(\rho|\mathbf{u}|^2\mathbf{u}) - \rho\mathbf{u}\cdot\nabla\left(\frac{|\mathbf{u}|^2}{2}\right). \tag{2.23}$$

Note that

$$\rho\mathbf{u}\otimes\mathbf{u} : \nabla\mathbf{u} = \rho\mathbf{u}\cdot\nabla\left(\frac{|\mathbf{u}|^2}{2}\right). \tag{2.24}$$

Now it is straight forward to calculate the terms on the left hand side of (2.21). Beginning with the first term we get

$$\begin{aligned}
\nabla_{\boldsymbol{\Upsilon}}\phi\cdot\frac{\partial}{\partial t}\begin{bmatrix}\rho\\ \rho\mathbf{u}\\ E\end{bmatrix} &= -\frac{1}{T}\begin{bmatrix}\frac{|\mathbf{u}|^2}{2} + c_V T\left(\frac{S}{c_V}-\gamma\right)\\ -\mathbf{u}\\ 1\end{bmatrix}\cdot\begin{bmatrix}\partial_t\rho\\ \partial_t\rho\mathbf{u}+\rho\partial_t\mathbf{u}\\ \partial_t\rho\frac{|\mathbf{u}|^2}{2}+\rho\partial_t\frac{|\mathbf{u}|^2}{2}+\partial_t\rho c_V T+\rho c_V\partial_t T\end{bmatrix} \\
&= \frac{\partial}{\partial t}(\rho S)
\end{aligned} \tag{2.25}$$

and the second term on the left hand side of (2.21) is

$$\begin{aligned}
&\nabla_{\boldsymbol{\Upsilon}}\phi\odot(\nabla\odot\mathbf{f}(\boldsymbol{\Upsilon})) = \\
&= -\frac{1}{T}\begin{bmatrix}\frac{|\mathbf{u}|^2}{2} + c_V T\left(\frac{S}{c_V}-\gamma\right)\\ -\mathbf{u}\\ 1\end{bmatrix}\odot\begin{Bmatrix}\nabla\cdot(\rho\mathbf{u})\\ \nabla\cdot(\rho\mathbf{u}\otimes\mathbf{u})+\nabla p\\ \left(\nabla\cdot\left(\rho\frac{|\mathbf{u}|^2}{2}\mathbf{u}\right)+\nabla\rho\cdot c_V T\mathbf{u}+\rho c_V\nabla T\cdot\mathbf{u}\right.\\ \left.+\rho c_V T\nabla\cdot\mathbf{u}+\nabla p\cdot\mathbf{u}+p\nabla\cdot\mathbf{u}\right)\end{Bmatrix}
\end{aligned} \tag{2.26}$$

$$= \nabla\cdot(\rho S\mathbf{u}).$$

A more detailed calculation of (2.26) is done in Appendix A. The Euler entropy equation is thus

$$\frac{\partial}{\partial t}(\rho S) + \nabla \cdot (\rho S \mathbf{u}) = 0.$$

Integrating over a fluid volume and applying the divergence theorem we obtain

$$\int_V \frac{\partial}{\partial t}(\rho S) dV + \oint_{\partial V} (\rho S \mathbf{u}) \cdot \hat{\mathbf{n}} dS = 0.$$

The subject of the next two sections will be the the calculations of the diffusive terms of entropy for the NS and NSS systems.

2.4 Navier-Stokes Entropy Diffusion

The following equations have already been calculated for the two dimensional case in [9]. The diffusive terms in the Navier-Stokes equations are

$$\nabla \odot F = \begin{Bmatrix} 0 \\ \nabla \cdot \sigma \\ \nabla \cdot (\sigma \cdot \mathbf{u}) + \nabla \cdot (\kappa \nabla T) \end{Bmatrix}$$

If we insert the Newtonian viscous stress tensor (1.5) we can equate this to

$$\nabla \odot F = \begin{Bmatrix} 0 \\ \nabla \cdot \left(\left(\zeta - \frac{2}{3}\mu \right) (\nabla \cdot \mathbf{u}) \mathbb{I} + \mu (\nabla \mathbf{u} + (\nabla \mathbf{u})^\top) \right) \\ \nabla \cdot \left(\left(\zeta - \frac{2}{3}\mu \right) (\nabla \cdot \mathbf{u}) \mathbb{I} \cdot \mathbf{u} + \mu (\nabla \mathbf{u} + (\nabla \mathbf{u})^\top) \cdot \mathbf{u} + \nabla \cdot (\kappa \nabla T) \right) \end{Bmatrix}.$$

Using the product rule integration by parts we can compactly express it as

$$\nabla_{\boldsymbol{\Upsilon}} \phi \odot (\nabla \odot F) = \nabla \cdot (\nabla_{\boldsymbol{\Upsilon}} \phi \cdot F) - \nabla \nabla_{\boldsymbol{\Upsilon}} \phi : F.$$

Integrating over a control volume and applying the divergence theorem we obtain the perhaps more familiar form

$$\int_V \nabla_{\boldsymbol{\Upsilon}} \phi \odot (\nabla \odot F) \; = \oint_{\partial V} \nabla_{\boldsymbol{\Upsilon}} \phi \cdot (F \cdot \hat{\mathbf{n}}) dS - \int_V \nabla \nabla_{\boldsymbol{\Upsilon}} \phi : F dV \tag{2.27}$$

where $\hat{\mathbf{n}}$ is a unit vector pointing perpendicularly outward from the surface of the volume of fluid. We will now ccalculate the two terms on the right hand side of (2.27). $\nabla \nabla_{\boldsymbol{\Upsilon}} \phi$ is

$$\nabla \nabla_{\boldsymbol{\Upsilon}} \phi = \begin{Bmatrix} c_V \frac{\nabla T}{T} - c_V (\gamma - 1) \frac{\nabla \rho}{\rho} + \frac{\mathbf{u} \cdot \nabla \mathbf{u}}{T} - \frac{|\mathbf{u}|^2}{2T^2} \nabla T \\ -\frac{\nabla \mathbf{u}}{T} + \frac{\mathbf{u}}{T^2} \otimes \nabla T \\ -\frac{1}{T^2} \nabla T \end{Bmatrix}. \tag{2.28}$$

Calculating $\nabla_{\boldsymbol{\Upsilon}}\phi \cdot (F \cdot \hat{\mathbf{n}})$ (the abuse of notation is explained by equation 14) gives us

$$\begin{aligned}\nabla_{\boldsymbol{\Upsilon}}\phi \cdot (F \cdot \hat{\mathbf{n}}) &= -\frac{1}{T}\begin{bmatrix} \frac{|\mathbf{u}|^2}{2} + c_V T\left(\frac{S}{c_V} - \gamma\right) \\ -\mathbf{u} \\ 1 \end{bmatrix} \cdot \left[\begin{Bmatrix} 0 \\ \sigma \\ \sigma \cdot \mathbf{u} + \kappa\nabla T \end{Bmatrix} \cdot \hat{\mathbf{n}}\right] \\ &= -\kappa\frac{\nabla T}{T} \cdot \hat{\mathbf{n}}.\end{aligned}$$

Calculating $\nabla\nabla_{\boldsymbol{\Upsilon}}\phi : F$ ((the abuse of notation is explained by 15) gives us

$$\begin{aligned}\nabla\nabla_{\boldsymbol{\Upsilon}}\phi : \nabla F &= \begin{Bmatrix} c_V\frac{\nabla T}{T} - c_V(\gamma-1)\frac{\nabla\rho}{\rho} + \frac{\mathbf{u}\cdot\nabla\mathbf{u}}{T} - \frac{|\mathbf{u}|^2}{2T^2}\nabla T \\ -\frac{\nabla\mathbf{u}}{T} + \frac{\mathbf{u}}{T^2}\otimes\nabla T \\ -\frac{1}{T^2}\nabla T \end{Bmatrix} : \begin{Bmatrix} 0 \\ \sigma \\ \sigma\cdot\mathbf{u} + \kappa\nabla T \end{Bmatrix} \\ &= \sigma : \frac{\nabla\mathbf{u}}{T} + \kappa\frac{|\nabla T|^2}{T^2}\end{aligned}$$

where we have used the fact that

$$\sigma : \frac{\mathbf{u}}{T^2} \otimes \nabla T = (\sigma \cdot \mathbf{u}) \cdot \frac{\nabla T}{T^2}.$$

If we now insert the Newtonian viscous stress tensor for σ we can express (2.29) as

$$\sigma : \frac{\nabla\mathbf{u}}{T} + \kappa\frac{|\nabla T|^2}{T^2} = \left[\left(\zeta - \frac{2}{3}\mu\right)\nabla\cdot\mathbf{u}\mathbb{I} + \mu(\nabla\mathbf{u} + (\nabla\mathbf{u})^\top)\right] : \frac{\nabla\mathbf{u}}{T} + \kappa\frac{|\nabla T|^2}{T^2} \quad (2.29)$$

Since the entropy diffusion must be non-negative for the second law of thermodynamics to hold and obtain the entropy inequality, (2.5), we must use two vector-calculus identities and some algebraic manipulation to prove that the diffusive terms in the Navier-Stokes entropy equation is non-negative. First we split the second term in (2.29) into its diagonal and not diagonal parts and distribute the $\nabla\mathbf{u}/T$ term

$$\begin{aligned}&\left(\zeta - \frac{2}{3}\mu\right)\nabla\cdot\mathbf{u}\mathbb{I} : \frac{\nabla\mathbf{u}}{T} + 2\mu\nabla\mathbf{u}\mathbb{I} : \frac{\nabla\mathbf{u}}{T} + \mu(\nabla\mathbf{u} + (\nabla\mathbf{u})^\top(1-\mathbb{I}) : \frac{\nabla\mathbf{u}}{T} + \kappa\frac{|\nabla T|^2}{T^2} \\ &\left(\zeta + \frac{4}{3}\mu\right)\nabla\cdot\mathbf{u}\mathbb{I} : \frac{\nabla\mathbf{u}}{T} + \mu(\nabla\mathbf{u} + (\nabla\mathbf{u})^\top(1-\mathbb{I}) : \frac{\nabla\mathbf{u}}{T} + \kappa\frac{|\nabla T|^2}{T^2}. \quad (2.30)\end{aligned}$$

$(1-\mathbb{I})$ is a matrix with zero in its diagonal entries and one in all the other entries. Now we use the two following vector calculus identities on the three first terms

$$\nabla\cdot\mathbf{u}\mathbb{I} : \nabla\mathbf{u} = (\nabla\cdot\mathbf{u})^2$$

and

$$\begin{aligned}(\nabla\mathbf{u}+(\nabla\mathbf{u})^\top)(1-\mathbb{I}):\nabla\mathbf{u} &= \left(\frac{1}{2}\left(\nabla\mathbf{u}+(\nabla\mathbf{u})^\top\right)+\frac{1}{2}\left(\nabla\mathbf{u}+(\nabla\mathbf{u})^\top\right)\right)(1-\mathbb{I}):\nabla\mathbf{u}\\ &= \left(\frac{1}{2}\left(\nabla\mathbf{u}+(\nabla\mathbf{u})^\top\right):\nabla\mathbf{u}+\frac{1}{2}\left(\nabla\mathbf{u}+(\nabla\mathbf{u})^\top\right):(\nabla\mathbf{u})^\top\right)(1-\mathbb{I})\\ &= \left[\frac{1}{2}\nabla\mathbf{u}:\nabla\mathbf{u}+(\nabla\mathbf{u})^\top:\nabla\mathbf{u}+\frac{1}{2}(\nabla\mathbf{u})^\top:(\nabla\mathbf{u})^\top\right](1-\mathbb{I})\\ &= \frac{1}{2}\left[\left(\nabla\mathbf{u}+(\nabla\mathbf{u})^\top\right):\left(\nabla\mathbf{u}+\left(\nabla\mathbf{u}\right)^\top\right)\right](1-\mathbb{I})\\ &= \frac{1}{2}\left(\nabla\mathbf{u}+(\nabla\mathbf{u})^\top\right)^{:2}(1-\mathbb{I})\end{aligned}$$

where we have used the fact that the double dot product, :, is a linear operator and the fact that the double dot product is transpose invariant, meaning that $A:B^\top=A^\top:B$ if either A and/or B are symmetric. In our case this means that $(\nabla\mathbf{u}+(\nabla\mathbf{u})^\top):\nabla\mathbf{u}=((\nabla\mathbf{u})^\top+\nabla\mathbf{u}):(\nabla\mathbf{u})^\top$ since $(\nabla\mathbf{u}+(\nabla\mathbf{u})^\top)$ is symmetric. We can now recast (2.30) as

$$\frac{1}{T}\left[\left(\zeta+\frac{4}{3}\mu\right)(\nabla\cdot\mathbf{u})^2+\frac{\mu}{2}(\nabla\mathbf{u}+(\nabla\mathbf{u})^\top)^{:2}(1-\mathbb{I})+\kappa\frac{|\nabla T|^2}{T}\right].$$

which shows that all the terms are non-negative, satisfying the second law of thermodynamics. The integral form of the entropy equation for the Navier-Stokes equations is

$$\begin{aligned}\int_V\frac{\partial}{\partial t}(\rho S)dV+\oint_{\partial V}(\rho S\mathbf{u})\cdot\hat{\mathbf{n}}dS = \oint_{\partial V}\kappa\nabla T\cdot\hat{\mathbf{n}}dS\\ +\frac{1}{T}\int_V\left[\left(\zeta+\frac{4}{3}\mu\right)(\nabla\cdot\mathbf{u})^2+\frac{\mu}{2}(\nabla\mathbf{u}+(\nabla\mathbf{u})^\top)^{:2}(1-\mathbb{I})\right.\\ \left.+\kappa\frac{|\nabla T|^2}{T}\right]dV\end{aligned}$$

and when assuming an infinitely big or periodic domain (which is relevant for this thesis) we can neglect the boundary integral terms, leaving us with

$$\int_V\frac{\partial(\rho S)}{\partial t}dV=\frac{1}{T}\int_V\left[\left(\zeta+\frac{4}{3}\mu\right)(\nabla\cdot\mathbf{u})^2+\frac{\mu}{2}(\nabla\mathbf{u}+(\nabla\mathbf{u})^\top)^{:2}(1-\mathbb{I})+\kappa\frac{|\nabla T|^2}{T}\right]dV. \tag{2.31}$$

where the vertical bars, $|\cdot|$, denote the Euclidean norm.

2.5 Navier-Stokes-Svärd Entropy Diffusion

Now we look at the diffusive terms on the Navier-Stokes-Svärd equations, which are

$$\nabla \odot (\nu \nabla \boldsymbol{\Upsilon}) = \nabla \odot \begin{Bmatrix} \nu \nabla \rho \\ \nu \nabla (\rho \mathbf{u}) \\ \nu \nabla E \end{Bmatrix}.$$

and by using the product rule as well as (2) and (3) we can recast it as

$$\nabla \odot \begin{Bmatrix} \nu \nabla \rho \\ \nu (\mathbf{u} \otimes \nabla \rho + \rho \nabla \mathbf{u}) \\ \nu (\nabla \rho \frac{|\mathbf{u}|^2}{2} + \rho \nabla \frac{|\mathbf{u}|^2}{2} + \nabla \rho c_V T + \rho c_V \nabla T) \end{Bmatrix}.$$

Parts of these calculations can be found in [22]. By integration by parts we can express them as

$$\int_V \nabla_{\boldsymbol{\Upsilon}} \phi \odot \nabla \odot (\nu \nabla \boldsymbol{\Upsilon}) dV = \oint_{\partial V} \nabla_{\boldsymbol{\Upsilon}} \phi \cdot (\nu \nabla \boldsymbol{\Upsilon} \cdot \hat{\mathbf{n}}) dS - \int_V \nabla \nabla_{\boldsymbol{\Upsilon}} \phi : (\nu \nabla \boldsymbol{\Upsilon}) dV.$$

The first term on the right hand side is the exact same as (2.25) except we now differentiate with respect to the spatial variables and it equates to

$$\begin{aligned} &\nabla_{\boldsymbol{\Upsilon}} \phi \cdot (\nu \nabla \boldsymbol{\Upsilon} \cdot \hat{\mathbf{n}}) = \\ &\quad = -\frac{1}{T} \begin{bmatrix} \frac{|\mathbf{u}|^2}{2} + c_V T \left(\frac{S}{c_V} - \gamma \right) \\ -\mathbf{u} \\ 1 \end{bmatrix} \cdot \left[\nu \begin{Bmatrix} \nabla \rho \\ \mathbf{u} \otimes \nabla \rho + \rho \nabla \mathbf{u} \\ \nabla \rho \frac{|\mathbf{u}|^2}{2} + \rho \nabla \frac{|\mathbf{u}|^2}{2} + \nabla \rho c_V T + \rho c_V \nabla T \end{Bmatrix} \cdot \hat{\mathbf{n}} \right] \\ &\quad = \nu \nabla (\rho S) \cdot \hat{\mathbf{n}}. \end{aligned}$$

To calculate the second term on the right hand side we use (2.28) obtained in the previous section.

$$\begin{aligned} &\nabla \nabla_{\boldsymbol{\Upsilon}} \phi : \nu \nabla (\boldsymbol{\Upsilon}) dx = \\ &\begin{Bmatrix} -\frac{1}{2T} \nabla |\mathbf{u}|^2 + \frac{|\mathbf{u}|^2}{2T^2} \nabla T - \frac{c_V}{T} \nabla T + \frac{c_V}{\rho} (\gamma - 1) \nabla \rho \\ \frac{1}{T} \nabla \mathbf{u} - \frac{\mathbf{u}}{T^2} \otimes \nabla T \\ \frac{1}{T^2} \nabla T \end{Bmatrix} : \nu \begin{Bmatrix} \nabla \rho \\ \mathbf{u} \otimes \nabla \rho + \rho \nabla \mathbf{u} \\ \nabla \rho \frac{|\mathbf{u}|^2}{2} + \rho \nabla \frac{|\mathbf{u}|^2}{2} + \nabla \rho c_V T + \rho c_V \nabla T \end{Bmatrix} \\ &= \nu \rho \frac{c_V}{\rho^2} (\gamma - 1) |\nabla \rho|^2 + \frac{\nu \rho}{T} |\nabla \mathbf{u}|^2 + \nu \rho \frac{c_V}{T^2} |\nabla T|^2. \end{aligned} \tag{2.32}$$

The steps of this calculation are shown in Appendix B. (The abuse of notation is explained by equations (14) and (15)). Here all the terms are non-negative,

satisfying the second law of thermodynamics and allowing for entropy inequality (2.5). The integral form of the Navier-Stokes-Svärd entropy equation can thus be expressed as

$$\int_V \frac{\partial}{\partial t}(\rho S)dV + \oint_{\partial V}(\rho S\mathbf{u})\cdot\hat{\mathbf{n}}dS = \oint_{\partial V}\nu\nabla(\rho S)\cdot\hat{\mathbf{n}}dS + \int_V\left[\nu\rho\frac{c_V}{\rho^2}(\gamma-1)|\nabla\rho|^2+\frac{\nu\rho}{T}|\nabla\mathbf{u}|^2+\nu\rho\frac{c_V}{T^2}|\nabla T|^2\right]dV$$

And again, assuming an infinitely big (or periodic) domain we can neglect the boundary terms leaving us with

$$\int_V \frac{\partial(\rho S)}{\partial t}dV = \int_V\left[\nu\rho\frac{c_V}{\rho^2}(\gamma-1)|\nabla\rho|^2+\frac{\nu\rho}{T}|\nabla\mathbf{u}|^2+\nu\rho\frac{c_V}{T^2}|\nabla T|^2\right]dV. \quad (2.33)$$

Chapter 3

Sound Absorption Coefficient

The following derivations are from Landau and Lifschitz [13]. In this chapter we will calculate the amount of energy dissipated due to viscosity and thermal conductivity. To do so we assume that all the energy that is dissipated, is dissipated from the mechanical energy, which is the sum of the kinetic and potential energy. The maximum amount of work occurs when the process is reversible which means that the entropy must stay constant. This leads us to the following energy relation

$$E_{mech} = E - E(S)$$

where E is the total energy, and is a constant, and $E(S)$ is the energy when the system is at thermal equilibrium but with the same amount of entropy as the total energy. Taking the time derivative of this we get

$$\frac{dE_{mech}}{dt} = -\frac{\partial E}{\partial S}\frac{dS}{dt}$$

where S is the entropy of any given volume, not just a unit volume, and is equal to $\int(\rho S)dV$. $\partial_S E$ is the temperature if the system was in a thermodynamic equilibrium,

$$T_0 = \frac{\partial E}{\partial S}$$

which allows us to express the time derivative of mechanical energy as

$$\frac{dE_{mech}}{dt} = -T_0\frac{d}{dt}\int \rho s dV \tag{3.1}$$

3.1 Coefficient of Absorption for Navier-Stokes

We will now calculate the coefficient of absorption for the Navier-Stokes equation. Using the entropy equation (2.31), (3.1) can be expressed as

$$\frac{dE_{mech}}{dt} = -T_0 \frac{1}{T} \int_V \left[\left(\zeta + \frac{4}{3}\mu \right) (\nabla \cdot \mathbf{u})^2 + \frac{\mu}{2} (\nabla \mathbf{u} + (\nabla \mathbf{u})^\top)^{:2} (1 - \mathbb{I}) + \kappa \frac{|\nabla T|^2}{T} \right] dV.$$

If we now assume that the temperature fluctuation is small we can treat it as a constant and set $T \approx T_0$ leaving us with

$$\frac{dE_{mech}}{dt} = - \int_V \left[\left(\zeta + \frac{4}{3}\mu \right) (\nabla \cdot \mathbf{u})^2 + \frac{\mu}{2} (\nabla \mathbf{u} + (\nabla \mathbf{u})^\top)^{:2} (1 - \mathbb{I}) + \kappa \frac{|\nabla T|^2}{T} \right] dV.$$

If we assume that the sound wave is a plane wave (a wave where the field variables only change in one spatial direction and are constant in the others) the PDE reduces to a one dimensional problem

$$\begin{aligned} \frac{dE_{mech}}{dt} &= - \int \left(\zeta + \frac{4}{3}\mu \right) \left(\frac{\partial u}{\partial x} \right)^2 + \frac{\kappa}{T} \left(\frac{\partial T}{\partial x} \right)^2 dV \\ &= - \left(\zeta + \frac{4}{3}\mu \right) \int \left(\frac{\partial u}{\partial x} \right)^2 dV - \frac{\kappa}{T} \int \left(\frac{\partial T}{\partial x} \right)^2 dV. \end{aligned}$$

Using (10), and then (11), we can simplify further:

$$\begin{aligned} \frac{dE_{mech}}{dt} &= - \left(\zeta + \frac{4}{3}\mu \right) \int \left(\frac{\partial u}{\partial x} \right)^2 dV - \frac{T\kappa\beta^2 c^2}{c_p^2} \int \left(\frac{\partial u}{\partial x} \right)^2 dV \\ &= - \left(\zeta + \frac{4}{3}\mu \right) \int \left(\frac{\partial u}{\partial x} \right)^2 dV - \frac{\kappa}{c_p} \left(\frac{c_p}{c_v} - 1 \right) \int \left(\frac{\partial u}{\partial x} \right)^2 dV \\ &= - \left(\frac{4}{3}\mu + \zeta + \kappa \left(\frac{1}{c_v} - \frac{1}{c_p} \right) \right) \int \left(\frac{\partial u}{\partial x} \right)^2 dV \end{aligned} \tag{3.2}$$

If we assume the velocity, u is a sinusoidal wave of the form $u_0 \cos(kx - \omega t)$ the integral term in (3.2) can be expressed as

$$\int \left(\frac{\partial u}{\partial x} \right)^2 dV = u_0^2 k^2 \int \sin^2(kx - \omega t) dV$$

and taking the time average after one period we end up with

$$u_0^2 k^2 \int \sin^2(kx - \omega t) dV = u_0^2 k^2 \frac{1}{2} V \tag{3.3}$$

where V is the volume of the fluid. Inserting (3.3) into (3.2) we get

$$\overline{\frac{dE_{mech}}{dt}} = -\left(\frac{4}{3}\mu + \zeta + \kappa\left(\frac{1}{c_v} - \frac{1}{c_p}\right)\right) u_0^2 k^2 \frac{1}{2} V.$$

which is the mean value of the energy dissipation. We can now calculate Γ in (1.2) using the fact that $\rho u_0^2 V/2$ is the total mechanical energy (1.1):

$$\begin{aligned}\Gamma_{NS} &= \frac{\frac{1}{2}k^2 u_0^2 V\left(\frac{4}{3}\mu + \zeta + \kappa\left(\frac{1}{c_v} - \frac{1}{c_p}\right)\right)}{\frac{1}{2}\rho u_0^2 V} \\ &= \frac{k^2}{\rho}\left(\frac{4}{3}\mu + \zeta + \kappa\left(\frac{1}{c_v} - \frac{1}{c_p}\right)\right). \end{aligned} \tag{3.4}$$

Using the relation

$$k = \frac{2\pi f}{c} = \frac{\omega}{c}$$

we can express (3.4) in terms of the angular frequency as well

$$\Gamma_{NS} = \frac{\omega^2}{c^2\rho}\left(\frac{4}{3}\mu + \zeta + \kappa\left(\frac{1}{c_v} - \frac{1}{c_p}\right)\right). \tag{3.5}$$

For an ideal monoatomic gas we can use the following two values $\gamma = 5/3$ and $\kappa = 5c_p\mu/2\gamma$ to calculate Γ.

$$\Gamma_{NS} = \frac{\omega^2}{c^2\rho}\frac{7}{3}\mu \tag{3.6}$$

3.2 Coefficient of Absorption for Navier-Stokes-Svärd

By the (almost) same procedure as in the previous section we can calculate the coefficient of absorption for the NSS equations. Using (2.33) we can express (3.1) as

$$\frac{dE_{mech}}{dt} = -T_0 \int_V \left[\nu\rho\frac{c_V}{\rho^2}(\gamma - 1)|\nabla\rho|^2 + \frac{\nu\rho}{T}|\nabla\mathbf{u}|^2 + \nu\rho\frac{c_V}{T^2}|\nabla T|^2\right] dV.$$

As in the precious section, we assume that the sound wave can be moddeled as a plane wave, $T \approx T_0$, and that $\nu = \mu/\rho$, simplifying the equation as follows

$$\frac{dE_{mech}}{dt} = -\int_V \left[T_0\mu\frac{c_V}{\rho^2}(\gamma - 1)\left(\frac{\partial\rho}{\partial x}\right)^2 + \mu\left(\frac{\partial u}{\partial x}\right)^2 + \mu\frac{c_V}{T}\left(\frac{\partial T}{\partial x}\right)^2\right] dV. \tag{3.7}$$

Now using (1.13) and (10), (3.7) reduces to

$$\frac{dE_{mech}}{dt} = -\mu \left[T\frac{c_V(\gamma-1)}{\rho^2}\frac{\rho_0^2}{c^2} + 1 + T\frac{c_V c^2\beta^2}{c_p^2} \right] \int_V \left(\frac{\partial u}{\partial x}\right)^2 dx$$

and by assuming that $\rho \approx \rho_0$ we can simplify further

$$\frac{dE_{mech}}{dt} = -\mu \left[T\frac{c_V(\gamma-1)}{c^2} + 1 + T\frac{c_V c^2\beta^2}{c_p^2} \right] \int_V \left(\frac{\partial u}{\partial x}\right)^2 dx.$$

Now, using (11), (3.3) and then $c_V(\gamma-1) = R$, and $1 - c_V/c_p = 1 - 1/\gamma$

$$\begin{aligned}\frac{dE_{mech}}{dt} &= -\mu \left(T\frac{c_V(\gamma-1)}{c^2} + 1 + c_V\left(\frac{1}{c_V} - \frac{1}{c_p}\right)\right)\frac{1}{2}k^2u_0^2V \\ &= -\mu\left(\frac{TR}{c^2} + 2 - \frac{1}{\gamma}\right)\frac{1}{2}k^2u_0^2V.\end{aligned}$$

The absorption coefficient, Γ in (1.2), is thus

$$\frac{\frac{1}{2}k^2u_0^2V\left(\mu\left(\frac{TR}{c^2}+2-\frac{1}{\gamma}\right)\right)}{\frac{1}{2}\rho u_0^2V} = \frac{k^2}{\rho}\left(\mu\left(\frac{TR}{c^2}+2-\frac{1}{\gamma}\right)\right)$$

and expressing this in terms on angular frequency we get

$$\Gamma_{NSS} = \frac{\omega^2}{c^2\rho}\left(\mu\left(\frac{TR}{c^2}+2-\frac{1}{\gamma}\right)\right).$$

For an ideal monoatomic gas we can again use the values $\gamma = 5/3$ and $c^2 = \gamma RT$. Γ becomes

$$\Gamma_{NSS} = 2\frac{\omega^2}{c^2\rho}\mu.$$

Comparing with (3.6) we see that Γ_{NS} is $7/6$ times greater than Γ_{NSS}, which was first pointed out in [16].

Chapter 4

Spectral Methods

The content in this chapter is mainly based on the outstanding book "Spectral Method in Matlab" by Lloyd Nicholas Trefethen [27] with supplementary insights from [10] and [6].

4.1 Finite Difference Methods via Interpolation

Given a PDE such as

$$\frac{\partial u}{\partial t} + \frac{\partial F}{\partial x} = \frac{\partial^2 G}{\partial x^2}$$

one can solve it numerically using the finite difference method

$$\frac{\partial u}{\partial t} + DF = D^2 G$$

where D and D^2 are finite difference matrices that approximate the first and second order derivative respectively and u is the vector with unknowns such that $[u]_i \approx u(x_i)$. Normally, finite-difference stencils are derived by Taylor series. Given a point $f(x_n)$ one can approximate a nearby point by using its derivative as follows

$$f(x_n{+}h) = f(x_n){+}h\frac{\partial f(x_n)}{\partial x}{+}\mathcal{O}(h^2) \qquad \text{and} \qquad f(x_n{-}h) = f(x_n){-}h\frac{\partial f(x_n)}{\partial x}{+}\mathcal{O}(h^2)$$

which can be combined to approximate the derivative as

$$\frac{\partial f(x_n)}{\partial x} = \frac{f(x_n + h) - f(x_n - h)}{2h} + \mathcal{O}(h).$$

This is referred to as the three point stencil. The $\mathcal{O}(h)$ is the truncation error, i.e., the error of the derivative approximation is proportional to h. One can obtain higher order stencils (meaning smaller truncation error) by combining

more Taylor series. One can also create a stencil that approximates higher order derivatives by combining higher order Taylor series. (For a thorough introduction to finite difference methods we recommend the book [8]).

An alternative way of computing the finite difference stencil is by first making a polynomial interpolation of the grid function and then differentiating it. We will now demonstrate that by Lagrangian interpolation we can find the coefficients of the finite difference scheme given an equispaced grid. Given three points (x_1, x_2, x_3) with corresponding values (f_1, f_2, f_3) we can interpolate the points using Lagrangian interpolation as follows

$$p(x) = f_1 \frac{(x-x_2)(x-x_3)}{(x_1-x_2)(x_1-x_3)} + f_2 \frac{(x-x_1)(x-x_3)}{(x_2-x_1)(x_2-x_3)} + f_3 \frac{(x-x_1)(x-x_2)}{(x_3-x_1)(x_3-x_2)}.$$

Upon differentiation we get

$$\frac{d}{dx}p(x) = f_1 \frac{2x-(x_3+x_2)}{(x_1-x_2)(x_1-x_3)} + f_2 \frac{2x-(x_1+x_3)}{(x_2-x_1)(x_2-x_3)} + f_3 \frac{2x-(x_1+x_2)}{(x_3-x_1)(x_3-x_2)}$$

and evaluating this at $x = x_2$ we get

$$\frac{d}{dx}p(x_2) = f_1 \frac{x_2-x_3}{(x_1-x_2)(x_1-x_3)} + f_2 \frac{2x_2-(x_1+x_3)}{(x_2-x_1)(x_2-x_3)} + f_3 \frac{x_2-x_1}{(x_3-x_1)(x_3-x_2)}$$

and using the fact that the difference between two neighboring x's is a step of size h, we can recast this expression as

$$\begin{aligned} \frac{d}{dx}p(x_2) &= f_1 \frac{-h}{(-h)(-2h)} + f_2 \frac{0}{(h)(-h)} + f_3 \frac{h}{(2h)(h)} \\ &= \frac{f_3 - f_1}{2h} \end{aligned}$$

or written in a more familiar manner

$$\frac{d}{dx}p(x_2) = \frac{f(x+h) - f(x-h)}{2h}.$$

Note that the middle term equates to zero because the x's are equispaced allowing us to express x_1 and x_3 as $(x_2 - h)$ and $(x_2 + h)$ respectively, which in turn enables us to express the numerator as $2x_2 - (x_2 - h + x_2 + h) = 0$. The accuracy of this stencil is $\mathcal{O}(h^2)$. This method of generating finite difference stencils also applies to higher order stencils. When the number of grid points used in the creation of a finite difference stencil, it approaches the spectral method. One can either calculate the stencil for larger and larger Lagrange interpolants and see what

the stencil converges to, or one can interpolate using trigonometric functions and benefit from their periodicity. The latter approach is the approach we will use in this thesis. We will first show how to interpolate functions in the semi-discrete domain (discrete in space and continuous frequency) with help from the Dirac distribution and then find the periodic interpolants and their derivatives in a fully discrete domain.

4.2 Semi-Discrete Domain

Given a set of points $\{x_n\}$, and their corresponding function values $f(x_n)$, on an evenly spaced grid, we can interpolate these points using trigonometric functions. First, we interpolate our function using the discrete delta distribution

$$\delta(x_n) = \begin{cases} 1, & x_n = 0 \\ 0, & x_n \neq 0 \end{cases} .$$

This is equivalent to "measuring" the function at discrete points to obtain a list of pairs of points corresponding to the input space and output space, $(x, f(x))$. Then take the Fourier transform of all discrete delta distributions. The Fourier transform of a single discrete delta distribution is

$$\hat{\delta} = \frac{h}{\sqrt{2\pi}} \sum_{n=1}^{N} \delta(x_n) \exp(-i\omega x_n) = \frac{h}{\sqrt{2\pi}}.$$

To get a smooth and analytical interpolate, we take the inverse Fourier transform. The inverse Fourier transform of a delta distribution is:

$$\begin{aligned} p(x) &= \frac{1}{\sqrt{2\pi}} \int_{-\frac{\pi}{h}}^{\frac{\pi}{h}} \hat{\delta} \exp(i\omega x) d\omega \\ &= \frac{h}{2\pi} \frac{1}{ix} [\exp(i\omega x)]_{-\frac{\pi}{h}}^{\frac{\pi}{h}} \\ &= \frac{h}{\pi x} \sin\left(\frac{\pi}{h} x\right) \\ &= \frac{\sin\left(\frac{\pi}{h} x\right)}{\frac{\pi}{h} x}, \qquad \frac{\pi}{h} = \frac{N}{2} \\ &= \frac{\sin\left(\frac{N}{2} x\right)}{\frac{N}{2} x}. \end{aligned}$$

This is known as the sinc function, which, like the delta distribution, is translationally invariant. That is, if you have some points $(x, f(x))$ you can

simply interpolate one point at a time without the interpolation of one point ruining the interpolation of any other point. In other words, the interpolation of one point is independent of all the other points. (This is not the case for the Lagrange interpolant). To demonstrate translational invariance, we first show that the sinc function can be expressed as as series of cosine functions and then show that those cosine functions exactly cancel each other at all points except when $x = 0$. We begin by a famous equality discovered by Euler in [4], namely

$$\frac{\sin(x)}{x} = \lim_{N\to\infty} \prod_{n=1}^{N} \cos\left(\frac{x}{2^n}\right).$$

Using the trigonometric identity

$$\cos(\theta_1)\cos(\theta_2) = \frac{1}{2}(\cos(\theta_1+\theta_2) + \cos(\theta_1-\theta_2)),$$

any product of cosines can be turned into a sum of cosines. For the product of N cosines we can express the same function as the sum of 2^{N-1} cosines as follows

$$\prod_{n=1}^{N} \cos(\theta_n) = \frac{1}{2^{N-1}} \sum_{n=1}^{2^{N-1}} \cos(P_n(\theta)),$$

where $P_n(\theta)$ is 2^{N-1} permutations of the sum of N θ's. For example, if $N = 3$, then

$$P_n(\theta) = \{\theta_1+\theta_2+\theta_3, \theta_1+\theta_2-\theta_3, \theta_1-\theta_2+\theta_3, \theta_1-\theta_2-\theta_3\}.$$

Note that θ_1 always comes with positive sign while all the others change signs. We now set $\theta_n = x/2^n$ and ignore x to simplify notation. The first term in $P_n(\theta)$ (the one with all positive values) is a geometric series

$$P_1(\theta) = \frac{1}{2} + \frac{1}{2^2} + \frac{1}{2^3} + \cdots + \frac{1}{2^{N-2}} + \frac{1}{2^{N-1}} + \frac{1}{2^N}$$

which can be solved using the following formula for a geometric series

$$\sum_{n=1}^{N} r^n = r\frac{1-r^{N+1}}{1-r}$$

and we obtain

$$P_1(\theta) = \frac{1}{2} + \frac{1}{2^2} + \frac{1}{2^3} + \cdots + \frac{1}{2^{N-2}} + \frac{1}{2^{N-1}} + \frac{1}{2^N} = 1 - \left(\frac{1}{2}\right)^N. \tag{4.1}$$

Recasting (4.1) with a common denominator of 2^N

$$P_1(\theta) = \frac{2^{N-1} + 2^{N-2} + 2^{N-3} + \cdots + 2^2 + 2 + 1}{2^N} = \frac{2^N - 1}{2^N} \tag{4.2}$$

we obtain a straightforward way of expressing all the values of $P_n(\theta)$ by using (4.2). The next term in $P_n(\theta)$, $P_2(\theta)$, will be the same, except the last term will be negative, giving us

$$P_2(\theta) = \frac{2^{N-1} + 2^{N-2} + 2^{N-3} + \cdots + 2^2 + 2 - 1}{2^N} = P_1(\theta) - \frac{2}{2^N} = \frac{2^N - 3}{2^N}$$

and $P_3(\theta)$ will be

$$P_3(\theta) = \frac{2^{N-1} + 2^{N-2} + 2^{N-3} + \cdots + 2^2 - 2 + 1}{2^N} = P_1(\theta) - \frac{4}{2^N} = \frac{2^N - 5}{2^N}$$

and so on, giving us the following values

$$\begin{aligned} P_n\left(\frac{x}{2^n}\right) &= \left\{ \left(\frac{2^N - 1}{2^N}\right) x, \left(\frac{2^N - 3}{2^N}\right) x, \left(\frac{2^N - 5}{2^N}\right) x, \cdots, \left(\frac{5}{2^N}\right) x, \left(\frac{3}{2^N}\right) x, \left(\frac{1}{2^N}\right) x \right\} \\ &= \left\{ \left(\frac{2n-1}{2^N}\right) x \right\}, \qquad n = 2^{N-1}, 2^{N-1} - 1, 2^{N-1} - 2, \cdots, 3, 2, 1. \end{aligned} \tag{4.3}$$

We can now express the sinc function both as a product of cosines and as a sum of cosines as follows

$$\frac{\sin(x)}{x} = \lim_{N\to\infty} \prod_{n=1}^{N} \cos\left(\frac{x}{2^n}\right) = \lim_{N\to\infty} \frac{1}{2^{N-1}} \sum_{n=1}^{2^{N-1}} \cos\left(\frac{2n-1}{2^N} x\right)$$

and since we will eventually use this equality in a computer using finite precision arithmetic, we use the approximation,

$$\frac{\sin(x)}{x} \approx \prod_{n=1}^{N} \cos\left(\frac{x}{2^n}\right) = \frac{1}{2^{N-1}} \sum_{n=1}^{2^{N-1}} \cos\left(\frac{2n-1}{2^N} x\right)$$

where the error can be made sufficiently small by increasing N. Consequently

$$\begin{aligned} \frac{\sin\left(\frac{2^{N-1}}{2} x\right)}{\frac{2^{N-1}}{2} x} &= \frac{1}{2^{N-1}} \sum_{n=1}^{2^{N-1}} \cos\left(\frac{2n-1}{2^N} \left(\frac{2^{N-1}}{2} x\right)\right) \\ &= \frac{1}{2^{N-1}} \sum_{n=1}^{2^{N-1}} \cos\left(\frac{2n-1}{4} x\right). \end{aligned}$$

We will now show that for an even or odd number of equidistant points, N, between 0 and 2π the following equation

$$\frac{\sin\left(\frac{N}{2}x\right)}{\frac{N}{2}x} = \frac{1}{N}\sum_{n=1}^{N}\cos\left(\frac{2n-1}{4}x\right) \tag{4.4}$$

equates to one at $x = 0$ and zero at all the other points. We begin by writing the first, middle, and last values of the series (4.4)

$$\begin{aligned}\frac{\sin\left(\frac{N}{2}x\right)}{\frac{N}{2}x} = \frac{1}{N}\Bigg[&\cos\left(\frac{1}{4}x\right) + \cos\left(\frac{3}{4}x\right) + \cos\left(\frac{5}{4}x\right) + \cdots \\ &+ \cos\left(\frac{N-1}{4}x\right) + \cos\left(\frac{N+1}{4}x\right) + \cdots \\ &+ \cos\left(\left(\frac{N}{2} - \frac{5}{4}\right)x\right) + \cos\left(\left(\frac{N}{2} - \frac{3}{4}\right)x\right) + \cos\left(\left(\frac{N}{2} - \frac{1}{4}\right)x\right)\Bigg].\end{aligned} \tag{4.5}$$

Now, using the fact that the nodes are equally spaced, we can express the discrete x values as

$$\begin{aligned}x_n &= \left\{\frac{2\pi}{N}, 2\frac{2\pi}{N}, 3\frac{2\pi}{N}, \cdots, (N-2)\frac{2\pi}{N}, (N-1)\frac{2\pi}{N}, N\frac{2\pi}{N}\right\} \\ &= n\frac{2\pi}{N}, \qquad n = \{1, \cdots, N\}\end{aligned}$$

and inserting x_n into (4.5) we obtain

$$\begin{aligned}\frac{\sin\left(\frac{N}{2}(x-x_n)\right)}{\frac{N}{2}(x-x_n)} = \frac{1}{N}\Big[&\cos\left(n\frac{\pi}{2N}\right) + \cos\left(n\frac{\pi}{2N}3\right) + \cos\left(n\frac{\pi}{2N}5\right) + \cdots \\ &+ \cos\left(n\frac{\pi}{2} - n\frac{\pi}{2N}\right) + \cos\left(n\frac{\pi}{2} + n\frac{\pi}{2N}\right) + \cdots \\ &+ \cos\left(n\pi - n\frac{\pi}{2N}5\right) + \cos\left(n\pi - n\frac{\pi}{2N}3\right) + \cos\left(n\pi - n\frac{\pi}{2N}\right)\Big].\end{aligned}$$

We now see that if n is an odd number then the last term cancels with the first term and the second to last term with the second and so on, for all values of x_n except for $x_n = 0$ in which case all the N cosines equate to 1 and we are left with $N/N = 1$. See figure (4.1) for a visual representation of the cancellation. Turning to the case when n is an even number, the first and last terms cancel with the terms in the middle. Finally, given an odd number of points the only difference is that we have one more cosine term which sits in the middle and is $\cos(n\pi/2)$ which is zero for all integer n's, as seen in figure (4.2). This gives insight into

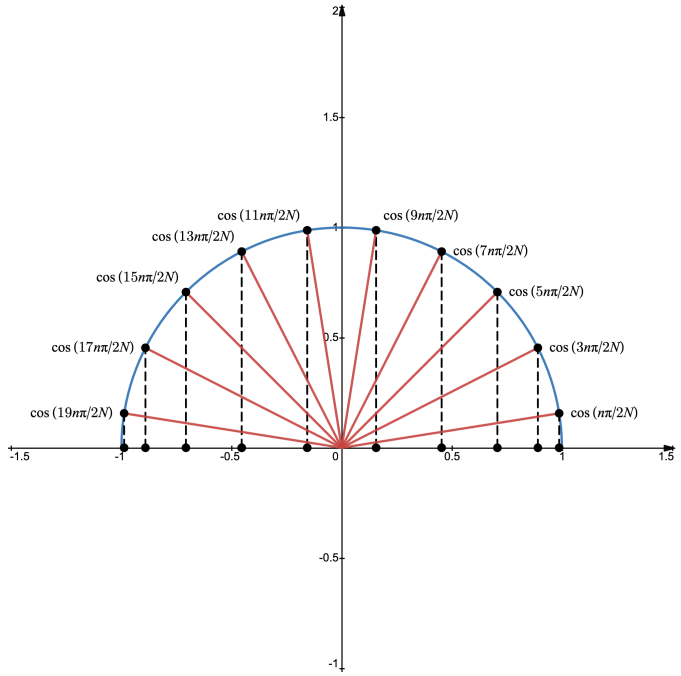

Figure 4.1: The cancelation of the sinc function on the complex unit circle where $n = 1$ and $N = 10$.

the interpolation of points using trigonometric functions. For each interpolation point, $f(x_n)$, one multiplies each point with a $\sin(x_n N/2)/(x_n N/2)$ and one will be left with whatever value is at that point and zero everywhere else.

A small detail that has been tacitly ignored is that although we have been using discrete spatial points, we have applied the *continuous* Fourier transform (i.e., we have been using infinitely many frequencies). This is obviously not possible on today's computers but the continuous math has given us a good preparation for the discrete case.

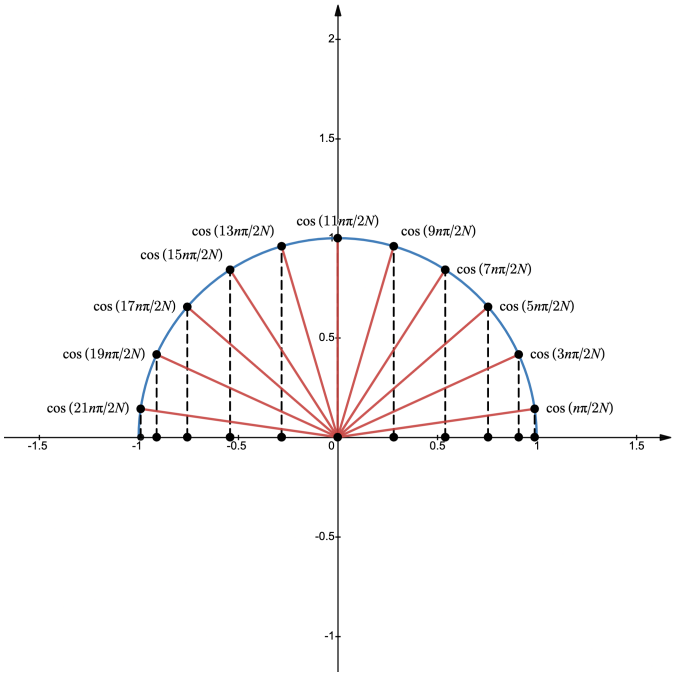

Figure 4.2: The cancelation of the sinc function on the complex unit circle where $n = 1$ and $N = 11$.

4.3 Discrete Domain

4.3.1 Odd Number of Grid Points

To analyze finitely many frequencies we use the *discrete* inverse Fourier transform. The interpolant now takes the form

$$p(x) = \frac{1}{N} \sum_{\omega=-\frac{N}{2}}^{\frac{N}{2}} \exp(i\omega x)$$

and is calculated using the formula for a geometric series, yielding

$$p(x) = \frac{1}{N} \frac{\sin\left(\frac{N}{2}x\right)}{\sin\left(\frac{x}{2}\right)}.$$

Differentiating $p(x)$ we get

$$\frac{d}{dx}p(x) = \frac{\cos\left(\frac{N}{2}x\right)}{2\sin\left(\frac{x}{2}\right)} - \frac{1}{2N}\frac{\sin\left(\frac{N}{2}x\right)}{\sin^2\left(\frac{x}{2}\right)}\cos\left(\frac{x}{2}\right)$$

and inserting $x = n \cdot 2\pi/N$ and using the relation $N/2 = \pi/h$ we get the following scheme

$$\frac{d}{dx}p(x) = \begin{cases} 0, & n = 0 \\ \frac{1}{2}(-1)^n \frac{1}{\sin\left(n\frac{h}{2}\right)}, & n \neq 0 \end{cases}.$$

In matrix form this takes the form

$$D = \begin{bmatrix} 0 & -\frac{1}{2}\csc\left(\frac{h}{2}\right) & \frac{1}{2}\csc\left(\frac{2h}{2}\right) & \cdots & \frac{1}{2}\csc\left(\frac{2h}{2}\right) & -\frac{1}{2}\csc\left(\frac{h}{2}\right) \\ -\frac{1}{2}\csc\left(\frac{h}{2}\right) & \ddots & \ddots & \ddots & \ddots & \frac{1}{2}\csc\left(\frac{2h}{2}\right) \\ \frac{1}{2}\csc\left(\frac{2h}{2}\right) & \ddots & \ddots & \ddots & \ddots & -\frac{1}{2}\csc\left(\frac{3h}{2}\right) \\ -\frac{1}{2}\csc\left(\frac{3h}{2}\right) & \ddots & \ddots & \ddots & \ddots & \vdots \\ \vdots & \ddots & \ddots & \ddots & \ddots & -\frac{1}{2}\csc\left(\frac{h}{2}\right) \\ -\frac{1}{2}\csc\left(\frac{h}{2}\right) & \frac{1}{2}\csc\left(\frac{2h}{2}\right) & -\frac{1}{2}\csc\left(\frac{3h}{2}\right) & \ldots & -\frac{1}{2}\csc\left(\frac{h}{2}\right) & 0 \end{bmatrix} \tag{4.6}$$

where D is referred to as the *differentiation matrix*. The function $p(x)$ and dp/dx can be seen in figure (4.3). The spectral difference matrix, D, is symmetric with zeros on its main diagonal. Thus, numerically differentiating the function evaluated at each grid point is equivalent to taking a convolution of the discrete function with the derivative of the interpolant. Matrix operators for n'th order derivatives can be constructed by taking the product of the first order derivative n times. Hence, the second order derivative is

$$\frac{d^2}{dx^2}p(x) = D^2 p(x). \tag{4.7}$$

4.3.2 Even Number of Grid Points

For an even number of grid points the interpolant takes the form

$$p(x) = \frac{1}{N} \sum_{\omega=-\frac{N}{2}+1}^{\frac{N}{2}} \exp(i\omega x). \tag{4.8}$$

This is slightly different compared to the case with an odd number of grid points. For an even number of grid points we obtain an odd number of *non-constant* complex exponential functions, $\exp(0)$ being the constant exponential function. Differentiating this interpolant as it stands will give the wrong result because when evaluating the highest frequency, $N/2$, there is no negative counterpart to turn it into an pure and real cosine wave. In other words, for all values of ω except for $\omega = N/2$, (4.8) will give us two values we can combine as follows

$$\exp(i\omega x) + \exp(-i\omega x) = 2\cos(\omega x)$$

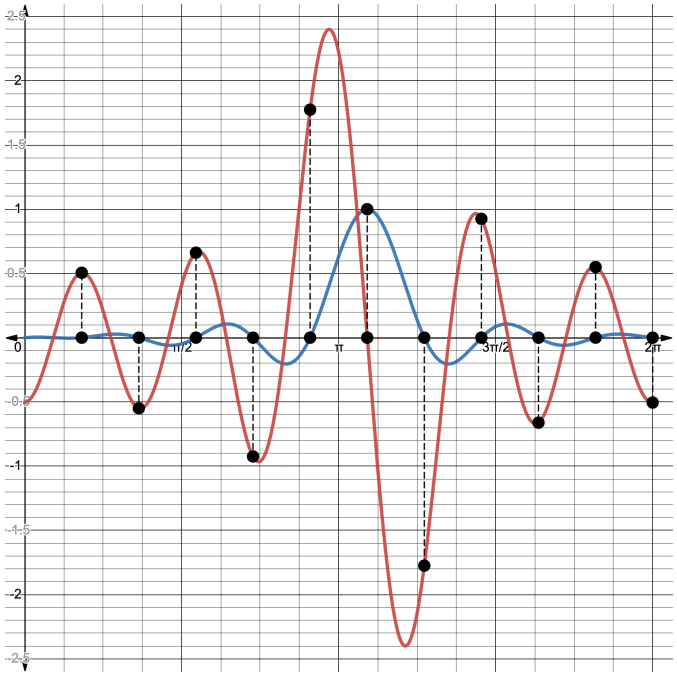

Figure 4.3: $p(x)$ and its derivative with and odd number of grid points. $p(x)$ is the blue function and its derivative is the red function. Note how the red function dp/dx is periodic.

and the derivative will be

$$-2\omega \sin(\omega x).$$

For the highest frequency, $N/2$, we get

$$\exp\left(i\frac{N}{2}x\right)$$

whose derivative is

$$i\frac{N}{2}\exp\left(i\frac{N}{2}x\right)$$

since there is no $\exp(-iN/2x)$ term. To fix this problem, we evaluate the grid function at zero as well as at 2π instead of just evaluating it at 2π. Since these points are the same we must divide them by 2. Our new interpolant can be neatly written as

$$p(x) = \frac{1}{N}\left(\frac{1}{2}\sum_{\omega=-\frac{N}{2}}^{-\frac{N}{2}-1}\exp(i\omega x) + \frac{1}{2}\sum_{\omega=-\frac{N}{2}+1}^{-\frac{N}{2}}\exp(i\omega x)\right). \tag{4.9}$$

By algebraic manipulation we can express (4.9) in a more compact form. We begin by writing the first, middle, and last terms in the sums

$$\begin{aligned}
p(x) = \frac{1}{N}\Bigg[&\frac{1}{2}\left(e^{i\left(-\frac{N}{2}\right)x} + e^{i\left(-\frac{N}{2}+1\right)x} + e^{i\left(-\frac{N}{2}+2\right)x} + \cdots + e^{i(0)x} + \cdots + e^{i\left(\frac{N}{2}-2\right)x} + e^{i\left(\frac{N}{2}-1\right)x}\right) \\
&+ \frac{1}{2}\left(e^{i\left(-\frac{N}{2}+1\right)x} + e^{i\left(-\frac{N}{2}+2\right)x} + \cdots + e^{i(0)x} + \cdots e^{i\left(\frac{N}{2}-2\right)x} + e^{i\left(\frac{N}{2}-1\right)x} + e^{i\left(\frac{N}{2}\right)x}\right)\Bigg] \\
= \frac{1}{N}\Bigg[&\frac{1}{2}e^{-i\frac{1}{2}x}\left(e^{i\left(-\frac{N}{2}+\frac{1}{2}\right)x} + e^{i\left(-\frac{N}{2}+\frac{3}{2}\right)x} + e^{i\left(-\frac{N}{2}+\frac{5}{2}\right)x} + \cdots + e^{i\left(\frac{1}{2}\right)x} + \cdots\right. \\
&\left. + e^{i\left(\frac{N}{2}-\frac{3}{2}\right)x} + e^{i\left(\frac{N}{2}-\frac{1}{2}\right)x}\right) + \frac{1}{2}e^{i\frac{1}{2}x}\left(e^{i\left(-\frac{N}{2}+\frac{1}{2}\right)x} + e^{i\left(-\frac{N}{2}+\frac{3}{2}\right)x} + \cdots\right. \\
&\left. + e^{i\left(-\frac{1}{2}\right)x} + \cdots + e^{i\left(\frac{N}{2}-\frac{5}{2}\right)x} + e^{i\left(\frac{N}{2}-\frac{3}{2}\right)x} + e^{i\left(\frac{N}{2}-\frac{1}{2}\right)x}\right)\Bigg]. \qquad (4.10)
\end{aligned}$$

Here we can see that the first term in the first sum of (4.10) is the same as the last term in the second sum and the second term in the first sum the same as the second to last term in the second sum and so on. This lets us write our interpolate as

$$p(x) = \frac{1}{N}\cos\left(\frac{x}{2}\right)\sum_{\omega=-\frac{N}{2}+\frac{1}{2}}^{\frac{N}{2}-\frac{1}{2}}\exp(i\omega x).$$

This sum is a geometric series and can be recast by multiplying the numerator and denominator by $\exp(-i/2x)$ and some algebraic manipulation

$$\begin{aligned}
p(x) &= \frac{1}{N}\cos\left(\frac{x}{2}\right)\frac{\exp\left(i\left(-\frac{N}{2}+\frac{1}{2}\right)x\right) - \exp\left(i\left(\frac{N}{2}+\frac{1}{2}\right)x\right)}{1-\exp(ix)} \\
&= \frac{1}{N}\cos\left(\frac{x}{2}\right)\frac{\exp\left(-i\frac{N}{2}x\right) - \exp\left(i\frac{N}{2}x\right)}{\exp\left(-i\frac{1}{2}x\right) - \exp\left(i\frac{1}{2}x\right)} \\
&= \frac{1}{N}\cos\left(\frac{x}{2}\right)\frac{\sin\left(\frac{N}{2}x\right)}{\sin\left(\frac{x}{2}\right)}.
\end{aligned}$$

This is the discrete and periodic interpolant. To get the difference operator, we differentiate $p(x)$.

$$\frac{d}{dx}p(x) = \frac{1}{2}\cos\left(\frac{N}{2}x\right)\frac{1}{\tan\left(\frac{x}{2}\right)} - \frac{1}{2N}\sin\left(\frac{N}{2}x\right)\left(\frac{1}{\tan^2\left(\frac{x}{2}\right)}+1\right)$$

and inserting $x = \{n\cdot 2\pi/N\}$, where $n = 0, 1, 2, \cdots, N$ we get

$$\frac{d}{dx}p(x) = \frac{1}{2}(-1)^n\frac{1}{\tan\left(n\frac{\pi}{N}\right)} - \frac{1}{2N}\sin(n\pi)\left(\frac{1}{\tan^2\left(n\frac{\pi}{2}\right)}+1\right)$$

and using the relation $N/2 = \pi/h$ we get the following scheme

$$\frac{d}{dx}p(x) = \begin{cases} 0, & n = 0 \\ \frac{1}{2}(-1)^n \frac{1}{\tan\left(n\frac{h}{2}\right)}, & n \neq 0 \end{cases}.$$

In matrix form this takes the form

$$D = \begin{bmatrix} 0 & -\frac{1}{2}\cot\left(\frac{h}{2}\right) & \frac{1}{2}\cot\left(\frac{2h}{2}\right) & \cdots & \frac{1}{2}\cot\left(\frac{2h}{2}\right) & -\frac{1}{2}\cot\left(\frac{h}{2}\right) \\ -\frac{1}{2}\cot\left(\frac{h}{2}\right) & \ddots & \ddots & \ddots & \ddots & \frac{1}{2}\cot\left(\frac{2h}{2}\right) \\ \frac{1}{2}\cot\left(\frac{2h}{2}\right) & \ddots & \ddots & \ddots & \ddots & -\frac{1}{2}\cot\left(\frac{3h}{2}\right) \\ -\frac{1}{2}\cot\left(\frac{3h}{2}\right) & \ddots & \ddots & \ddots & \ddots & \vdots \\ \vdots & \ddots & \ddots & \ddots & \ddots & -\frac{1}{2}\cot\left(\frac{h}{2}\right) \\ -\frac{1}{2}\cot\left(\frac{h}{2}\right) & \frac{1}{2}\cot\left(\frac{2h}{2}\right) & -\frac{1}{2}\cot\left(\frac{3h}{2}\right) & \ldots & -\frac{1}{2}\cot\left(\frac{h}{2}\right) & 0 \end{bmatrix}. \tag{4.11}$$

A graphical representation of $p(x)$ and dp/dx can be seen in figure (4.4). The rows

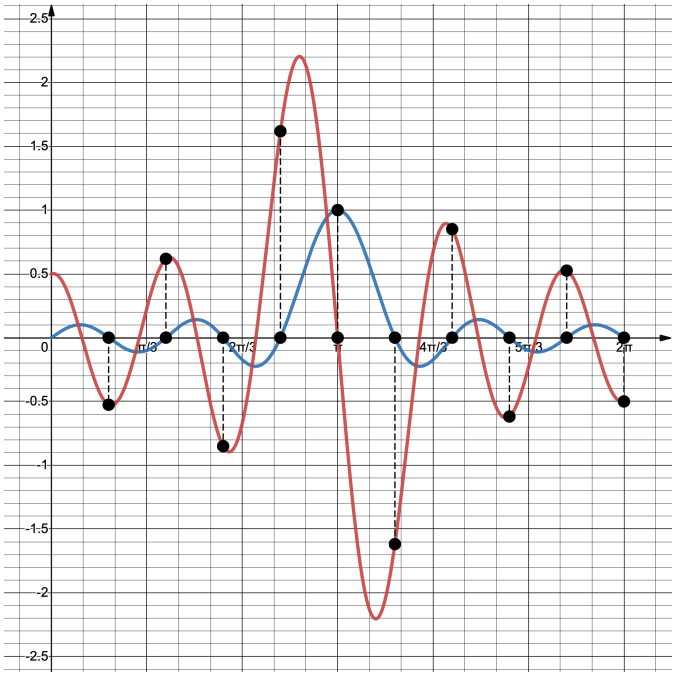

Figure 4.4: $p(x)$ and its derivative with and even number of grid points (10 points). $p(x)$ is the blue function and its derivative is the red function. Note how the derivative of $p(x)$ is not periodic. Compare with figure (4.3).

of the difference matrix is simply the the derivative of the interpolant centered at the corresponding grid point. Figure (4.5) shows the idea, and hopefully shows

that taking the derivative of a periodic function is equivalent to a convolution with dp/dx. The same visualization can be done for higher order derivatives and for an odd number of grid points. Since the basis functions for $p(x)$ with an even number

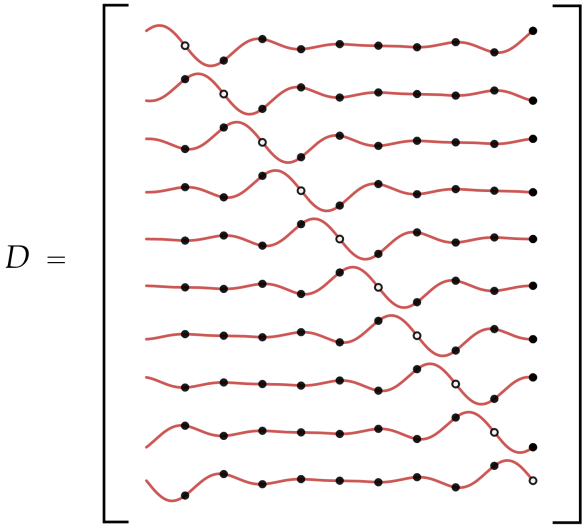

Figure 4.5: An alternative visualization of the spectral difference matrix for the first derivative for an even number of grid points. The height of each point corresponds to the value in the difference matrix. There are two things to note here. The only entries in the matrix that are zero are on the diagonal, which are marked with a circular dot, and the function in one row is the same function as in the row above just shifted one grid point to the right.

of grid points are $\cos(\omega x)$ and $\sin(\omega x)$, $\omega \in \{-N/2+1, N/2\}$ we *cannot* simply multiply the matrix operator for the first derivative with itself n times to obtain the n'th order derivative matrix as we did when we were dealing with an odd number of grid points. To see why, assume that our interpolant is just the highest frequency wave of the basis functions, $p(x) = \cos(x \cdot N/2)$. Upon differentiating two times we would get

$$\frac{d^2}{dx^2}p(x) = \cos(x \cdot (-N/2))$$

but this is not one of the basis functions for $p(x)$. In other words

$$\frac{d^2}{dx^2}p(x) \neq D^2 p(x).$$

Therefore we must redo the same calculations as when finding the first derivative once more. This results in

$$\frac{d^2}{dx^2}p(x) = \frac{1}{2N}\frac{\sin\left(\frac{Nx}{2}\right)\left(\tan^2\left(\frac{x}{2}\right)+1\right)^2}{\tan^3\left(\frac{x}{2}\right)} - \frac{\cos\left(\frac{Nx}{2}\right)}{2}\left(1+\frac{1}{\tan^2\left(\frac{x}{2}\right)}\right) - \frac{N}{4}\frac{\sin\left(\frac{Nx}{2}\right)}{\tan\left(\frac{x}{2}\right)} - \frac{\sin\left(\frac{Nx}{2}\right)}{2N}\left(1+\frac{1}{\tan\left(\frac{x}{2}\right)}\right)$$

and gives us the following scheme

$$\frac{d^2}{dx^2}p(x) = \begin{cases} -\frac{\pi^2}{3h^2} - \frac{1}{6}, & n = 0 \\ -\frac{(-1)^n}{2\sin^2\left(n\frac{h}{2}\right)}, & n \neq 0 \end{cases}.$$

which can be expressed in matrix form as

$$D^2 = \begin{bmatrix} -\frac{\pi^2}{3h^2} - \frac{1}{6} & \frac{1}{2}\csc^2\left(\frac{h}{2}\right) & -\frac{1}{2}\csc^2\left(\frac{2h}{2}\right) & \cdots & -\frac{1}{2}\csc^2\left(\frac{2h}{2}\right) & \frac{1}{2}\csc^2\left(\frac{h}{2}\right) \\ \frac{1}{2}\csc^2\left(\frac{h}{2}\right) & \ddots & \ddots & \ddots & \ddots & -\frac{1}{2}\csc^2\left(\frac{2h}{2}\right) \\ -\frac{1}{2}\csc^2\left(\frac{2h}{2}\right) & \ddots & \ddots & \ddots & \ddots & \frac{1}{2}\csc^2\left(\frac{3h}{2}\right) \\ \frac{1}{2}\csc^2\left(\frac{3h}{2}\right) & \ddots & \ddots & \ddots & \ddots & \vdots \\ \vdots & \ddots & \ddots & \ddots & \ddots & \frac{1}{2}\csc^2\left(\frac{h}{2}\right) \\ \frac{1}{2}\csc^2\left(\frac{h}{2}\right) & -\frac{1}{2}\csc^2\left(\frac{2h}{2}\right) & \frac{1}{2}\csc^2\left(\frac{3h}{2}\right) & \cdots & \frac{1}{2}\csc^2\left(\frac{h}{2}\right) & -\frac{\pi^2}{3h^2} - \frac{1}{6} \end{bmatrix} \tag{4.12}$$

For intervals other than $[0, 2\pi]$ we simply multiply the difference operator with a scaling factor s. Given an interval $[a, b]$, s is obtained by the following formula

$$s = \frac{2\pi}{b-a}.$$

For the unit interval, $x \in [0, 1]$, then the n'th order derivative is multiplied with $(2\pi)^n$. So the operator for the first derivative is multiplied with 2π, and the second derivative operator with $(2\pi)^2$ and so on. This is intuitive because the sinc function, $\sin(nx)/(nx)$, becomes steeper when its roots are closer to each other.

4.4 Convergence

Now that we have derived our spectral difference matrix, it is straightforward to see that it is a dense matrix, and more importantly, this is the same matrix you would obtain in the limit of higher and higher order Taylor series. The truncation error of a finite difference scheme using $n + 1$ points is $\mathcal{O}(h^n)$. By taking this to

the limit as $n+1 \to N+1$ the truncation error is then $\mathcal{O}(h^N)$ and using the fact that $h = 1/N$ we get $\mathcal{O}(N^{-N})$ or $\mathcal{O}(h^{1/h})$ which is referred to as exponential convergence. This only holds if the solution is infinitely differentiable. The solution to some initial boundary value problems are not infinitely differentiable and the smoothness of the solution becomes the limiting factor of convergence.

Chapter 5

Fourth Order Runge-Kutta Method

The theory in this chapter is based on [8], [27], and [21]. Now that we have introduced spectral methods to discretize our PDE in space we have the following system of coupled ODE's

$$\frac{d\mathbf{u}}{dt} = Q\mathbf{f}(\mathbf{u}(t), t) \tag{5.1}$$

where Q is a difference operator. The coupling occurs for two reasons. The first reason is because $\mathbf{f}(\mathbf{u}, t)$ itself depends nonlinearly on $\mathbf{u}$ and the second is due to the difference matrix. To analyze the stability of the time discretization scheme we must try to diagonalize (5.1). This is generally not possible for non-linear PDE's, but the linear theory gives good intuition for the stability of time discretization techniques. For a diagonalization of the linearized Navier-Stokes equations see [17].

Throughout the rest of this chapter we will assume that we are dealing with the linearized NS and NSS equations. The diagonalizationo of (5.1) can be expressed as

$$\frac{d\mathbf{v}}{dt} = Q\mathbf{g}(\mathbf{v})$$

where $\mathbf{v}$ and $\mathbf{g}$ are the diagonalizations of $\mathbf{u}$ and $\mathbf{f}$ respectively. The second reason of coupling is due to the differentiation matrices. As an example, consider the transport equation $\partial_t u + \partial_x u$ which can be discretized in space by a first order

periodic central difference stencil as follows

$$\frac{\partial v}{\partial t} + Qv = \frac{\partial}{\partial t}\begin{bmatrix} v_1 \\ v_2 \\ v_3 \\ \vdots \\ v_N \end{bmatrix} + \frac{1}{2h}\begin{bmatrix} 0 & 1 & 0 & \cdots & \cdots & -1 \\ -1 & 0 & 1 & 0 & \cdots & 0 \\ 0 & -1 & 0 & 1 & \cdots & 0 \\ \ddots & \ddots & \ddots & \ddots & \ddots & \ddots \\ -1 & 0 & \cdots & 0 & 1 & 0 \end{bmatrix}\begin{bmatrix} v_1 \\ v_2 \\ v_3 \\ \vdots \\ v_N \end{bmatrix}$$
$$= \frac{\partial}{\partial t}\begin{bmatrix} v_1 \\ v_2 \\ v_3 \\ \vdots \\ v_N \end{bmatrix} + \frac{1}{2h}\begin{bmatrix} v_2 - v_N \\ v_3 - v_1 \\ v_4 - v_2 \\ \vdots \\ v_{N-1} - v_1 \end{bmatrix}$$

where we have obtained a system of coupled ODE's. Diagonalizing $Q\mathbf{g}$ for the periodic case this is simple since the difference matrix approximating the first derivative is skew-symmetric and the difference matrix approximating the second derivative is symmetric. Both skew-symmetric and symmetric matrices can be diagonalized such that we get $T^{-1}QT = \Lambda \Leftrightarrow Q = T\Lambda T^{-1}$, where Λ is a diagonal matrix. This leaves us with the following system of ODE's

$$\frac{\partial \mathbf{v}}{\partial t} = T\Lambda T^{-1}\mathbf{g}$$
$$\frac{\partial \mathbf{w}}{\partial t} = \mathbf{h}$$

where $\mathbf{w} = T^{-1}\mathbf{v}$, $\mathbf{h} = \Lambda T^{-1}\mathbf{g}$ and the diagonal entries of Λ are $\lambda_1, \lambda_2, \cdots, \lambda_N$ (and are the eigenvalues of Q). We have now obtained a system of N decoupled ODE's and can solve for $\mathbf{w}(t + \Delta t)$ as follows

$$\mathbf{w}(t + \Delta t) = \mathbf{w}(t) + \int_t^{t+\Delta t} \mathbf{h}(\mathbf{u}(t), t)d\tau.$$

Often we don't know the solution to this integral and we need to discretize in time to solve it numerically resulting in the following equation

$$\mathbf{w}(t + \Delta t) = \mathbf{w}(t) + \Delta t \sum_i \omega_i \mathbf{h}(\mathbf{w}(t + \alpha_i), t + \beta_i)$$

where ω_i are the weights and α_i and β_i determine where $\mathbf{h}$ is to be evaluated. There are many ways to express the last term on the right hand side and in this thesis we will choose the fourth order Runge-Kutta method (RK4). We will not go into the same amount of detail as we did in the spectral methods chapter because

most of the accuracy improvements gained from solving PDE's numerically arise from the spatial discretization methods (especially for non-linear PDE's). That is to say that the errors resulting from the spatial discretization are often much greater than from time discretization. The fourth order Runge-Kutta method is

$$\mathbf{w}(t+\Delta t) = \mathbf{w}(t) + \Delta t(a\mathbf{h}_1 + b\mathbf{h}_2 + c\mathbf{h}_3 + d\mathbf{h}_4) \tag{5.2}$$

where

$$\begin{aligned}
\mathbf{h}_1 &= \mathbf{h}(\mathbf{w}, t) \\
\mathbf{h}_2 &= \mathbf{h}\left(\mathbf{w} + \frac{\Delta t}{2}\mathbf{h}_1, t + \frac{\Delta t}{2}\right) \\
\mathbf{h}_3 &= \mathbf{h}\left(\mathbf{w} + \frac{\Delta t}{2}\mathbf{h}_2, t + \frac{\Delta t}{2}\right) \\
\mathbf{h}_4 &= \mathbf{h}(\mathbf{u} + \Delta t\mathbf{h}_3, t + \Delta t).
\end{aligned}$$

and the weights a, b, c, d in (5.2) are to be determined. Using the first order Taylor expansion we can express $\mathbf{h}_2$ as follows

$$\mathbf{h}_2 = \mathbf{h}(\mathbf{w}, t) + \frac{\Delta t}{2}\frac{d}{dt}(\mathbf{h}(\mathbf{w}, t)) + \mathcal{O}(\Delta t^2).$$

Remember, after we have discretized in space $\mathbf{w}$ becomes a function of time only. Now that we have expressed $\mathbf{h}_2$ we can express $\mathbf{h}_3$ and $\mathbf{h}_4$. We will drop the $\mathcal{O}(\Delta t^2)$ term. $\mathbf{h}_3$ and $\mathbf{h}_4$ are

$$\begin{aligned}
\mathbf{h}_3 &= \mathbf{h}(\mathbf{w}, t) + \frac{\Delta t}{2}\frac{d\mathbf{h}_2}{dt} \\
&= \mathbf{h}(\mathbf{w}, t) + \frac{\Delta t}{2}\frac{d}{dt}\left(\mathbf{h}(\mathbf{w}, t) + \frac{\Delta t}{2}\frac{d}{dt}(\mathbf{h}(\mathbf{w}, t))\right) \\
&= \mathbf{h}(\mathbf{w}, t) + \frac{\Delta t}{2}\frac{d}{dt}\mathbf{h}(\mathbf{w}, t) + \frac{\Delta t^2}{4}\frac{d^2}{dt^2}\mathbf{h}(\mathbf{w}, t) \\
\mathbf{h}_4 &= \mathbf{h}(\mathbf{w}, t) + \Delta t\frac{d\mathbf{h}_3}{dt} \\
&= \mathbf{h}(\mathbf{w}, t) + \Delta t\frac{d}{dt}\left(\mathbf{h}(\mathbf{w}, t) + \frac{\Delta t}{2}\frac{d}{dt}\mathbf{h}(\mathbf{w}, t) + \frac{\Delta t^2}{4}\frac{d^2}{dt^2}\mathbf{h}(\mathbf{w}, t)\right) \\
&= \mathbf{h}(\mathbf{w}, t) + \Delta t\frac{d}{dt}\mathbf{h}(\mathbf{w}, t) + \frac{\Delta t^2}{2}\frac{d^2}{dt^2}\mathbf{h}(\mathbf{w}, t) + \frac{\Delta t^3}{4}\frac{d}{dt}\mathbf{h}(\mathbf{w}, t))
\end{aligned}$$

We can now insert $\mathbf{h}_1$, $\mathbf{h}_2$, $\mathbf{h}_3$, and $\mathbf{h}_4$ into (5.2) yielding

$$\begin{aligned}\mathbf{w}(t+h) &= \mathbf{w}(t) + a\Delta t\mathbf{h}(\mathbf{w},t) + b\Delta t\mathbf{h}(\mathbf{w},t) + b\frac{\Delta t^2}{2}\frac{d}{dt}(\mathbf{h}(\mathbf{w},t)) + c\Delta t\mathbf{h}f(\mathbf{w},t)\\ &\quad + c\frac{\Delta t^2}{2}\frac{d}{dt}\mathbf{h}(\mathbf{w},t) + c\frac{\Delta t^3}{4}\frac{d^2}{dt^2}\mathbf{h}(\mathbf{w},t) + d\Delta t\mathbf{h}(\mathbf{w},t) + d\Delta t^2\frac{d}{dt}\mathbf{h}(\mathbf{w},t)\\ &\quad + d\frac{\Delta t^3}{2}\frac{d^2}{dt^2}\mathbf{h}(\mathbf{w},t) + d\frac{\Delta t^4}{4}\frac{d}{dt}\mathbf{h}(\mathbf{w},t)\\ &= \Delta t\mathbf{h}(a+b+c+d) + \frac{\Delta t^2}{2}\frac{d}{dt}\mathbf{h}(\mathbf{w},t)(b+c+2d) + \frac{\Delta t^3}{4}\frac{d^2}{dt^2}\mathbf{h}(\mathbf{w},t)(c+2d)\\ &\quad + d\frac{\Delta t^4}{4}\frac{d^3}{dt^3}\mathbf{h}(\mathbf{w},t).\end{aligned}$$

If we compare this with the fifth order Taylor series of $\mathbf{w}(t+h)$, namely

$$\begin{aligned}\mathbf{w}(t+h) &= \mathbf{w} + \Delta t\frac{\partial\mathbf{w}}{\partial t} + \frac{\Delta t^2}{2!}\frac{\partial^2\mathbf{w}}{\partial t^2} + \frac{\Delta t^3}{3!}\frac{\partial^3\mathbf{w}}{\partial t^3} + \frac{\Delta t^4}{4!}\frac{\partial^4\mathbf{w}}{\partial t^4} + \mathcal{O}(\Delta t^5)\\ &= \mathbf{w} + \Delta t\mathbf{h}(\mathbf{w},t) + \frac{\Delta t^2}{2!}\frac{\partial}{\partial t}\mathbf{h}(\mathbf{w},t) + \frac{\Delta t^3}{3!}\frac{\partial^2}{\partial t^2}\mathbf{h}(\mathbf{w},t) + \frac{\Delta t^4}{4!}\frac{\partial^3}{\partial t^3}\mathbf{h}(\mathbf{w},t) + \mathcal{O}(\Delta t^5)\end{aligned}$$

we get the four following equations

$$\begin{aligned}a+b+c+d &= 1\\ \frac{1}{2}(b+c)+d &= \frac{1}{2}\\ \frac{1}{4}c+\frac{1}{2}d &= \frac{1}{6}\\ \frac{1}{4}d &= \frac{1}{24}\end{aligned}$$

which gives us

$$a = \frac{1}{6}, \quad b = \frac{1}{3}, \quad c = \frac{1}{3}, \quad d = \frac{1}{6}.$$

Technically, our calculations for the RK4 method only show $\mathcal{O}(\Delta t^3)$ convergence since we only expanded $\mathbf{h}_2$ with a first order Taylor expansion. Had we expanded $\mathbf{h}_2$ using a fourth order Taylor expansion we would get additional equations which would show a $\mathcal{O}(\Delta t^5)$ order convergence. It turns out that, a, b, c, and d would be the exact same as we derived above. For the full proof of the fifth order convergence, consult [15]. Now that we have a temporal approximation we make the ansatz that

$$\begin{aligned}u' + \delta_{n+1} = u_{n+1} &= f(u'+\delta_n) = f(u') + \dot{f}(u')\delta_n + \mathcal{O}(\delta_n^2)\\ \delta_{n+1} &= \dot{f}(u')\delta_n + \mathcal{O}(\delta_n^2)\end{aligned}$$

where u' is a fixed point such that $f(u') = u'$ and δ_n is to be viewed as a small step away from the fixed point. The difference equation is stable if $\dot{f}(u_n) < 1$ where $\dot{f}(u_n) \in \mathbb{C}$. The stability region of the Runge Kutta method is thus stable when

$$\dot{f}(u_n) = 1 + z + \frac{z^2}{2} + \frac{z^3}{6} + \frac{z^4}{24} < 1$$

where $z \in \mathbb{C}$. $\dot{f}(u_n) = 1$ is shown in figure 5.1 with the eigenvalues of the spectral difference matrices approximating the first and second derivatives. Note that the first derivatives have purely imaginary eigenvalues and the second derivative has purely real eigenvalues.

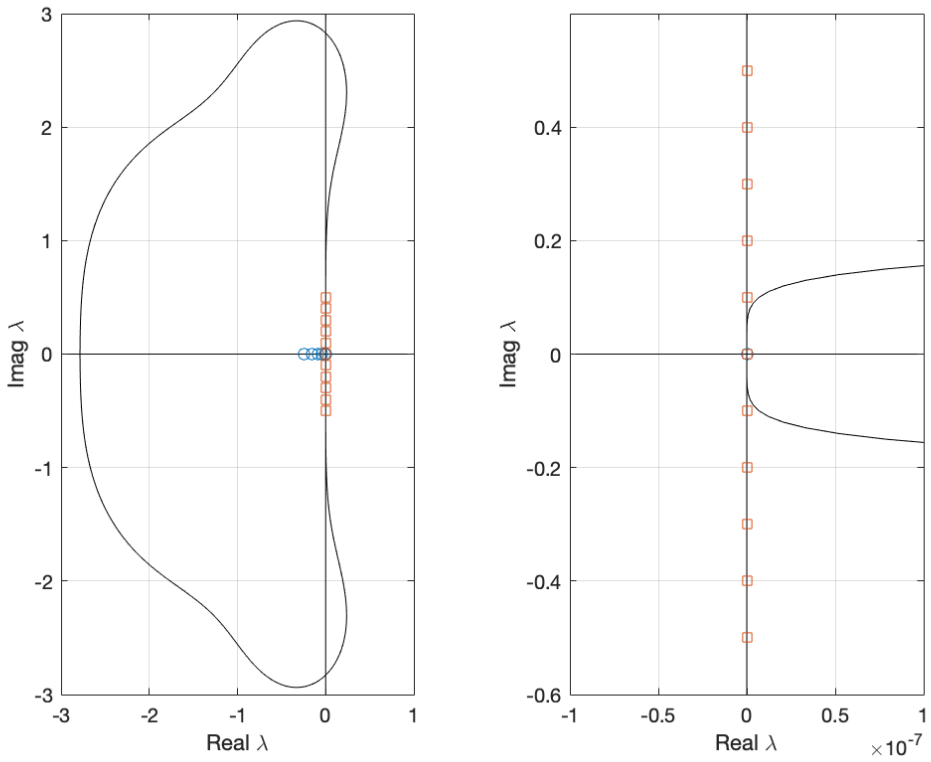

Figure 5.1: Stability region of the fourth order Runge-Kutta method including eigenvalues of the 11 point first and second order spectral difference operators.

Chapter 6

Code Verification

In this chapter we will verify that our code has the correct convergence rate by use of the method of manufactured solution.

6.1 Method of Manufactured Solution

Given a time dependent PDE

$$\frac{\partial u}{\partial t} + Qu = S \tag{6.1}$$

where Q is some difference operator and S is a source term which we assume is given. By measuring the error between the analytical solution and the numerical solution we can check if the convergence rate is correct. This is often referred to as the method of exact solutions. But, in the case where we do not know the analytical solution (such as for the NS and NSS equations) we need to construct our own solution. This is done by determining a solution, v, and constructing a source term such that it satisfies the PDE. Doing this for (6.1) we get

$$\frac{\partial v}{\partial t} + Qv = R.$$

R will almost certainly not be equal to S, but the source term does not affect stability, which we will prove shortly. The following definition and proof are adapted from [8].

Definition 6.1.1. *An initial value problem (IVP) is considered to be well posed if there is a unique solution satisfying*

$$\|u(\cdot, t)\| \leq \|f(\cdot)\| K \exp(\alpha t)$$

where the K and α are constants independent of $f(x)$.

Theorem 6.1.1. *Adding a source term to some* well posed *initial value problem, the contribution of the source term will not affect the well posedness. Here $\hat{u}$ and $\hat{F}$ are the Fourier transform of u and F respectively.*

Proof.

$$\begin{aligned}
\frac{\partial u(x,t)}{\partial t} &= F(x,t) \\
\frac{u(x,t_{n+1}) - u(x,t_n)}{k} &= F(x,t_n) \\
\hat{u}(\omega,t_{n+1}) &= \hat{u}(\omega,t_n) + k\hat{F}(\omega,t_n), \qquad \hat{u}(\omega,t_n) = \hat{u}(\omega,t_{n-1}) + k\hat{F}(\omega,t_{n-1}) \\
&= \hat{u}(\omega,t_{n-1}) + k(\hat{F}(\omega,t_n) + \hat{F}(\omega,t_{n-1})) \\
&\vdots \\
&= \hat{u}(\omega,t_0) + k\sum_{i=0}^{n} \hat{F}(\omega,t_i)
\end{aligned}$$

Now, if we take the norm of both sides, use the triangle inequality, and Parsevals relation we get

$$\begin{aligned}
\|u(\cdot,t_{n+1})\| &= \|\hat{u}(\cdot,t_{n+1})\| \\
&= \|\hat{u}(\cdot,t_0) + k\sum_{i=0}^{n} \hat{F}(\cdot,t_i)\| \\
&\leq \|\hat{u}(\cdot,t_0)\| + \|k\sum_{i=0}^{n} \hat{F}(\cdot,t_i)\| \\
&= \|f\| + k\|\sum_{i=0}^{n} \hat{F}(\cdot,t_i)\| \\
&\leq \|f\| + k(n+1)\max_{0\leq i\leq n} \|\hat{F}(\cdot,t_i)\| \\
&\leq K\|f\|
\end{aligned}$$

assuming that $\|f\| \neq 0$. In plain English: a source term will always have a norm that can be made smaller than or equal to the norm of the PDE without the source term. □

The procedure of the method of manufactured solution is as follows: First we determine a solution v, then we insert it into our equation and calculate the source term, R. Since the source term doesn't affect stability, we have a analytical solution we can compare our approximation to. This method of determining a solution and then calculating the source term is referred to as the Method of Manufactured solution. For more information about on the method of manufactured solution consult [19].

6.1.1 Errors by Method of Manufactured Solution

When constructing a manufactured solution one must keep in mind to have the same boundary conditions and make sure to keep in mind various assumptions that were assumed when making the equations. In this case, we have periodic boundary conditions and assume that density can only have positive values. It isn't necessary to strive for any sort of physical realism in the solutions and the solutions must be at least as differentiable as the highest derivative in the equations. With this in mind we chose the following solutions for the NS and NSS equations.

$$\begin{aligned}\rho &= \cos(2\pi(x+t)) + \sin(2\pi(x+t)) + 2\\ m &= \cos(2\pi(x+t)) - \sin(2\pi(x+t))\\ E &= -\cos(2\pi(x+t)) + \sin(2\pi(x+t))\end{aligned}$$

with the following constants in SI units

$$\begin{aligned}\mu &= 1\\ \kappa &= 1\\ c_p &= 2\\ c_V &= 1\end{aligned}$$

We obtained the following errors for both equations after running the code with time step 10^{-6} seconds for 10^{-2} seconds, 10^4 steps in total. The error is calculated using the following formula

$$\text{error} = \sqrt{\sum_{n=0}^{N} h(u_n - u)^2}$$

and the results for the NS and NSS equations are tabulated and plotted in tables 6.1 and 6.2 and figures 6.1 and 6.2 respectively. Notice in the figures that for each increase in the number of grid points, N, the error decreases at a greater rate than in the previous increase in N until it hits the rounding error at around 10^{-14}. This is the telltale sign of spectral convergence and differs from normal finite difference schemes where the rate of change of the error would not change for each increase of N (it would be constant).

Table 6.1: Error using manufactured solution for Navier-Stokes

N	h	ρ error	m error	E error
11	1/10	$1.916 \cdot 10^{-3}$	$1.535 \cdot 10^{-2}$	$2.050 \cdot 10^{-2}$
21	1/20	$2.861 \cdot 10^{-5}$	$6.009 \cdot 10^{-5}$	$8.810 \cdot 10^{-5}$
41	1/40	$2.219 \cdot 10^{-9}$	$3.404 \cdot 10^{-9}$	$8.434 \cdot 10^{-9}$
81	1/80	$1.129 \cdot 10^{-14}$	$3.610 \cdot 10^{-14}$	$2.797 \cdot 10^{-14}$
161	1/160	$1.841 \cdot 10^{-14}$	$3.641 \cdot 10^{-13}$	$3.118 \cdot 10^{-13}$

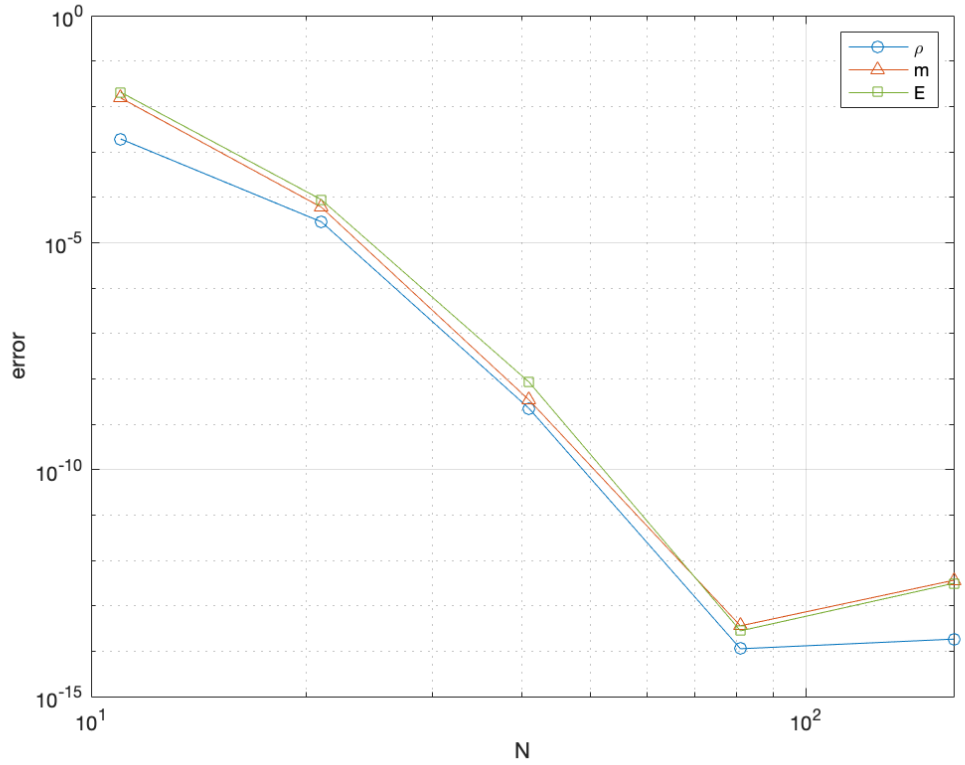

Figure 6.1: Plot of the error of the Navier-Stokes equations.

Table 6.2: Error using manufactured solution for Navier-Stokes-Svärd

N	h	ρ error	m error	E error
11	1/10	$6.137 \cdot 10^{-3}$	$9.146 \cdot 10^{-3}$	$3.476 \cdot 10^{-2}$
21	1/20	$4.344 \cdot 10^{-5}$	$3.476 \cdot 10^{-5}$	$4.470 \cdot 10^{-5}$
41	1/40	$2.601 \cdot 10^{-9}$	$3.515 \cdot 10^{-9}$	$8.902 \cdot 10^{-9}$
81	1/80	$5.710 \cdot 10^{-15}$	$1.780 \cdot 10^{-14}$	$1.655 \cdot 10^{-14}$
161	1/160	$1.879 \cdot 10^{-14}$	$5.125 \cdot 10^{-14}$	$4.747 \cdot 10^{-14}$

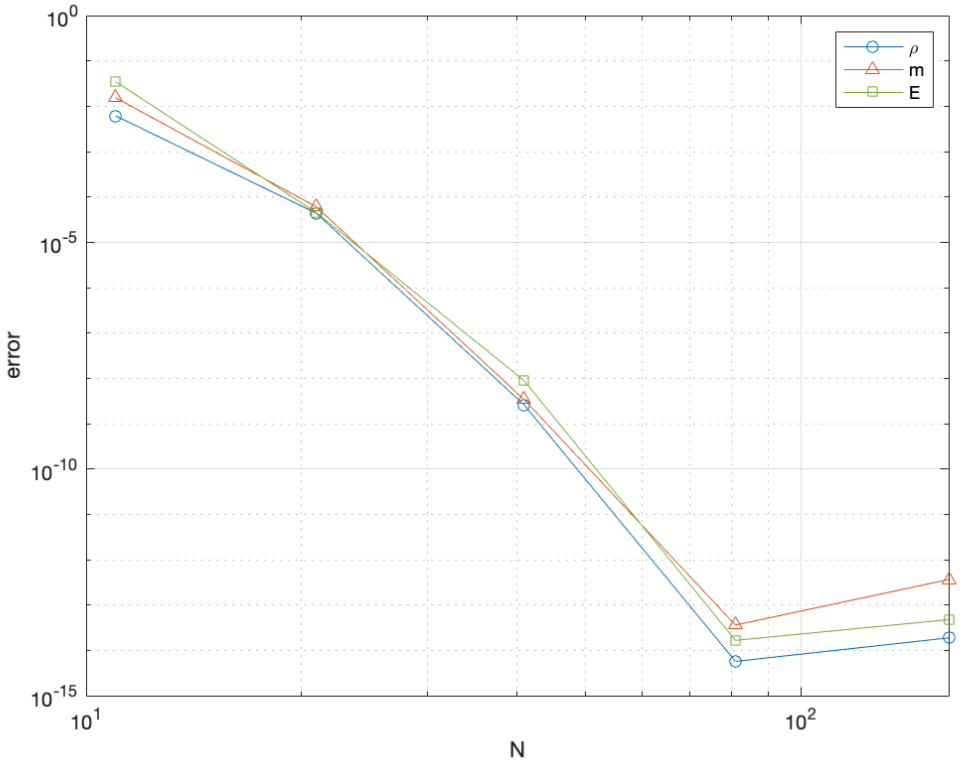

Figure 6.2: Plot of the error of the Navier-Stokes-Svärd equations.

Chapter 7

Acoustic Attenuation Simulation Results

In this chapter we will describe the procedures used to analyze the data obtained from our simulations of acoustic attenuation. We will then explain various sources of errors and present our results. The scheme used was

$$\frac{\partial}{\partial t}u + Q_1 f = Q_2 g$$

where $u = (\rho, m, E)^\top$ and $Q_1 f = D_1(\rho, m^2 + p, (E+p)m/\rho)^\top$ for both the NS and NSS system. $Q_2 g = (0, \mu 4/3 D_2(m/\rho), \mu 4/6 D_2(m/\rho)^2 + D_1(\kappa D1T))^\top$ for the NS system and $Q_2 g = D_1 \nu D_1(\rho, m, E)^\top$ for the NSS system. Q_1 and Q_2 are difference operators approximating the first and second derivative and D_1 and D_2 are the difference matrices obtained from (4.6), (4.11) and (4.7), (4.12) respectively. The fourth order Runge Kutta method was used in time.

7.1 Post Simulation Analysis

After having run the simulation we have had to analyse the data to obtain the rate of decay obtained from the two fluid models. The data we have chosen to extract is the work, $\int \rho u^2/2$, because it was used when deriving the absorption coefficient. We divided the work data into chunks such that one data chunk approximately equals one full period of sound. One would expect the frequency to be the same as two times the speed of sound. For example, in oxygen, $c \approx 312$m/s so one would expect that the period would be approximately $1.6 \cdot 10^{-3} s^{-1}$ but according to the simulations it is closer to $1.3 \cdot 10^{-3} s^{-1}$. Thus, we did not know the period a priori and had to measure it directly from the simulation.

Finding the approximate rate of decay was done in the following four step process.

1. We integrated $\rho u^2/2$ in space giving us a scalar work value at each time step.
2. We divided the work from step 1 into chunks that contained approximately one wavelength in time of work.
3. We created a vector with the maximum value of each wavelength from the chunks obtained in step 2.
4. We took the natural logarithm of the vector from step 3 (since we are assuming exponential decay) and then computed a linear regression of the points giving us an approximation of the coefficient of absorption.

7.2 Sources of Errors

When conducting experiments, both numerically and physically, with gases there are numerous sources of errors. Here we will list a few of these sources for the simulations run in this thesis. The list is most definitely not complete and we have therefore been conservative when trying to find a suitable value for the error estimate.

Conservation Accuracy

For a differentiation matrix with entries with more than 15 significant figures we must consider what we call *conservation accuracy*. Conservation accuracy is defined as the maximum value of the vector obtained when multiplying a *constant* vector with the differentiation matrix. For matrices with less than 15 significant figures (if you are using double precision) the conservation accuracy will be 0 since multiplying a constant vector with the differentiation matrix will exactly equate to zero. If the entries have more than 15 significant figures (as in spectral methods), which we will refer to discretely irrational matrices, then they will be rounded up or down and unless you are exceedingly lucky you will not have a conservation accuracy of 0. Multiplying a 10×10 discretely irrational differentiation matrix with with a vector with one in all its entries we get a new vector with entries of magnitude 10^{-15} due to floating point arithmetic. If we increase the differentiation matrix (which occurs when you increase points on the grid) by one order of magnitude then we lose one order of magnitude in conservation accuracy. If we have a differentiation matrix of the size $10^n \times 10^n$ we will in the worst case lose n orders of magnitude in conservation accuracy.

Similarly, if the constant vector has entries of magnitude 10^n then we will also lose n orders of magnitude in conservation accuracy in the worst case scenario. In our case, the background pressure is 10^5 Pa setting a limit to our conservation accuracy at $10^{-15+5} = 10^{-10}$.

Rounding Error in Small Magnitudes

The magnitude of work is approximately 10^{-8}. This small value puts a limiting factor on how accurate our simulations can be. We use double precision accuracy which has an precision of at least 10^{-15} decimal points. This means that in the case when the work is of order 10^{-8} we can *at best* get a 7 significant digit accuracy.

7.3 Numerical Results

We ran a total of four simulations. Two simulations of oxygen with background pressures of $p_0 = \{10^3, 10^5\}$ and two simulations of argon with the same background pressures. We simulated sound waves for oxygen to compare with the results of [3] and for argon to compare with [7]. In both cases temperature was set to 273.15 Kelvin. The initial values were

$$\begin{aligned} \rho &= \frac{p_0}{RT_0} + 10^{-6}\sin(2\pi x) \\ p &= \rho^\gamma \\ u &= 0 \\ E &= \rho c_V T_0 \end{aligned}$$

The reason we chose the amplitude of the fluctuation of ρ to be 10^{-6} was because the simulation run with a fluctuation amplitude of 10^{-5} showed non-linearities as can be seen in figure 7.1. When $p_0 = 10^3$ the simulations were run such that the wave oscillated 100 times and when $p_0 = 10^5$ the simulations were runu such that the wave oscillated 1000 times. Note that the sound waves used in [3] and [7] have greater amplitude and a higher frequency which both contribute to making the waves nonlinear and. The simulations were run on a 12 point grid (the calculations were done with 11 points and the 12th point was added for periodicity). For oxygen, the following fluid values were used

$$\begin{aligned} \mu &= 20.64 \cdot 10^{-6} \\ \kappa &= 26.58 \cdot 10^{-3} \\ c_p &= 915 \\ c_V &= 659, \end{aligned}$$

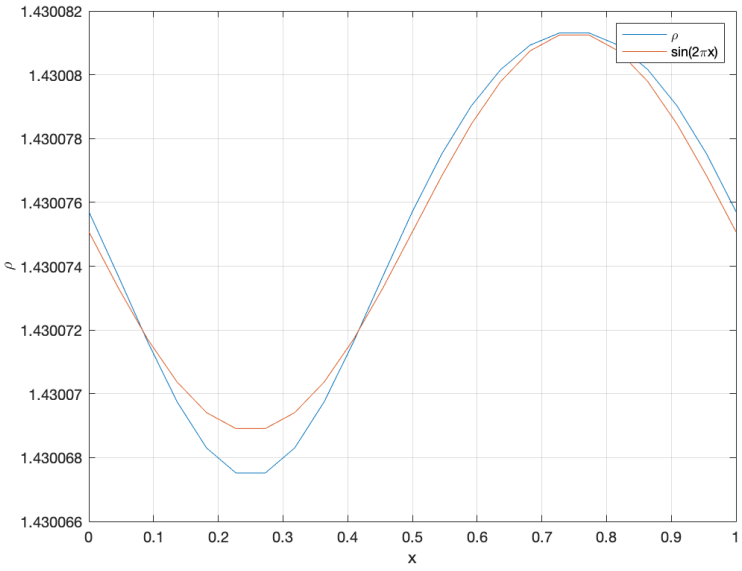

Figure 7.1: Non-linearities occurring when fluctuation amplitude is 10^{-5}.

and for argon we used the following fluid values

$$\begin{aligned} \mu &= 22.61 \cdot 10^{-6} \\ \kappa &= 1.78 \cdot 10^{-2} \\ c_p &= 520 \\ c_V &= 313. \end{aligned}$$

All the coefficients are in SI units. The numerical absorption coefficient was calculated three times in each test. The first 10% of the wave was removed to account for inaccuracies in the initial condition. Then, the remaining data was divided into three even parts and the numerical absorption coefficient was calculated for each part. The data for oxygen is presented in tables 7.2 and 7.1 and the last third of the simulation is plotted in figures 7.3 and 7.2 for the oxygen simulations with background pressure at 10^3 and 10^5 respectively. The data for argon is presented in tables 7.4 and 7.3 and the last third of the simulation is plotted in figures 7.5 and 7.4 for the argon simulations with background pressure at 10^3 and 10^5 respectively.

Table 7.1: Oxygen with background pressure at 10^5 Pa

	NS	NSS
Theoretical	$-1.0712351 \cdot 10^{-3}$	$-1.1395689 \cdot 10^{-3}$
1/3	$-1.0708588 \cdot 10^{-3}$	$-1.1391873 \cdot 10^{-3}$
2/3	$-1.0709171 \cdot 10^{-3}$	$-1.1392333 \cdot 10^{-3}$
3/3	$-1.0709835 \cdot 10^{-3}$	$-1.1392861 \cdot 10^{-3}$

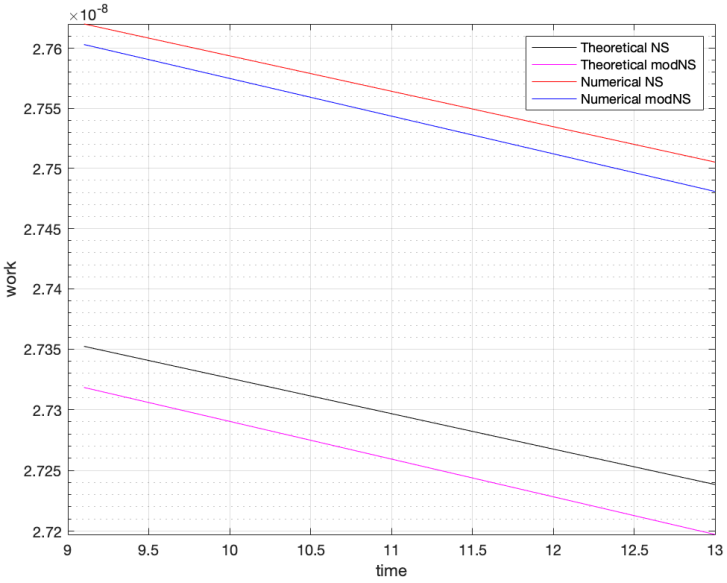

Figure 7.2: Plot of numerical absorption coefficient obtained from the last third of the data with $p_0 = 10^5$.

Table 7.2: Oxygen with background pressure at 10^3 Pa

	NS	NSS
Theoretical	$-1.0712351 \cdot 10^{-1}$	$-1.1395689 \cdot 10^{-1}$
1/3	$-1.0677959 \cdot 10^{-1}$	$-1.1358931 \cdot 10^{-1}$
2/3	$-1.0677645 \cdot 10^{-1}$	$-1.1358495 \cdot 10^{-1}$
3/3	$-1.0677069 \cdot 10^{-1}$	$-1.1357976 \cdot 10^{-1}$

Table 7.3: Argon with background pressure at 10^5 Pa

	NS	NSS
Theoretical	$-1.1782598 \cdot 10^{-3}$	$-1.0093966 \cdot 10^{-3}$
1/3	$-1.1779069 \cdot 10^{-3}$	$-1.0090695 \cdot 10^{-3}$
2/3	$-1.1778993 \cdot 10^{-3}$	$-1.0090807 \cdot 10^{-3}$
3/3	$-1.1779807 \cdot 10^{-3}$	$-1.0091486 \cdot 10^{-3}$

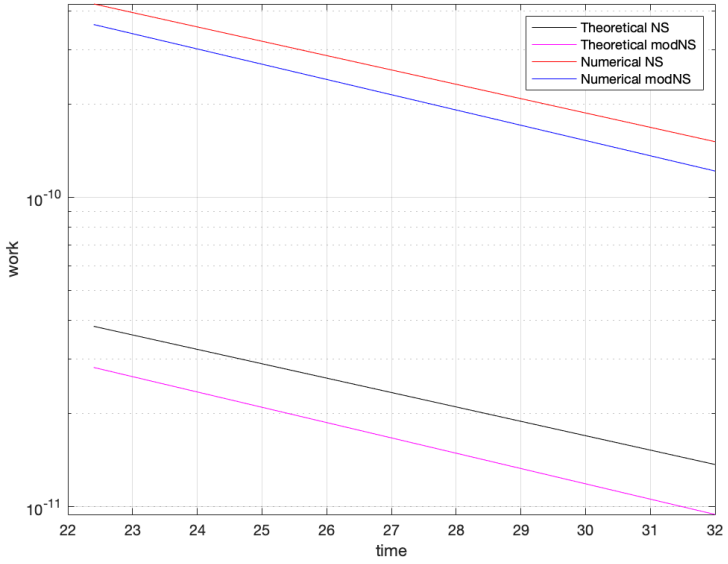

Figure 7.3: Plot of numerical absorption coefficient obtained from the last third of the data with $p_0 = 10^3$.

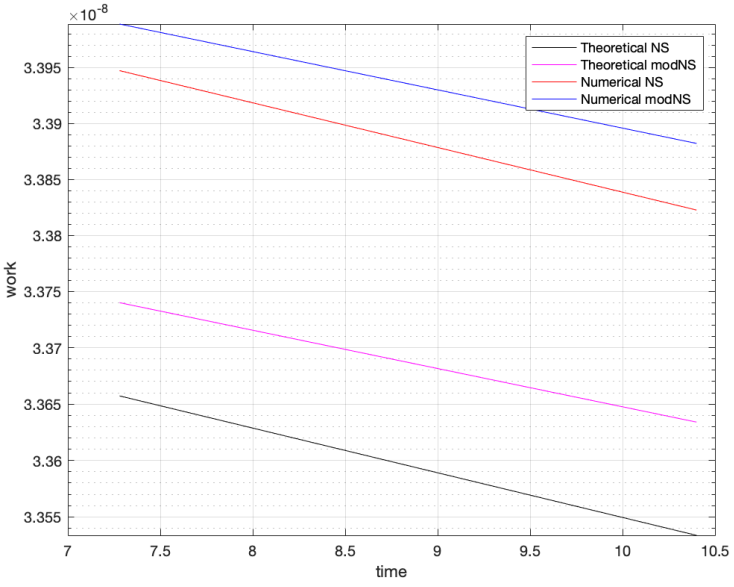

Figure 7.4: Plot of numerical absorption coefficient obtained from the last third of the data with $p_0 = 10^5$.

Table 7.4: Argon with background pressure at 10^3 Pa

	NS	NSS
Theoretical	$-1.178258 \cdot 10^{-1}$	$-1.0093966 \cdot 10^{-1}$
1/3	$-1.1743132 \cdot 10^{-1}$	$-1.0060407 \cdot 10^{-1}$
2/3	$-1.1738801 \cdot 10^{-1}$	$-1.0056609 \cdot 10^{-1}$
3/3	$-1.1747385 \cdot 10^{-1}$	$-1.0063710 \cdot 10^{-1}$

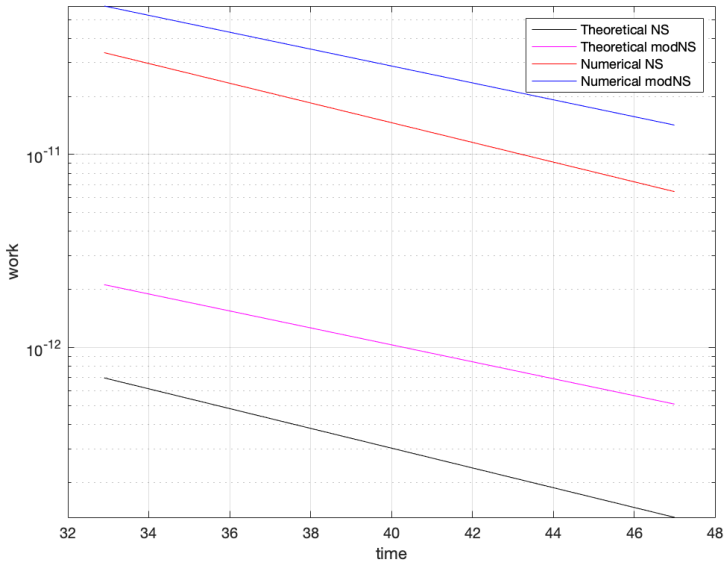

Figure 7.5: Plot of numerical absorption coefficient obtained from the last third of the data with $p_0 = 10^3$.

Although [3] and [7] have not used error bars or written anything about the accuracy of their results we believe that we are within the accuracy of their measuring devices because. Both [3] and [7] used higher frequencies and amplitudes than in our simulations which, according to our simulations give rise to non-linearities and non-linearities might increase the absorption coefficient. Our results show that the difference between the NS and NSS equations is less than can be measured experimentally and the difference between the numerical and linear solutions is similar. We thus conclude that none of the equations can be said to be invalid based on their ability to predict acoustic attenuation in the linear regime.

Chapter 8

Boundary Layer

Boundary layers are the parts of the fluid close to a boundary where viscosity plays a significant role. One example is the boundary layer that develops on the wing of a plan. Since viscosity plays a significant role, it is common to assume an incompressible fluid. In this chapter we will show that the NS and NSS systems simplify to the same system of equations under the assumption of incompressibility. The incompressible NS and NSS equations are used in the derivation of boundary layer equations. Additionally, we will show how the boundary layer equations were first solved analytically, and then solve them numerically.

8.1 Incompressible Navier-Stokes-Svärd Equations

To derive the boundary layer equations we must first derive the incompressible NS and NSS equations from the compressible NS and NSS equations. (For the NS equations this is standard theory and derivations of the incompressible NS equations can be found in [12]). We begin with the NS equations. The compressible NS equations (excluding the energy equation) are

$$\frac{\partial \rho}{\partial t} + \nabla \cdot (\rho \mathbf{u}) = 0. \tag{8.1}$$

$$\frac{\partial (\rho \mathbf{u})}{\partial t} + \nabla \cdot (\rho \mathbf{u} \otimes \mathbf{u}) + \nabla p = \nabla \cdot \left(\left(\zeta - \frac{2}{3}\mu \right) \nabla \cdot \mathbf{u} \mathbb{I} + \mu \left(\nabla \mathbf{u} + (\nabla \mathbf{u})^{\top} \right) \right). \tag{8.2}$$

Incompressiblility allows us to equate all gradients of ρ to zero (also the time derivative). The conservation of mass equation, (8.1), can then be simplified as

follows

$$\begin{aligned} \cancel{\frac{\partial \rho}{\partial t}} + \nabla \cdot (\rho \mathbf{u}) &= 0 \\ \rho \nabla \cdot \mathbf{u} + \cancel{\nabla \rho \cdot \mathbf{u}} &= 0 \\ \nabla \cdot \mathbf{u} &= 0. \end{aligned} \tag{8.3}$$

Now, the conservation of momentum equation (8.2) can be simplified by setting all gradients of ρ to zero as well as every term containing the divergence of $\mathbf{u}$ due to (8.3). Thus, we can recast (8.2) as follows

$$\frac{\partial(\rho \mathbf{u})}{\partial t} + \nabla \cdot (\rho \mathbf{u} \otimes \mathbf{u}) + \nabla p = \nabla \cdot \left(\cancel{\left(\zeta - \frac{2}{3} \mu \right) \nabla \cdot \mathbf{u} \mathbb{I}} + \mu \left(\nabla \mathbf{u} + (\nabla \mathbf{u})^\top \right) \right)$$

$$\rho \frac{\partial \mathbf{u}}{\partial t} + \cancel{\mathbf{u} \frac{\partial \rho}{\partial t}} + \cancel{(\nabla \cdot \rho \mathbf{u}) \mathbf{u}} + \rho \mathbf{u} \cdot \nabla \mathbf{u} + \nabla p = \mu \nabla \cdot (\nabla \mathbf{u} + (\nabla \cdot \mathbf{u})^\top)$$

$$\rho \frac{\partial \mathbf{u}}{\partial t} + \rho \mathbf{u} \cdot \nabla \mathbf{u} + \nabla p = \mu \nabla \cdot \nabla \mathbf{u} + \cancel{\mu \nabla (\nabla \cdot \mathbf{u} \mathbb{I})}$$

$$\frac{\partial \mathbf{u}}{\partial t} + \mathbf{u} \cdot \nabla \mathbf{u} + \frac{1}{\rho} \nabla p = \nu \nabla \cdot \nabla \mathbf{u}.$$

The NS conservation of mass and momentum equations have thus been simplified to

$$\nabla \cdot \mathbf{u} = 0 \tag{8.4}$$

$$\frac{\partial \mathbf{u}}{\partial t} + \mathbf{u} \cdot \nabla \mathbf{u} + \frac{1}{\rho} \nabla p = \nu \nabla \cdot \nabla \mathbf{u}. \tag{8.5}$$

We will now show that the NSS equations will simplify to these equations as well under the incompressibility assumption. The conservation of mass and momentum equations for the NSS system are

$$\frac{\partial \rho}{\partial t} + \nabla \cdot (\rho \mathbf{u}) = \nabla \cdot (\nu \nabla \rho) \tag{8.6}$$

$$\frac{\partial(\rho \mathbf{u})}{\partial t} + \nabla \cdot (\rho \mathbf{u} \otimes \mathbf{u}) + \nabla p = \nabla \cdot (\nu \nabla (\rho \mathbf{u})). \tag{8.7}$$

Assuming constant ρ, the conservation of mass equation, (8.6), simplifies as follows

$$\begin{aligned} \cancel{\frac{\partial \rho}{\partial t}} + \nabla \cdot (\rho \mathbf{u}) &= \cancel{\nabla \cdot (\nu \nabla \rho)} \\ \rho \nabla \cdot \mathbf{u} + \cancel{\mathbf{u} \cdot \nabla \rho} &= 0 \\ \nabla \cdot \mathbf{u} &= 0, \end{aligned}$$

compare with with (8.4). Now the conservation of momentum equation (8.7) can be simplified by using the chain rule and neglecting all terms that contain either the gradient of ρ or the divergence of $\mathbf{u}$.

$$\begin{aligned}
\frac{\partial \rho \mathbf{u}}{\partial t} + \nabla \cdot (\rho \mathbf{u} \otimes \mathbf{u}) + \nabla p &= \nabla \cdot (\nu \nabla (\rho \mathbf{u})) \\
\rho \frac{\partial \mathbf{u}}{\partial t} + \mathbf{u} \cancel{\frac{\partial \rho}{\partial t}} + \cancel{(\nabla \cdot \rho \mathbf{u}) \mathbf{u}} + \rho \mathbf{u} \cdot \nabla \mathbf{u} + \nabla p &= \nabla \cdot (\nu (\cancel{\nabla \rho \otimes \mathbf{u}} + \rho \nabla (\mathbf{u}))) \\
\rho \frac{\partial \mathbf{u}}{\partial t} + \rho \mathbf{u} \cdot \nabla \mathbf{u} + \nabla p &= \cancel{\nabla (\nu \rho) \cdot \nabla \mathbf{u}} + \nu \rho \nabla \cdot \nabla \mathbf{u} \\
\rho \frac{\partial \mathbf{u}}{\partial t} + \rho \mathbf{u} \cdot \nabla \mathbf{u} + \nabla p &= \mu \nabla \cdot \nabla \mathbf{u} \\
\frac{\partial \mathbf{u}}{\partial t} + \mathbf{u} \cdot \nabla \mathbf{u} + \frac{1}{\rho} \nabla p &= \nu \nabla \cdot \nabla \mathbf{u}.
\end{aligned}$$

compare with (8.5). Thus, the incompressible NSS equations are the exact same as the incompressible NS equations.

8.2 Boundary Layer Equation for Laminar Flow

Boundary layers can be analyzed under two more assumption (in addition to incompressibility). Namely, the assumption that the flow is steady (independent of time) and two dimensional. For more information about boundary layers and the following calculations we recommend [12]. The steady, incompressible and two dimensional NS- or NSS equations can be expressed as

$$\frac{\partial u}{\partial x} + \frac{\partial v}{\partial y} = 0 \tag{8.8}$$

$$u \frac{\partial u}{\partial x} + v \frac{\partial u}{\partial y} = -\frac{1}{\rho} \frac{\partial p}{\partial x} + \nu \left(\frac{\partial^2 u}{\partial x^2} + \frac{\partial^2 u}{\partial y^2} \right) \tag{8.9}$$

$$u \frac{\partial v}{\partial x} + v \frac{\partial v}{\partial y} = -\frac{1}{\rho} \frac{\partial p}{\partial y} + \nu \left(\frac{\partial^2 v}{\partial x^2} + \frac{\partial^2 v}{\partial y^2} \right). \tag{8.10}$$

Prandtl first derived the two dimensional steady boundary layer equations in [18] by using two assumptions (in addition to incompressibility) which are:

1. The length of the boundary, L, is a lot bigger than the boundary layer itself δ, namely $L >> \delta$.

2. The convective terms and the diffusive terms are of the same magnitude, namely $\mathbf{u} \cdot \nabla \mathbf{u} \sim \nu \nabla \cdot \nabla \mathbf{u}$.

These two assumptions allow us to use scale analysis to determine the order of magnitude of the relevant terms

$$u \sim U_\infty, \quad x \sim L, \quad y \sim \delta$$
$$\frac{\partial u}{\partial x} \sim \frac{U_\infty}{L}, \quad \frac{\partial u}{\partial y} \sim \frac{U_\infty}{\delta}, \quad \frac{\partial^2 u}{\partial x^2} \sim \frac{U_\infty}{L^2}, \quad \frac{\partial^2 u}{\partial y^2} \sim \frac{U_\infty}{\delta^2}.$$

By the first assumption we can deduce that

$$\left|\frac{U_\infty}{\delta^2}\right| >> \left|\frac{U_\infty}{L^2}\right| \Rightarrow \left|\frac{\partial^2 u}{\partial y^2}\right| >> \left|\frac{\partial^2 u}{\partial x^2}\right|$$

so the majority of the diffusion is due to $\partial_y^2 u$ in (8.9). Moreover, (8.8) indicates that $\partial_x u$ is of the same order of magnitude as $\partial_y v$, namely

$$\frac{\partial u}{\partial x} \sim \frac{U_\infty}{L} \sim \frac{\partial v}{\partial y} \sim \frac{U_\infty}{\delta} \Rightarrow v \sim \delta \frac{U_\infty}{L}. \tag{8.11}$$

and since $\delta << L$, it is safe to assume that the majority of the convection occurs due to the $u\partial_x u$ term in (8.9). Using the second assumption and looking at the terms that contribute most to convection and diffusion, namely $u\partial_x u$ and $\partial_y^2 u$ we can determine their appropriate magnitudes.

$$\frac{U_\infty^2}{L} \sim \frac{\nu U_\infty}{\delta^2} \Rightarrow \frac{\delta^2}{L^2} \sim \frac{\nu}{L U_\infty} \Rightarrow \frac{\delta}{L} \sim \sqrt{\frac{\nu}{U_\infty L}} \sim \frac{1}{\sqrt{Re}} \tag{8.12}$$

where Re is Reynolds number. Now we can write out our Navier-Stokes equation in non-dimensional form

$$\begin{aligned}
&\frac{U_\infty}{L} + \frac{1}{\sqrt{Re}}\frac{U_\infty}{\delta} = 0 \\
&\frac{U_\infty^2}{L} + \frac{1}{\sqrt{Re}}\frac{U_\infty^2}{\delta} = -\frac{1}{\rho}\frac{\partial p}{\partial x} + \nu\left(\frac{U_\infty}{L^2} + \frac{U_\infty}{\delta^2}\right) \\
&\frac{1}{\sqrt{Re}}\frac{U_\infty^2}{L} + \frac{1}{Re}\frac{U_\infty^2}{\delta} = -\frac{1}{\rho}\frac{\partial p}{\partial y} + \frac{1}{\sqrt{Re}}\left(\frac{U_\infty}{L^2} + \frac{U_\infty}{\delta^2}\right)
\end{aligned} \tag{8.13}$$

and in the second equation, (8.13), $1/\sqrt{Re}$ appeared in the diffusive terms because

$$\nu v \sim \nu U_\infty \frac{\delta}{L} \sim \frac{U_\infty}{\sqrt{Re}}.$$

by the similarities found in (8.11) and (8.12). From (8.12) we can deduce that

$$\frac{1}{\delta\sqrt{Re}} \sim \frac{1}{L}$$

which allows us to rewrite our equations and neglect the terms with Re in the denominator and U_∞/L^2 in favor of U_∞/δ^2.

$$\begin{aligned}
\frac{U_\infty}{L} + \frac{U_\infty}{L} &= 0 \\
\frac{U_\infty^2}{L} + \frac{U_\infty^2}{L} &= -\frac{1}{\rho}\frac{\partial p}{\partial x} + \nu\left(\cancel{\frac{U_\infty}{L^2}} + \frac{U_\infty}{\delta^2}\right) \\
\cancel{\frac{1}{\sqrt{Re}}\frac{U_\infty^2}{L}} + \cancel{\frac{1}{Re}\frac{U_\infty^2}{\delta}} &= -\frac{1}{\rho}\frac{\partial p}{\partial y} + \cancel{\frac{1}{\sqrt{Re}}}\left(\cancel{\frac{U_\infty}{L^2}} + \cancel{\frac{U_\infty}{\delta^2}}\right).
\end{aligned}$$

Converting back to normal variables we get

$$\begin{aligned}
\frac{\partial u}{\partial x} + \frac{\partial v}{\partial y} &= 0 \\
u\frac{\partial u}{\partial x} + v\frac{\partial u}{\partial y} &= -\frac{1}{\rho}\frac{\partial p}{\partial x} + \nu\frac{\partial^2 u}{\partial y^2} \\
\frac{1}{\rho}\frac{\partial p}{\partial y} &= 0,
\end{aligned}$$

and because the $\partial_y p/\rho$ term is indepeendent of the two other equations it too can be neglected. Thus, the boundary layer equations are

$$\begin{aligned}
\frac{\partial u}{\partial x} + \frac{\partial v}{\partial y} &= 0 \\
u\frac{\partial u}{\partial x} + v\frac{\partial u}{\partial y} &= -\frac{1}{\rho}\frac{\partial p}{\partial x} + \nu\frac{\partial^2 u}{\partial y^2}.
\end{aligned}$$

Now we must determine the boundary conditions. We know that for $y = 0$ we must use the no slip boundary condition and that $x = x_0$ we can simply set the flow velocity to u_{in}. But we need a condition at the top. Assuming that the fluid is also irrotational and barotropic ($p = p(\rho)$) we can use the steady Bernoulli equation. Also, since we assume the boundary layer is thin, we drop the body term. This leaves us with

$$\frac{p}{\rho} + \frac{1}{2}U_\infty^2 = C$$

where U_∞ is the free stream velocity. Differentiating both sides with respect to x we get

$$-\frac{1}{\rho}\frac{\partial p}{\partial x} = U_\infty\frac{\partial U_\infty}{\partial x}$$

which closes the system of PDE's because we assume that U_∞ is given and then we simply have two coupled PDE's of u and v.

8.2.1 Blausius Solution to a Boundary Layer of a Flat Plate

The solution to the Boundary layer equations for a semi-infinte flat plate with a constant free-stream velocity was first done by Blasius in [2] and we will outline his process here. In the case of constant free-stream velocity the pressure gradient equation reduces to

$$-\frac{1}{\rho}\frac{\partial p}{\partial x} = U_\infty \frac{\partial U_\infty}{\partial x} = 0. \tag{8.14}$$

since U_∞ is constant. So the boundary equations reduce to

$$\frac{\partial u}{\partial x} + \frac{\partial v}{\partial y} = 0 \tag{8.15}$$

$$u\frac{\partial u}{\partial x} + v\frac{\partial u}{\partial y} = \nu \frac{\partial^2 u}{\partial^2 y}. \tag{8.16}$$

Now (8.15) tells us that the fluid is incomprerssible, meaning that we can solve for a stream function. Using the stream function equations

$$u = \frac{\partial \Psi}{\partial y} \quad \text{and} \quad v = -\frac{\partial \Psi}{\partial x}$$

(8.15) and (8.16) can be expressed as

$$\frac{\partial^2 \Psi}{\partial y \partial x} - \frac{\partial^2 \Psi}{\partial x \partial y} = 0 \tag{8.17}$$

$$\frac{\partial \Psi}{\partial y}\frac{\partial^2 \Psi}{\partial y \partial x} - \frac{\partial \Psi}{\partial x}\frac{\partial^2 \Psi}{\partial y^2} = \nu \frac{\partial^3 \Psi}{\partial y^3}. \tag{8.18}$$

Blasius assumed that if the free stream velocity is zero then the boundary layer, $\delta(x)$, is zero. Thus, Blasius guessed that the stream function must take the form

$$\Psi = U_\infty \delta(x) f(\eta).$$

When $x \to 0$ then $\delta(x) \to 0$ which in turn means that $\Psi \to 0$. $f(\eta)$ must now be chosen to help satisfy (8.15). Using the fact that the system of equations is unchanged under the following transformation

$$x' = C^2 x. \quad y' = Cy, \quad u' = u, \quad v' = \frac{v}{C},$$

where C is some positive constant, we must look for a variable which is also unchanged under this transformation. One variable that Blasius guessed might work was

$$\eta = \frac{y}{\delta(x)} = y\sqrt{\frac{U_\infty}{\nu x}}$$

which is unchanged under the transformation. We are now ready to calculate the derivatives needed in equations (8.17) and (8.18). To aid us with these calculations we use the following equality

$$\frac{d\eta}{dx} = -\frac{y}{\delta^2}\frac{d\delta}{dx} = -\frac{\eta}{\delta}\frac{d\delta}{dx}.$$

The relative derivatives for (8.17) and (8.18) are

$$\begin{aligned}
\frac{\partial\Psi}{\partial y} &= U_\infty \frac{df}{d\eta} \\
\frac{\partial^2\Psi}{\partial y^2} &= U_\infty \frac{d^2f}{d\eta^2}\frac{1}{\delta} \\
\frac{\partial^3\Psi}{\partial y^3} &= U_\infty \frac{d^3f}{d\eta^3}\frac{1}{\delta^2} \\
\frac{\partial\Psi}{\partial x} &= -U_\infty \frac{d\delta}{dx}\left(\frac{df}{d\eta}\eta - f\right) \\
\frac{\partial^2\Psi}{\partial y\partial x} &= \frac{\partial^2\Psi}{\partial x\partial y} = -U_\infty \frac{d^2f}{d\eta^2}\frac{\eta}{\delta}\frac{d\delta}{dx}.
\end{aligned}$$

The last equation obviously ensures us that (8.17) is satisfied. Plugging these values into (8.18) we get

$$\begin{aligned}
-U_\infty\frac{df}{d\eta}U_\infty\frac{d^2f}{d\eta^2}\frac{\eta}{\delta}\frac{d\delta}{dx} + U_\infty\frac{d\delta}{dx}\left(\frac{df}{d\eta}\eta - f\right)U_\infty\frac{d^2f}{d\eta^2}\frac{1}{\delta} &= \nu U_\infty\frac{d^3f}{d\eta^3}\frac{1}{\delta^2} \\
-U_\infty\frac{df}{d\eta}\frac{d^2f}{d\eta^2}\eta\frac{d\delta}{dx} + U_\infty\frac{df}{d\eta}\frac{d^2f}{d\eta^2}\eta\frac{d\delta}{dx} - U_\infty\frac{d\delta}{dx}\frac{d^2f}{d\eta^2}f &= \frac{\nu}{\delta}\frac{d^3f}{d\eta^3} \\
-U_\infty\frac{d\delta}{dx}\frac{d^2f}{d\eta^2}f &= \frac{\nu}{\delta}\frac{d^3f}{d\eta^3} \qquad (8.19)
\end{aligned}$$

Now using the fact that

$$\delta(x) = \sqrt{\frac{\nu x}{U_\infty}} \Rightarrow \frac{d\delta}{dx} = \frac{1}{2}\frac{1}{\delta}\frac{\nu}{U_\infty},$$

(8.19) becomes

$$\begin{aligned}
-U_\infty\frac{1}{2}\frac{1}{\delta}\frac{\nu}{U_\infty}\frac{d^2f}{d\eta^2}f &= \frac{\nu}{\delta}\frac{d^3f}{d\eta^3} \\
\frac{1}{2}\frac{d^2f}{d\eta^2}f &= \frac{d^3f}{d\eta^3} \\
\frac{d^3f}{d\eta^3} + \frac{1}{2}f\frac{d^2f}{d\eta^2} &= 0. \qquad (8.20)
\end{aligned}$$

Thus, the nonlinear coupled PDE's (8.15) and (8.16) have been reduced to a nonlinear ordinary differential equation (ODE) (8.20). To figure out the boundary conditions, we note that that $u = v = 0$ when $y = 0$ due to the no slip boundary condition, which means that

$$u = \frac{\partial \Psi}{\partial y} \Leftrightarrow \frac{df(0)}{d\eta} = 0$$

and for the v component we get

$$v = -\frac{\partial \Psi}{\partial x} = U_\infty \frac{d\delta}{dx}\left((0)\eta - f\right) = -U_\infty \frac{d\delta}{dx} f = 0 \Leftrightarrow f(0) = 0$$

and finally we know that at the top of the boundary equation the velocity must equal that of the free stream velocity so we can write

$$\lim_{\eta \to \infty} \frac{df(\eta)}{d\eta} = 1.$$

The way to interpret $\lim \eta \to \infty$ is to assume a fixed point in space (x, y) and let $\delta(x)$ go to zero, and in doing so the boundary layer is beneath the fixed point so its velocity must be the free stream velocity. Or, you can do the opposite, fix the boundary layer at some distance x and then let y go to infinity, and then again we are far above the boundary layer so the velocity must equal the freestream velocity. Thus, the ODE is

$$\frac{d^3 f}{d\eta^3} + \frac{1}{2} f \frac{d^2 f}{d\eta^2} = 0$$

with the following boundary conditions

$$f(0) = 0, \quad \frac{df(0)}{d\eta} = 0, \quad \frac{df(\infty)}{d\eta} = 1. \tag{8.21}$$

The non-linearity leads us to solve the equation numerically, which is the subject of the next chapter.

Chapter 9

Non-Dimensional Boundary Layer Simulation

To simulate a boundary layer predicted by the NSS equations we create a rectangular domain where an inlet and outlet boundary are imposed on the western and eastern boundaries respectively (i.e., the fluid is moving from left to right). The southern boundary simulates an adiabatic flat plate so the momentum in x and y direction (m and n, respectively) are set to zero and $\partial_n \rho$ and $\partial_n T$ are set to zero. On the norther boundary we impose a far field boundary condition. On the western, northern, and eastern boundaries we use the injection method by injecting the solution of the Blasius equation (8.20). On the southern boundary we also use the injection method and set $\partial_n \rho$, $\partial_n T$, m, and n to zero. Since the western, northern, and eastern boundary conditions are not the correct boundary conditions for the NSS equations we expect the errors will propagate out from the boundaries but decrease the further away from the boundary they travel. Therefore, all comparisons between the Blasius solution and the NSS solution are done in the middle between the two boundaries.
The outline of this chapter is as follows

1. Numerically solve the Blasius ODE (8.20).

2. Derive the finite volume method.

3. Set boundary conditions, initial conditions, and non-dimensional fluid properties.

4. Transform grid to obtain a higher resolution near the flat plate and lower resolution far away from the boundary.

5. Simulate and compare the solutions of Blasius equation and NSS equations.

9.1 Numerical Solution of Blasius Boundary Layer

The Blasius ODE (8.20) is a third order non-linear ODE with two initial conditions and one boundary condition (8.21). We solve the nonlinear ODE using the shooting method, which turns an ODE with boundary conditions into an ODE with initial conditions (For an introduction to the shooting method we recommend [20]). We first transform (8.20) into a system of first order ODE's

$$\begin{aligned}\dot{f}_1 &= f_2\\ \dot{f}_2 &= f_3\\ \dot{f}_3 &= -\frac{1}{2}f_1 f_3.\end{aligned}$$

The root finding method used to determine the appropriate initial condition was the bisection method because it is guaranteed to converge as long as the two initial values are on each side of the root. Since the boundary condition was set for $df/d\eta$ we solved for $df/d\eta$ and numerically integrated to obtain f. The error tolerance between the true boundary condition and the numerical boundary condition was set to 10^{-15} and the fourth order Runge-Kutta method was used as the time discretization method. Figure 9.1 shows some of the attempts. Figure 9.2 shows $f, df/d\eta, d^2f/d\eta^2$, and $\eta df/d\eta - f$. f is the stream function, $df/d\eta$ is the non-dimensional velocity, and $d^2f/d\eta^2$ is the shear stress. We now have u and v

$$\begin{aligned}\frac{u}{U_\infty} &= \frac{\partial \Psi}{\partial y} = \frac{df}{d\eta}\\ \frac{v}{U_\infty} &= -\frac{\partial \Psi}{\partial x} = \frac{d\delta}{dx}\left(\frac{df}{d\eta}\eta - f\right).\end{aligned}$$

Now that we have the numerical approximation of the Blasius solution we can set boundary conditions and initial conditions for the NSS equations.

9.2 Finite Volume Method

We have chosen the finite volume method (FVM) as our numerical scheme because it is the method used to derive a convergent scheme for the NSS system in [23]. The explanations in this section are based on the book [8]. For the following PDE

$$\frac{\partial}{\partial t}u + \nabla \cdot \mathbf{f} = \nabla \cdot \nabla g$$

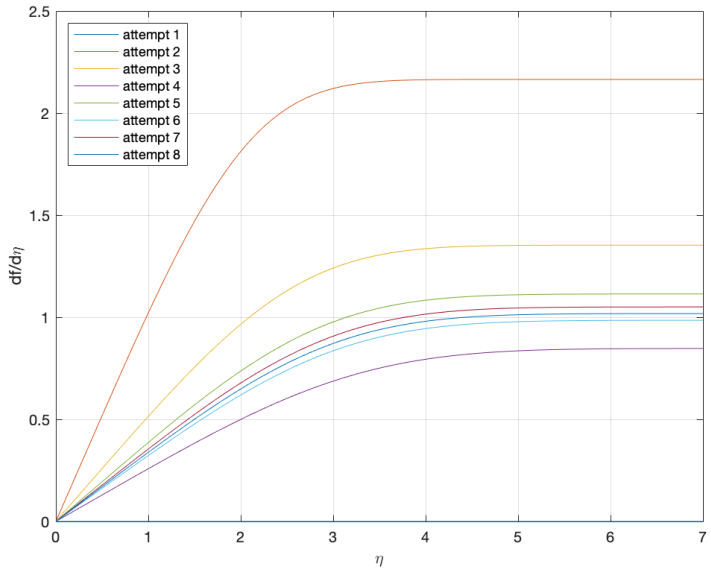

Figure 9.1: The first eight attempts of the shooting method for solving Blasius's ODE.

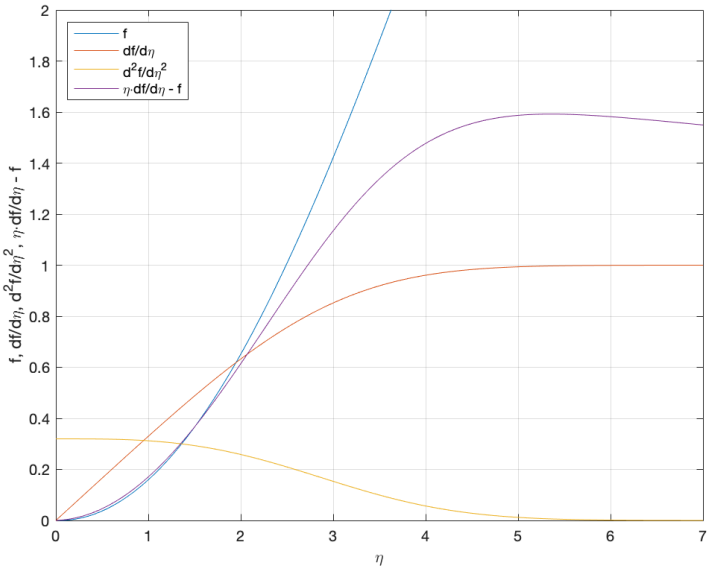

Figure 9.2: Plots of the stream function f, the x-component of the velocity, $df/d\eta$, the y-component of the velocity, $\eta df/d\eta - f$, and the shear stress $d^2f/d\eta^2$

where $u : \mathbb{R} \to \mathbb{R}$, $\mathbf{f} : \mathbb{R}^d \to \mathbb{R}^d$, and $g : \mathbb{R} \to \mathbb{R}$ where $d \in \mathbb{N}$. We can integrate over each control volume, denoted V

$$\int_V \frac{\partial}{\partial t} u dV + \int_V \nabla \cdot \mathbf{f} dV = \int_V \nabla \cdot \nabla g dV$$

and apply the divergence theorem to the spatial fluxes.

$$\int_V \frac{\partial}{\partial t} u dV + \oint_{\partial V} \mathbf{f} \cdot \hat{\mathbf{n}} dS = \oint_{\partial V} \nabla g \cdot \hat{\mathbf{n}} dS$$

where $\hat{\mathbf{n}}$ is a unit vector pointing orthogonally outward from the surface of the volume. For the time derivative, we assume that the fluid in the volume is approximately constant such that the midpoint of the fluid multiplied by the volume is a good approximation of the integral of time derivative of the volume. This assumption holds if fluxes in the fluid are very small or the volumes containing the fluid are very small or both.

$$V \frac{\partial}{\partial t} \overline{u} + \oint_{\partial V} \mathbf{f} \cdot \hat{\mathbf{n}} dS = \oint_{\partial V} \nabla g \cdot \hat{\mathbf{n}} dS.$$

If we now assume that our volume is a polygon with N sides we can express the surface integral as the sum of flux over all the sides

$$V \frac{\partial}{\partial t} \overline{u} + \sum_{n=1}^{N} \mathbf{f}(\mathcal{B}) \cdot \hat{\mathbf{n}} dS_n = \sum_{n=1}^{N} \nabla g(\mathcal{B}) \cdot \hat{\mathbf{n}} dS_n$$

where $\mathbf{f}(\mathcal{B})$ and $g(\mathcal{B})$ are $\mathbf{f}$ and g evaluated at the boundaries of the control volume respectively. Since we are working with discrete points we must approximate $\mathbf{f} \cdot \hat{\mathbf{n}}$ and $\nabla \mathbf{g} \cdot \hat{\mathbf{n}}$ at the interface between the volumes. A common choice is to approximate the flux linearly. This is done as follows

$$\mathbf{f}_{n+\frac{1}{2}} \approx \frac{\mathbf{f_n} + \mathbf{f}_{n+1}}{2} \tag{9.1}$$

and

$$\frac{\partial}{\partial x} g_{n+\frac{1}{2}} \approx \frac{g_{n+1} - g_n}{x_{n+1} - x_n} \tag{9.2}$$

where x_n are points on an arbitrary affine coordinate system. This enables us to recast our scheme in the following semi-discrete form

$$V \frac{\partial}{\partial t} \overline{\mathbf{\Upsilon}} + \sum_{n=1}^{N} \frac{\mathbf{f} + \mathbf{f}_{adj}}{2} \hat{\mathbf{n}} dS_n = \sum_{n=1}^{N} \frac{g - g_{adj}}{x - x_{adj}} \hat{\mathbf{n}} dS_n$$

$$\frac{\partial}{\partial t} \overline{\mathbf{\Upsilon}} = -\frac{1}{V} \sum_{n=1}^{N} \frac{\mathbf{f} + \mathbf{f}_{adj}}{2} \hat{\mathbf{n}} dS_n + \frac{1}{V} \sum_{n=1}^{N} \frac{g - g_{adj}}{x - x_{adj}} \hat{\mathbf{n}} dS_n$$

where the subscript *adj* denotes the adjacent volume. In this thesis we will numerically solve the two dimensional NSS system on a rectangular grid. The two dimensional NSS equations are

$$\frac{\partial}{\partial t}\begin{pmatrix}\rho\\ m\\ n\\ E\end{pmatrix}+\frac{\partial}{\partial x}\begin{pmatrix}m\\ \frac{m^2}{\rho}+p\\ \frac{mn}{\rho}\\ E\frac{m}{\rho}+p\frac{m}{\rho}\end{pmatrix}+\frac{\partial}{\partial y}\begin{pmatrix}n\\ \frac{mn}{\rho}\\ \frac{n^2}{\rho}+p\\ E\frac{n}{\rho}+p\frac{n}{\rho}\end{pmatrix}=\frac{\partial}{\partial x}\left(\nu\frac{\partial}{\partial x}\begin{pmatrix}\rho\\ m\\ n\\ E\end{pmatrix}\right)+\frac{\partial}{\partial y}\left(\nu\frac{\partial}{\partial y}\begin{pmatrix}\rho\\ m\\ n\\ E\end{pmatrix}\right).$$

After applying the divergence theorem for a rectangular grid, we get the following scheme

$$\begin{aligned}\frac{\partial}{\partial t}\begin{pmatrix}\rho\\ m\\ n\\ E\end{pmatrix}=&-\frac{1}{V}\left(\begin{pmatrix}m\\ \frac{m^2}{\rho}+p\\ \frac{mn}{\rho}\\ E\frac{m}{\rho}+p\frac{m}{\rho}\end{pmatrix}_{east}-\begin{pmatrix}m\\ \frac{m^2}{\rho}+p\\ \frac{mn}{\rho}\\ E\frac{m}{\rho}+p\frac{m}{\rho}\end{pmatrix}_{west}\right)\\ &-\frac{1}{V}\left(\begin{pmatrix}n\\ \frac{mn}{\rho}\\ \frac{n^2}{\rho}+p\\ E\frac{n}{\rho}+p\frac{n}{\rho}\end{pmatrix}_{north}-\begin{pmatrix}n\\ \frac{mn}{\rho}\\ \frac{n^2}{\rho}+p\\ E\frac{n}{\rho}+p\frac{n}{\rho}\end{pmatrix}_{south}\right)\\ &+\frac{1}{V}\left(\nu\frac{\partial}{\partial x}\begin{pmatrix}\rho\\ m\\ n\\ E\end{pmatrix}_{east}-\nu\frac{\partial}{\partial x}\begin{pmatrix}\rho\\ m\\ n\\ E\end{pmatrix}_{west}\right)\\ &+\frac{1}{V}\left(\nu\frac{\partial}{\partial y}\begin{pmatrix}\rho\\ m\\ n\\ E\end{pmatrix}_{north}-\nu\frac{\partial}{\partial y}\begin{pmatrix}\rho\\ m\\ n\\ E\end{pmatrix}_{south}\right)\end{aligned}$$

where *east*, *west*, *north*, and *south* are the boundaries of the control volume. The *nodal* finite volume method was used, meaning that the centers of the volumes are known values and the boundaries of the volumes are not (in contrast with cell-centered finite volume schemes). The various entities ρ, m, n, E, and p were evaluated at the boundaries using 9.1 for the convective terms and 9.2 for the diffusive terms. The time discretization method used was the fourth order Runge-Kutta method.

9.3 Boundary Conditions, Initial Conditions, and Fluid Properties

To simulate a boundary layer developed by convection from west to east over a semi-infinite plate we create a rectangular domain. Inlet and outlet boundaries are set on the western and eastern boundaries respectively. The northern boundary is treated as a far field boundary and the southern boundary is has boundary conditions of an adiabatic wall with no slip condition. The western, northern, and eastern boundaries are Dirichlet boundaries where we set the Blasius boundary solution obtained from section 9.1. The southern boundary is a Robin boundary where $\partial_n \rho$ and $\partial_n T$ are set to zero, satisfying the adiabatic wall, and the x and y components of momentum are set to zereo in accordance with the no slip condition. All boundary conditions were imposed by the injection method. For the eastern, northern, and western boundaries, we calculated $\eta = y\sqrt{U_\infty/\nu x}$ at each point set the the corresponding value for u and v. ρ and T were assumed to be constant in accordance with the assumptions used to derive the Blasius boundary layer.
The initial condition was calculated the same was as the boundary conditions. Namely, we calculated $\eta = y\sqrt{U_\infty/\nu x}$ for each point on the grid and then determined the corresponding value of u and v at that point. ρ was the same for each grid point and $E = \rho c_V T + \rho(u^2 + v^2)/2$ at each grid point. We used the nondimensionalized fluid properties.

$$T = 1, \quad p = 1, \quad \mu = 1, \quad c_p = 2, \quad c_V = 1$$

9.4 Grid Transformation

Boundary layers are known to exhibit steep gradients near the wall, which in this case is the southern boundary. At the northern far-field boundary the gradients are almost zero (which is supported by the plots depicted in figure 9.2). Therefore, we have transformed our grid such that the volumes close to the southern boundary are small and the volumes increase in size the further away they are from the southern boundary. To keep the second order convergence rate we need to apply an affine transformation (preserving parallelism and lines). We have chosen the following transformation

$$y' = A + B\exp(\alpha y).$$

where A, B, and α are constants. y' must equal y at the boundaries, y_0 and y_N. The coefficients A and B are then easily obtained by the following system of

algebraic equations

$$\begin{bmatrix} y_0 \\ y_N \end{bmatrix} = \begin{bmatrix} 1 & \exp(\alpha y_0) \\ 1 & \exp(\alpha y_N) \end{bmatrix} \begin{bmatrix} A \\ B \end{bmatrix}.$$

A and B are thus computed to be

$$A = \frac{y_0 \exp(\alpha y_N) - y_N \exp(\alpha y_0)}{\exp(\alpha y_N) - \exp(\alpha y_0)}$$
$$B = \frac{y_N - y_0}{\exp(\alpha y_N) - \exp(\alpha y_0)}.$$

Note that α is a coefficient that determines how quickly the volumes change and it can be tuned to obtained the desired grid. α has no affect on A or B. The transformed grid is thus

$$y' = \frac{y_0 \exp(\alpha y_N) - y_N \exp(\alpha y_0)}{\exp(\alpha y_N) - \exp(\alpha y_0)} + \left(\frac{y_N - y_0}{\exp(\alpha y_N) - \exp(\alpha y_0)} \right) \exp(\alpha y) \tag{9.3}$$

and x remains unchanged.

9.5 Numerical Results

The simulation was run on the grid $x \in [9, 11]$ with 33 cells and $y \in [0, 200]$ with 128 cells. y was transformed using (9.3) and α was set to $1/30$ (y_0 and y_N are 0 and 200 respectively). Figure 9.3 depicts the transformed grid. The smallest volume had a measure of approximately $2.1 \cdot 10^{-4}$. The time step, Δt, was set to 10^{-5} and the simulation was run until the l^2 norm of the difference between the error in ρ from one time step to the next was less than 10^{-14}. The error was calculated as follows

$$\text{error} = \sqrt{\sum h(\rho(t - \Delta t) - \rho(t))^2} \tag{9.4}$$

where $\rho_{t-\Delta t}$ and $\rho_{t-\Delta t}$ is ρ at times t and $t - \Delta t$ respectively. h is the measure of the size of each cell. This informed us that we had reached a steady state solution. The solution seemed to converge uniformly to to a steady state solution. The errors in table 9.5 are the l^2 norm of difference between the Blasius solution and the NSS solution at $x = 10$, i.e., in the middle between the eastern and western boundaries.

$$\text{error} = \sqrt{\sum h(f_{Blas} - f_{NSS})^2} \tag{9.5}$$

where h is the volume size of each cell and f is either ρ, u, v, T or a combination of those values. f_{Blas} is the solution to the Blasius equations and f_{NSS} is the solution to the NSS equations.

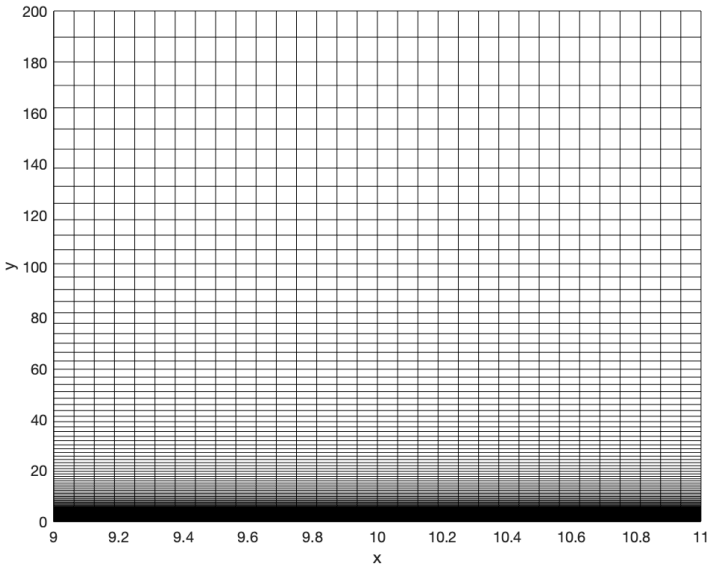

Figure 9.3: The grid used to solve for the boundary profile of the NSS equations.

Table 9.1: Error between Blasius and NSS equations

variables	error
ρ	0.00202
u	0.00362
v	0.0142
Internal energy	0.00503
Mechanical energy	0.00322

Internral energy was calculated as $\rho c_V T$ and Mechanical energy was calculated as $\rho(u^2 + v^2)/2$. The differences between the Blasius solution and the NSS solution are less than one percent except for v. This indicates a good match between the NSS equations and the Blasius equations. Figures 9.4 and 9.5 depict the Blasius solution and the NSS solution for u and v respectively

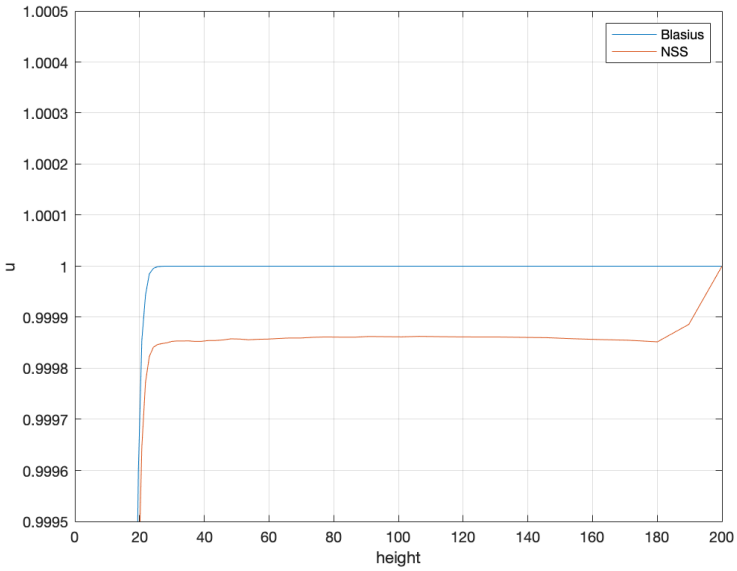

Figure 9.4: Numerical NSS Boundary layer plotted on the analytical Blasius solution

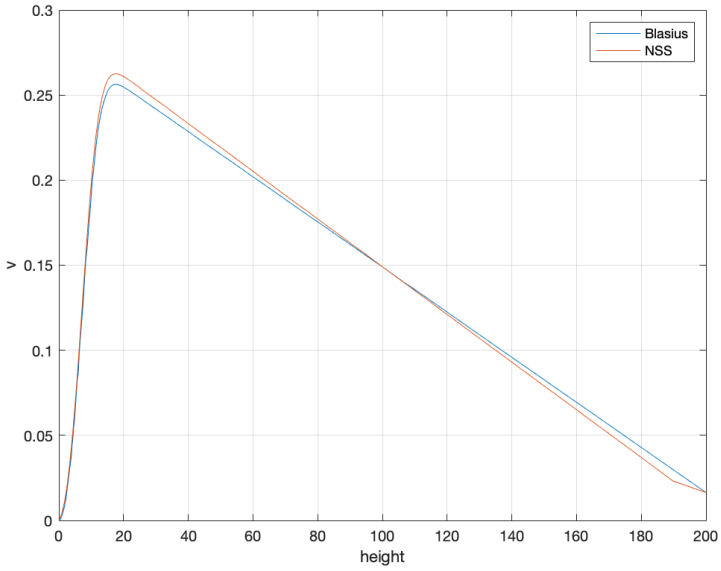

Figure 9.5: Numerical NSS Boundary layer plotted on the analytical Blasius solution

Conclusion and Outlook

In this thesis we have tested the validity of the NSS equations compared to the NS equations and experimental results found in the literature. The fluids being simulated were pure argon and oxygen. We found that for acoustic attenuation, the difference between the two systems in the linear regime is smaller than what can be measured using modern acoustic measuring devices. Further research should examine simulations of other gases and experiments should be conducted in the linear regime. Also, changes in pressure, temperature, density etc. should be examined to see if a combination of changes to those values increase the absorption coefficient without making the wave non-linear. This would help bridge the gap between accurate computer simulations and accurate physical experiments.

For the boundary layer case, the NSS equations were in good agreement with the Blasius solution, but further research should run the simulations on different grids and experiment with the dimensionalized equations. Additionally, the computer simulations should be compared with experimental results. The Blasius boundary layer for a flat plate is one of the simplest boundary layers. Therefore, more research should be done on more complicated boundary layers such as a boundary layer that does not assume constant temperature or boundary layers on a non-flat plate, such as the Falkner–Skan boundary layer. Finally, the NS equations should also be compared to the Blasius boundary layer to compare efficiency and accuracy between the NS and NSS equations.

Appendix A

Here we provide a detailed calculation of (2.26) where we use the notation explained in definition .

$$\begin{bmatrix} -\frac{|\mathbf{u}|^2}{2T} - c_V\left(\frac{S}{c_V} - \gamma\right) \\ \frac{\mathbf{u}}{T} \\ -\frac{1}{T} \end{bmatrix} \odot \begin{Bmatrix} \nabla\cdot(\rho\mathbf{u}) \\ \nabla\cdot(\rho\mathbf{u}\otimes\mathbf{u}) + \nabla p \\ \left(\nabla\cdot\left(\rho\frac{|\mathbf{u}|^2}{2}\mathbf{u}\right) + \nabla\rho\cdot c_V T\mathbf{u} + \rho c_V\nabla T\cdot\mathbf{u}\right. \\ \left. + \rho c_V T\nabla\cdot\mathbf{u} + \nabla p\cdot\mathbf{u} + p\nabla\cdot\mathbf{u}\right) \end{Bmatrix}$$

The first row is

$$-\frac{|\mathbf{u}|^2}{2T}\nabla\cdot(\rho\mathbf{u}) - S\nabla\cdot(\rho\mathbf{u}) + c_V\gamma\nabla\cdot(\rho\mathbf{u}). \tag{A.1}$$

Using the relation the product rule and the following relation

$$\gamma\nabla\rho = \frac{\nabla T}{T}\rho + \nabla\rho - \frac{\rho}{c_V}\nabla S$$

we can recast (A.1) as

$$-\frac{|\mathbf{u}|^2}{2T}\nabla\cdot(\rho\mathbf{u}) - S\nabla\cdot(\rho\mathbf{u}) + c_V\gamma\rho\nabla\cdot\mathbf{u} + c_V\mathbf{u}\frac{\nabla T}{T}\rho + c_V\nabla\rho\cdot\mathbf{u} - \mathbf{u}\cdot\rho\nabla S. \tag{A.2}$$

The product of the middle entries are

$$\frac{\rho|\mathbf{u}|^2}{T}\nabla\cdot(\rho\mathbf{u}) + \frac{|\mathbf{u}|^2}{T}\nabla\cdot(\rho\mathbf{u}) + \frac{\mathbf{u}}{T}\nabla p \tag{A.3}$$

and the product of the last entries are

$$-\frac{|\mathbf{u}|^2}{2T}\nabla\cdot(\rho\mathbf{u}) - \frac{\rho\mathbf{u}}{2T}\cdot\nabla|\mathbf{u}|^2 - c_V\nabla\rho\cdot\mathbf{u} - \frac{c_V\rho}{T}\nabla T\cdot\mathbf{u} - c_V\rho\nabla\cdot\mathbf{u} - \frac{\mathbf{u}}{T}\cdot\nabla p - \frac{p}{T}\nabla\cdot\mathbf{u}. \tag{A.4}$$

The first terms in (A.2) and (A.4) cancel with the second term in (A.3) and the first and last term in (A.3) cancels the second and second to last term in (A.4) respectively. The second to last and third to last terms in (A.2) cancel with third and fourth term in (A.4) respectively. After all the cancellations we are left with

$$-S\nabla\cdot(\rho\mathbf{u}) + c_V\gamma\rho\nabla\cdot\mathbf{u} - \mathbf{u}\cdot\rho\nabla S - c_V\rho\nabla\cdot\mathbf{u} + \frac{p}{T}\nabla\cdot\mathbf{u}.$$

Now, using the fact that $\gamma c_V = c_p$, $R = c_p - c_V$, and $p/T = \rho R$ we aree simply left with

$$-\nabla\cdot(\rho\mathbf{u}S)$$

Appendix B

Here we provide a detailed calculation of (2.32).

$$\begin{Bmatrix} -\frac{1}{2T}\nabla|\mathbf{u}|^2 + \frac{|\mathbf{u}|^2}{2T^2}\nabla T - \frac{c_V}{T}\nabla T + \frac{c_V}{\rho}(\gamma-1)\nabla\rho \\ \frac{1}{T}\nabla\mathbf{u} - \frac{\mathbf{u}}{T^2}\otimes\nabla T \\ \frac{1}{T^2}\nabla T \end{Bmatrix} : \nu \begin{Bmatrix} \nabla\rho \\ \mathbf{u}\otimes\nabla\rho + \rho\nabla\mathbf{u} \\ \nabla\rho\frac{|\mathbf{u}|^2}{2} + \rho\nabla\frac{|\mathbf{u}|^2}{2} + \nabla\rho c_V T + \rho c_V \nabla T \end{Bmatrix}$$

where we start by taking the dot product of each row. To simplify notation we multiply ν at the end. The dot product of the first rows are

$$-\frac{\nabla\rho}{2T}\cdot\nabla|\mathbf{u}|^2 + \frac{|\mathbf{u}|^2}{2T^2}\nabla T\cdot\nabla\rho - \frac{c_V}{T}\nabla T\cdot\nabla\rho + \frac{c_V}{\rho}(\gamma-1)\nabla\rho\cdot\nabla\rho \tag{B.1}$$

the product of the second row is

$$\frac{1}{T}\nabla\mathbf{u} : (\mathbf{u}\otimes\nabla\rho) + \frac{\rho}{T}\nabla\mathbf{u} : \nabla\mathbf{u} - \frac{\mathbf{u}}{T^2}\otimes\nabla T : (\mathbf{u}\otimes\nabla\rho) - \rho\frac{\mathbf{u}}{T^2}\otimes\nabla T : \nabla\mathbf{u}.$$

We can recast the the tensor product terms as dot products as follows

$$\frac{1}{2T}\nabla|\mathbf{u}|^2\cdot\nabla\rho + \frac{\rho}{T}\nabla\mathbf{u} : \nabla\mathbf{u} - \frac{|\mathbf{u}|^2}{T^2}\nabla T\cdot\nabla\rho - \frac{\rho}{2T^2}\nabla|\mathbf{u}|^2\cdot\nabla T \tag{B.2}$$

and the product of the last rows are

$$\frac{1}{T^2}\nabla T\cdot\nabla\rho\frac{|\mathbf{u}|^2}{2} + \frac{\rho}{T}\nabla\frac{|\mathbf{u}|^2}{2}\cdot\nabla T + \frac{c_V}{T}\nabla\rho\cdot\nabla T + \frac{\rho c_V}{T}\nabla T\cdot\nabla T. \tag{B.3}$$

Now we can see all the terms that cancel out. The first and third term in (B.1) cancel out with the first term in (B.2) and third term in (B.3) respectively. The second term of (B.1) and first term of (B.3) cancel with the third term of (B.2). And finally, the second term in (B.3) cancels with the last term in (B.2). We are therefor left with

$$\nu\rho\frac{c_V}{\rho^2}(\gamma-1)|\nabla\rho|^2 + \frac{\nu\rho}{T}|\nabla\mathbf{u}|^2 + \nu\rho\frac{c_V}{T^2}|\nabla T|^2$$

Bibliography

[1] Rutherford Aris. *Vectors, Tensors and the Basic Equations of Fluid Mechanics*. DOVER PUBN INC, Jan. 1990. 320 pp. ISBN: 0486661105. URL: https://www.ebook.de/de/product/3303126/rutherford_aris_vectors_tensors_and_the_basic_equations_of_fluid_mechanics.html.

[2] Paul Richard Heinrich Blasius. "Grenzschichten in Flüssigkeiten mit kleiner Reibung". In: *Z. Angew. Math. Phys.* (1908).

[3] Sally G. Ejakov et al. "Acoustic attenuation in gas mixtures with nitrogen: Experimental data and calculations". In: *The Journal of the Acoustical Society of America* 113.4 (Apr. 2003), pp. 1871–1879. DOI: 10.1121/1.1559177.

[4] Leonhard Euler. "On the sums of series of reciprocals". In: (June 2005). arXiv: math/0506415 [math.HO].

[5] Lawrence Evans. *Partial differential equations*. Providence, R.I: American Mathematical Society, 2010. ISBN: 0821849743.

[6] Bengt Fornberg. *A Practical Guide to Pseudospectral Methods*. Cambridge University Press, Jan. 1996. DOI: 10.1017/cbo9780511626357.

[7] Martin Greenspan. "Propagation of Sound in Five Monatomic Gases". In: *The Journal of the Acoustical Society of America* 28.4 (July 1956), pp. 644–648. DOI: 10.1121/1.1908432.

[8] Bertil Gustafsson. *High Order Difference Methods for Time Dependent PDE*. Springer-Verlag GmbH, Dec. 2007. ISBN: 3540749934. URL: https://www.ebook.de/de/product/8900071/bertil_gustafsson_high_order_difference_methods_for_time_dependent_pde.html.

[9] Amiram Harten. "On the symmetric form of systems of conservation laws with entropy". In: *Journal of Computational Physics* 49.1 (Jan. 1983), pp. 151–164. DOI: 10.1016/0021-9991(83)90118-3.

[10] Jan Hesthaven. *Spectral methods for time-dependent problems*. Cambridge: Cambridge University Press, 2007. ISBN: 9780511618352.

[11] T.J.R. Hughes, L.P. Franca, and M. Mallet. "A new finite element formulation for computational fluid dynamics: I. Symmetric forms of the compressible Euler and Navier-Stokes equations and the second law of thermodynamics". In: *Computer Methods in Applied Mechanics and Engineering* 54.2 (Feb. 1986), pp. 223–234. DOI: 10.1016/0045-7825(86)90127-1.

[12] Pijush Kundu. *Fluid mechanics*. Amsterdam: Academic Press, 2015. ISBN: 9780124059351.

[13] E. M. Lifshitz L D Landau. *Fluid Mechanics*. Elsevier Science Techn., Sept. 2013. 554 pp. URL: https://www.ebook.de/de/product/22314839/l_d_landau_e_m_lifshitz_fluid_mechanics.html.

[14] L. D. Landau. *Statistical physics*. Amsterdam London: Elsevier Butterworth Heinemann, 1980. ISBN: 9780750633727.

[15] Ling-Hsiao Lyu. *Numerical Simulation of Space Plasmas (I) Lecture Notes*. 2016. URL: http://www.ss.ncu.edu.tw/~lyu/lecture_files_en/lyu_NSPP_Notes/lyu_NSPP_Content.html.

[16] Melissa Morris. "Analysis of an alternative Navier-Stokes system: Attenuation of sound waves". en. In: (2021). DOI: 10.13140/RG.2.2.29383.01442.

[17] Jan Nordström and Magnus Svärd. "Well-Posed Boundary Conditions for the Navier–Stokes Equations". In: *SIAM Journal on Numerical Analysis* 43.3 (Jan. 2005), pp. 1231–1255. DOI: 10.1137/040604972.

[18] Ludwig Prandtl. "Über Flüssigkeitsbewegung bei sehr kleiner Reibung". In: *Verhandlinger 3. Int. Math. Kongr. Heidelberg* (1904).

[19] KAMBIZ SALARI and PATRICK KNUPP. *Code Verification by the Method of Manufactured Solutions*. Tech. rep. June 2000. DOI: 10.2172/759450.

[20] Tim Sauer. *Numerical analysis*. Harlow, Essex: Pearson, 2014. ISBN: 9781292023588.

[21] Steven Strogatz. *Nonlinear dynamics and chaos : with applications to physics, biology, chemistry, and engineering*. Boulder, CO: Westview Press, a member of the Perseus Books Group, 2015. ISBN: 9780813349107.

[22] Magnus Svärd. "A new Eulerian model for viscous and heat conducting compressible flows". In: *Physica A: Statistical Mechanics and its Applications* 506 (Sept. 2018), pp. 350–375. DOI: 10.1016/j.physa.2018.03.097.

[23] Magnus Svärd. "Analysis of an alternative Navier-Stokes system: Weak entropy solutions and a convergent numerical scheme". en. In: (2021). DOI: 10.13140/RG.2.2.16184.47366.

[24] Magnus Svärd. "Weak solutions and convergent numerical schemes of modified compressible Navier–Stokes equations". In: *Journal of Computational Physics* 288 (May 2015), pp. 19–51. DOI: 10.1016/j.jcp.2015.02.013.

[25] Eitan Tadmor. "Entropy stability theory for difference approximations of nonlinear conservation laws and related time-dependent problems". In: *Acta Numerica* 12 (May 2003), pp. 451–512. DOI: 10.1017/s0962492902000156.

[26] Terence Tao. "Finite time blowup for an averaged three-dimensional Navier-Stokes equation". In: (Feb. 2014). arXiv: 1402.0290 [math.AP].

[27] Lloyd N. Trefethen. *Spectral Methods in MATLAB*. CAMBRIDGE, July 2000. 183 pp. ISBN: 0898714656. URL: https://www.ebook.de/de/product/6906321/lloyd_n_trefethen_spectral_methods_in_matlab.html.

[28] Hugh Young. *Sears and Zemansky's university physics : with modern physics*. Boston: Pearson, 2016. ISBN: 9781292100319.